From: Emily Jeffers [mailto:ejeffers@biologicaldiversity.org]
Sent: Tuesday, March 21, 2023 3:17 PM
To: CityClerk <CityClerk@longbeach.gov>
Subject: CBD Sources, Part 3.1

-EXTERNAL-

Please see attached sources for our comment letter.

March 21, 2023

Tom Modica, City Manager
411 W. Ocean Blvd.
Long Beach, CA 90802

Re: Support of Setbacks in Long Beach

Dear Mr. Modica,

We, the undersigned organizations with membership and constituents in Long Beach – the traditional homelands of the Acjachemen and Tongva Peoples – are writing in support of Senate Bill 1137 (SB 1137) and setbacks between oil and gas wells and sensitive sites. We are deeply disappointed to see your office's letter to Governor Newsom in defiance of SB 1137[1]. This position undermines critical health and safety protection zones for your constituents. Furthermore, the City Council did not formally approve this letter.

This stance runs contrary to well-established science and fails to accurately represent the voices of the Long Beach community. We encourage you to retract your statements on SB 1137 and prohibit new oil drilling and rework permits within the 3,200 foot setback zone while we await the results of the referendum. Furthermore, we encourage your office to identify alternative sources of revenue to cover the cost of cleaning up oil wells and ensure a just transition for impacted workers.

---

[1] https://www.longbeach.gov/globalassets/city-manager/media-library/documents/government-affairs/position-letters---state/2021-2022/letter-to-governor-newsom-expressing-concerns-for-senate-bill-1137--gonzalez-and-limon-oil-and-gas.

The Referendum Process Undermines Democracy and Allows the Industry to Buy Their Way out of Regulation

As you know, last September the state legislature passed SB 1137, a historic and long overdue bill that prohibits new oil drilling within 3,200 feet of homes, schools, hospitals and other sensitive sites.

The oil industry spent over 20 million dollars to overturn this law with a referendum which will go to the ballot in 2024, delaying these long overdue health protections. Throughout the state, there have been numerous documented accounts of petitioners misleading voters while collecting signatures for the referendum.[2] In fact, the LA Times reported canvassers fabricating misinformation to voters that the referendum would ban new oil drilling within setbacks.[3]

Thousands of Residents in Long Beach Live Too Close to Oil Drilling Operations

Neighborhood oil drilling exposes Long Beach residents to toxic chemicals and smog-forming gasses, which can cause **respiratory illness, cardiovascular disease, leukemia, lymphoma, lung cancer, nervous system damage, reproductive and endocrine disruption, birth defects, and premature death.** Neighbors adjacent to urban oil drilling suffer the most from these health effects. Even once a well is no longer active, it can continue to leak oil, methane, and other gasses, leaving nearby communities at continued risk.

An estimated 140,138 Long Beach residents live within 3,200 feet of an operational oil and gas well within the city limits. This amounts to about 30.2% of the population. Of those, 101,498 (72.4%) are people of color.

Communities of color and low-income households are most affected by neighborhood oil drilling. Many neighborhoods with urban oil drilling operations are currently exposed to other environmental hazards and pollution, such as heavy transportation corridors and port operations.

The stance on setbacks as currently set by your office is allowing for the expansion of an already catastrophic public health crisis. And as evidenced by these organizations who have signed on, it does not represent the stance of the people you represent.

---

[2] https://www.kvpr.org/local-news/2022-12-30/why-an-oil-industrys-signature-gathering-effort-is-seen-as-misleading

[3] https://www.latimes.com/opinion/story/2023-02-07/oil-drilling-referendum-qualified

Instead of using city resources fighting these overdue health and safety protections, we urge you to use your time and resources to identify alternative revenue sources to fund oil well clean up and work with impacted workers and community members to enable a just transition.

Thank you for considering our comments.

Signed,

Nicole Levin - Campaigner, Sierra Club Dirty Fuels
Nancy Woo - Hub Coordinator, Sunrise Long Beach
Brady Bradshaw - Campaigner, Center for Biological Diversity
Tina Calderon - Director, Sacred Grounds ™
Jeannine Pearce - CEO, Fierce Courage
Jeannine Pearce - Convener, The Climate Council
Charles Miller - Chair, Los Angeles Climate Reality Project
Jan Victor Andasan - Community Organizer, East Yard Communities for Environmental Justice
Bill Sive - West Coast Coordinator, Queers 4 Climate
Karen Reside - Executive Director, Long Beach Grey Panthers
Ellie Cohen - Executive Director, The Climate Center
Maro Kakoussian - Climate Justice Organizing Manager, Physicians for Social Responsibility
Kobi Naseck - Coalition Coordinator, Voices in Solidarity Against Oil in Neighborhoods (VISIÓN)
Paulina Torres- Staff Attorney, Natural Resources Defense Council

ResearchGate

See discussions, stats, and author profiles for this publication at: https://www.researchgate.net/publication/357602225

Prior exposure to weathered oil influences foraging of an ecologically important saltmarsh resident fish

Article *in* PeerJ · January 2022

DOI: 10.7717/peerj.12593

CITATION
1

READS
29

4 authors:

Ashley M. McDonald
University of Florida
25 PUBLICATIONS **126** CITATIONS

SEE PROFILE

Charles W. Martin
University of Florida
76 PUBLICATIONS **996** CITATIONS

SEE PROFILE

Guillaume Rieucau
Louisiana Universities Marine Consortium
70 PUBLICATIONS **1,105** CITATIONS

SEE PROFILE

Brian Roberts
Louisiana Universities Marine Consortium
69 PUBLICATIONS **1,744** CITATIONS

SEE PROFILE

Some of the authors of this publication are also working on these related projects:

Project Saltmarsh vegetation dynamics of high disturbance area, Point aux Pins, AL View project

Project Salinity effects on Thalassia testudinum and Halodule wrightii ion ratios View project

All content following this page was uploaded by Brian Roberts on 05 January 2022.

The user has requested enhancement of the downloaded file.

Prior exposure to weathered oil influences foraging of an ecologically important saltmarsh resident fish

Ashley M. McDonald[1], Charles W. Martin[1], Guillaume Rieucau[2] and Brian J. Roberts[2]

[1] UF|IFAS Nature Coast Biological Station, University of Florida, Cedar Key, Florida, United States
[2] Louisiana Universities Marine Consortium, Chauvin, Louisiana, United States

ABSTRACT

Estuarine ecosystem balance typically relies on strong food web interconnectedness dependent on a relatively low number of resident taxa, presenting a potential ecological vulnerability to extreme ecosystem disturbances. Following the *Deepwater Horizon* (DwH) oil spill disaster of the northern Gulf of Mexico (USA), numerous ecotoxicological studies showed severe species-level impacts of oil exposure on estuarine fish and invertebrates, yet post-spill surveys found little evidence for severe impacts to coastal populations, communities, or food webs. The acknowledgement that several confounding factors may have limited researchers' abilities to detect negative ecosystem-level impacts following the DwH spill drives the need for direct testing of weathered oil exposure effects on estuarine residents with high trophic connectivity. Here, we describe an experiment that examined the influence of previous exposure to four weathered oil concentrations (control: 0.0 L oil m^{-2}; low: 0.1 L oil m^{-2}; moderate: 0.5–1 L oil m^{-2}; high: 3.0 L oil m^{-2}) on foraging rates of the ecologically important Gulf killifish (*Fundulus grandis*). Following exposure in oiled saltmarsh mesocosms, killifish were allowed to forage on grass shrimp (*Palaeomonetes pugio*) for up to 21 h. We found that previous exposure to the high oil treatment reduced killifish foraging rate by ~37% on average, compared with no oil control treatment. Previous exposure to the moderate oil treatment showed highly variable foraging rate responses, while low exposure treatment was similar to unexposed responses. Declining foraging rate responses to previous high weathered oil exposure suggests potential oil spill influence on energy transfer between saltmarsh and off-marsh systems. Additionally, foraging rate variability at the moderate level highlights the large degree of intraspecific variability for this sublethal response and indicates this concentration represents a potential threshold of oil exposure influence on killifish foraging. We also found that consumption of gravid *vs* non-gravid shrimp was not independent of prior oil exposure concentration, as high oil exposure treatment killifish consumed ~3× more gravid shrimp than expected. Our study findings highlight the sublethal effects of prior oil exposure on foraging abilities of ecologically valuable Gulf killifish at realistic oil exposure levels, suggesting that important trophic transfers of energy to off-marsh systems may have been impacted, at least in the short-term, by shoreline oiling at highly localized scales. This study provides support for further experimental testing of oil exposure effects on sublethal behavioral impacts of ecologically important estuarine species, due to the

Submitted 20 April 2021
Accepted 14 November 2021
Published 5 January 2022

Corresponding author
Ashley M. McDonald,
ashley.mcdonald@ufl.edu

Academic editor
Edmond Sanganyado

Additional Information and Declarations can be found on page 13

DOI 10.7717/peerj.12593

Copyright
2022 McDonald et al.

Distributed under
Creative Commons CC-BY 4.0

OPEN ACCESS

How to cite this article McDonald AM, Martin CW, Rieucau G, Roberts BJ. 2022. Prior exposure to weathered oil influences foraging of an ecologically important saltmarsh resident fish. PeerJ 9:e12593 DOI 10.7717/peerj.12593

likelihood that some ecological ramifications of DwH on saltmarshes likely went undetected.

Subjects Animal Behavior, Ecology, Marine Biology, Zoology, Environmental Contamination and Remediation
Keywords Fish behavior, Macondo, Nekton, Feeding effort, Mesocosm

INTRODUCTION

Trophic connectivity is of vital importance to the functionality and resilience of estuarine ecosystems (*Costanza, Kemp & Boynton, 1993*; *Tett et al., 2013*). Greater trophic connections optimize the transfer of primary production to upper trophic levels, increasing food web resilience and maintaining a domain of attraction towards ecosystem stability (*MacArthur, 1955*; *Holling, 1973*). Estuarine ecosystems have unique food webs because of the physiological flexibility that is required for resident species to deal with unpredictable abiotic extremes, combined with the limited geologic lifetimes of estuaries, leading to taxonomic diversity limitations (*Whitfield, 1994*; *Day et al., 1989*). Therefore, trophic interconnectedness between resident and transient species, and thus food web resilience, of estuarine ecosystems can often rely on a relatively small number of mid-trophic level nektonic estuarine residents (*Subrahmanyam & Drake, 1975*).

A supported paradigm of estuarine ecosystems is that they are comprised of relatively resilient biota (*Elliott & Whitfield, 2011*), however severe environmental disturbances may cause disruptions in trophic connectivity (*Matich, Moore & Plumlee, 2020*). This can stem from negative impacts to "critically resilient" species, described as a taxon with generally high perturbation resilience and an important role in the food web (*McCann et al., 2017*). In northern Gulf of Mexico (nGoM) estuarine saltmarshes, Gulf killifish (*Fundulus grandis*, Baird and Girard 1853) are a common, opportunistic saltmarsh resident species (*Able et al., 2015*) with high site fidelity that makes them valuable sentinel species and indicators of habitat disturbance (*Nelson, Sutton & DeVries, 2014*; *Vastano et al., 2017*; *Jensen et al., 2019*). This Cyprinodontiform species is considered highly important to marsh food webs, serving a key function in the "trophic relay" of marsh production to off-marsh open waters *via* predator/prey interactions with larger transient predators (*Rozas & LaSalle, 1990*; *Kneib, 2000*; *McCann et al., 2017*). The saltmarsh habitats of Gulf killifish are characterized by highly dynamic, and often extreme, environmental conditions (*e.g.*, extreme temperatures, wide salinity ranges, tidal exchange, hypoxia, *etc.* (*Vernberg, 1993*)), and are therefore naturally resilient to many interacting stressors, marking Gulf killifish as a "critically resilient" saltmarsh species (*Able et al., 2015*; *Vastano et al., 2017*; *McCann et al., 2017*).

The necessity of understanding how a large-scale disturbance event might disrupt a food web at the critically resilient species level arose with the *Deepwater Horizon* (DwH) oil spill, the largest industrial marine oil spill in American history that impacted nGoM coastlines from Louisiana to Florida (*BP Oil Spill Commission, 2011*). In 2010, at least 2,113 km of shoreline were subjected to oiling after the explosion of an offshore oil drilling

rig on April 20th led to the loss of 11 lives and the corresponding oil well blowout caused the subsequent release of ~4.1 M barrels (~560,000 metric tons) of crude oil into offshore waters (*McNutt et al., 2012*; *Nixon et al., 2016*). As the crude oil drifted into coastal areas, where wetlands accounted for ~53% of oiled shoreline (*Michel et al., 2013*), exposure to the weathered oil caused significant casualties of several critically sensitive species (*sensu McCann et al., 2017*) at low and high trophic levels, such that terrestrial marsh plants, gastropods, predatory birds, and dolphins experienced high levels of mortality. Alternatively, many coastal fish populations and community structures have shown resilience to, or rapid recovery from, the large-scale exposure to weathered oil (*Moody, Cebrian & Heck, 2013*; *Fodrie et al., 2014*; *Able et al., 2015*; *Schaefer, Frazier & Barr, 2016*; *Martin et al., 2020a*). A decade later, potential trophic implications from this marine disaster are still unclear, despite extensive analyses of community-wide data, with interpretation of oil spill effects on populations of estuarine and marine species further complicated by possible trophic release (*e.g.*, stark decline of mammal and bird predators), engineered efforts to protect shorelines from oil intrusion (*e.g.*, boom deployment and increased freshwater discharge), and the extensive temporary closure of Gulf of Mexico fisheries operations (*Upton, 2011*; *Fodrie et al., 2014*; *McCann et al., 2017*). Large gaps in understanding possible trophic repercussions of a marsh community to oil spill effects are therefore bolstered by experimental manipulations not constrained by the unethical re-creation of oiled field conditions, but are instead replicated in a hyper-realistic, controlled mesocosm environment.

Here, we describe the results of a foraging experiment carried out to test the hypothesis that prior oil exposure negatively affects natural predatory feeding rates of Gulf killifish, a dominant and ecologically important marsh resident (*Able et al., 2015*). Classic foraging experiments examining saltmarsh predator-prey interactions have used killifish (*Fundulus* sp.) and grass shrimp (*Palaeomonetes pugio*) as study species because of their abundance and trophic importance in Atlantic and Gulf coastal marshes (*Heck & Thoman, 1981*; *Kneib, 1987*; *Kneib, 1988*), and because grass shrimp are a common prey item for Gulf killifish of the size range used in this experiment (*Harrington & Harrington, 1961*). We therefore examined foraging rates of Gulf killifish on unexposed grass shrimp prey, following exposure to varying real-world DwH concentrations of weathered oil in large marsh mesocosms, to assess previous oil exposure impacts explicitly due to exposure of this important saltmarsh resident predator. We tested the hypothesis that foraging rate would decline concomitantly with increased levels of exposure concentration. This investigation was inspired by field reports of little evidence for Gulf killifish population-level effect following nGoM saltmarsh oiling (*Able et al., 2015*), despite strong negative individual-level physiological and developmental impacts from oil exposure (*Garcia et al., 2012*; *Whitehead et al., 2012*; *Dubansky et al., 2013*; *Crowe et al., 2014*; *Fodrie et al., 2014*). Ecotoxicological studies on fish have shown strong evidence that shifts in feeding behavior by sublethal exposure to toxic contaminants may impact community structure or trophic transfer caused in part by decreased motivation to feed, impaired feeding abilities, and decreased prey detection (*Atchison, Henry & Sandheinrich, 1987*; *Little et al., 1990*; *Weis et al., 2001*; *Fleeger, 2020*). Decreased Gulf killifish foraging rates

related to any previous sublethal oil exposure would provide further evidence that this type of environmental disturbance could influence nearshore food web connectivity.

MATERIALS AND METHODS

Oiled mesocosms and killifish exposure

During August/September 2019, an ongoing experimentally oiled marsh mesocosm experiment was being conducted at Louisiana Universities Marine Consortium (LUMCON) in Cocodrie, LA (29.254573°, −90.664031°). These oiled mesocosms were used to expose Gulf killifish for 10-15 days, a duration based on previous studies of site fidelity for *F. grandis* (*Nelson, Sutton & DeVries, 2014*; *Jensen et al., 2019*). Twelve hydrologically-independent, outdoor mesocosms (3.05 m diameter, 1.83 m height) were paired each with its own tidal surge tank that generates daily tidal cycles with range of 25 cm (flooding marsh ~10 cm at high tide) *via* a water control system of blowers and airlifts (*Alt, 2019*). Intact *Spartina alterniflora* saltmarsh plugs (30 cm diameter × 50 cm depth) at natural densities were collected from previously unoiled natural saltmarshes near the LUMCON mesocosm facility, planted in the mesocosms, and allowed to establish for approximately 18 months prior to oiling (*Roberts et al., 2019*; *Roberts et al., 2020*). During flooded marsh conditions (~40% of the time), Gulf killifish had access to ~7.3 m^2 of marsh platform (~10 cm at high tide) to allow for natural foraging opportunities, and adjacent deeper water (~40 cm at high tide) in the empty circular trough surrounding the saltmarsh platform. At low tide, Gulf killifish were restricted to the ~1.4 m^2 of area in the trough perimeter, with minimum water depths of 15 cm at low tide. Additional details on the saltmarsh mesocosm setup and design can be found in Fig. S1.

Oil used in mesocosm exposure periods was Light Louisiana Sweet (LLS) blended crude oil at API Gravity 40.1, similar to the oil released by the DwH spill, acquired from Placid Refining Company LLC in May 2018. The oil was then evaporatively weathered using a nitrogen gas sparging system over 150 days to obtain a loss of 30% of volatile components, as measured by gas chromatography, to attain chemical composition similar to that of weathered oil that washed ashore following DwH (*Passow & Overton, 2021*). Four exposure levels were randomly assigned to three replicate mesocosms in a randomized block design for a total of 12 experimental mesocosm units. Weathered oil exposure levels scaled roughly to Shoreline Cleanup and Assessment Team (SCAT) categories observed in Louisiana marshes following the DwH disaster (*Michel et al., 2013*; *Lin et al., 2016*): control/no oil at 0.0 L oil m^{-2}, low at 0.1 L oil m^{-2}, moderate at 0.5–1 L oil m^{-2}, and high at 3.0 L oil m^{-2}. For the oiled treatment mesocosms, a single application of weathered oil was applied to the saturated sediment surface under high tide conditions at uniformly spaced locations on July 8, 2019. After initial weathered oil application, oil was further naturally weathered in the open air of mesocosms 45 to 60 days prior to experiment initiation.

During the killifish exposure period, following 45 to 60 additional days of open-air oil weathering, the mean ± standard error surface soil (0-5 cm) total petroleum hydrocarbon (TPH) concentrations in the high oil treatments (419 ± 24 mg/g soil) were ~10 and ~40 times higher than in the moderate (39 ± 5 mg/g soil) and low (10 ± 0.4 mg/g soil) oil treatments (mean of 19 August and 9 September samplings; as previously described in

Martin et al., 2020b, and collected by E. Overton and B. J. Roberts, 2020). These concentrations are similar to those found in Louisiana saltmarsh field conditions following the DwH oil spill (Lin et al., 2016). Gulf killifish were collected from the nearby saltmarsh using baited minnow traps and held for 2–4 days in the same 450 liter, aerated aquarium with a constant salinity of 7 psu (equivalent to mesocosms at the time of collection) to minimize mortality due to handling. Then, 12 adult fish were added to each saltmarsh mesocosm on 22 August 2019, with six more Gulf killifish added to each mesocosm on 27 August to increase the number of fish available for the foraging behavior experiment after some mortality was observed after 5 days of holding in mesocosms. Total fish mortality during the exposure period resulted in no mortality in control treatments, 38% in low exposure treatments, 56.6% in medium exposure treatments, and 81.5% in high exposure treatments, however the causes of mortality were not determined and possibly arose from direct and indirect effects from oil exposure (see Martin et al., 2020b for further detail on fish additions). All surviving fish used in the subsequent foraging experiment (three to six fish per mesocosm) were within the size range of 57 to 105 mm (mean of lengths 79.4 + 1.8 mm standard error). Fish were exposed to oiled or control treatments for 10 (27 August additions) to 15 (22 August additions) days prior to behavioral experiments. Following the exposure period, fish were recaptured with dipnets and kept separated according to mesocosm assignment then held without food for 24 h at ambient room temperature conditions in aerated 37.9 L aquaria containing unoiled 7 psu filtered seawater prior to use in the foraging experiment performed at the LUMCON facility.

Foraging experiment

Gulf killifish foraging behavior response to previous oil exposure was examined over a one-day period. Foraging trials were conducted at the LUMCON facility in separate 19 L white plastic buckets filled with 10 L of filtered water with a salinity of 7 psu. Twenty grass shrimp (*Palaemonetes pugio*), captured by dipnet from the nearby bayou were added to each bucket and allowed to acclimate for 2 h prior to the start of the experiment. Shrimp densities were selected to represent natural field densities relative to the size of the experimental unit (~67 shrimp per m^2). As shrimp were added, we noted the number of gravid shrimp in each bucket as a potential foraging covariate due to the possibility that gravid shrimp may be more visually/olfactorily detectable or less capable of escape, making them more easily predated by impaired killifish (Welsh, 1975). However, we did not control for the same proportion of gravid to non-gravid across replicates. To better simulate the low marsh habitat structure where killifish forage most effectively (Vince et al., 1976), ten 18 cm length black needlerush (*Juncus roemerianus*) stems were added to each bucket in a haphazard fashion.

To initiate the experiment, killifish were transferred from the 37.9 L holding aquaria to 19 L buckets containing the grass shrimp that had been randomly assigned a killifish oil exposure or autogenic control treatment. Killifish from the same oiled mesocosm treatment were randomly paired by drawing numbers without replacement, and the two fish placed into one of nine replicates for control, low, or moderate treatment buckets but

only five replicates for high treatment buckets, which precluded equivalent replication for all treatments tested in the foraging experiment. No further criteria were used to select killifish inclusion in the experiment. An additional four autogenic control buckets contained only grass shrimp with no killifish addition for a total of 36 buckets arranged in a 6 × 6 grid with rows spaced 1 m apart. Every 4 h during the experiment we monitored factors that would affect foraging rates, specifically mortality of killifish and complete predation of all shrimp provided to a replicate. To minimize investigator influence on foraging, inspections consisted of identifying shrimp and killifish movement from a distance of 0.5 m, and randomization of experimental treatments within the grid array ensured that any observer influence was not grouped. Water temperatures ranged from 26.8–28.6 °C during trials (comparable to mesocosm conditions at time of collection) and dissolved oxygen remained near 100% saturation, determined by measurements at beginning and end of trial. At 21 h, all killifish were removed from the buckets and remaining gravid and nongravid shrimp were counted and these values deducted from gravid and nongravid shrimp counts taken at the beginning of the experiment. To calculate shrimp consumption rate per fish per minute (shrimp consumed $fish^{-1}$ min^{-1}), the number of shrimp consumed within each bucket was divided by the sum of foraging minutes for both fish in that bucket. If fish mortality or complete predation was noticed during routine checks, the reduced foraging time for that fish or bucket was noted and values adjusted accordingly. Mortality was recorded during the foraging experiment, with the following losses per oil exposure treatment: control-one, low-none, medium-four (two from the same bucket), and high-one. These losses corresponded to ~6% mortality in the control treatment, 0% mortality in low oil exposure treatment, ~22% mortality in medium oil exposure treatment, and 10% mortality in high oil exposure treatment. All experimental units were included in subsequent analyses.

STATISTICAL ANALYSES

Due to the unbalanced sample sizes (n = 9 for control, low, moderate prior oil exposure and n = 5 for high prior oil exposure) and heteroscedasticity of experimental results, a Welch's ANOVA was used to compare Gulf killifish foraging rates among weathered crude oil exposure treatments and a Games-Howell test was used for *post hoc* contrasts (*Moder, 2010*). A linear regression with combined fish lengths per replicate and foraging rate was used to determine whether killifish length should be included as a potential covariate with oil exposure treatment. To test the hypothesis that gravid grass shrimp consumption was independent of prior oil exposure concentrations, we constructed a chi square table on expected and observed gravid shrimp consumption. For this analysis, we excluded any buckets where the 20 shrimp provided for foraging during the experiment did not include gravid individuals (excluded one control, three moderate, and one high oil exposure treatment replicates). To estimate how many gravid shrimp we would expect to be eaten with the assumption killifish had no preference, we multiplied the proportion of gravid shrimp given to a treatment by the total number of shrimp eaten, noting that both values excluded nongravid shrimp counts from buckets that did not receive gravid shrimp. For example, if 10% of shrimp provided to a treatment were gravid and 50 shrimp were

consumed by that treatment group, our expected value for that treatment would be five gravid shrimp consumed. Analyses were performed in RStudio (Version 1.2.1335) and the accepted α was set at 0.05 for the Welch's ANOVA, Games-Howell contrasts, linear regression, and chi square test.

Vertebrate study animal ethics statement

Gulf killifish were collected from marsh sites adjacent to the LUMCON facility in Chauvin, LA. All field collections were made under Louisiana Department of Wildlife and Fisheries Scientific Collecting Permit #SCP 200. The use of vertebrate organisms was conducted with IACUC approval and staff training from University of Florida under protocol 201710044. Fish were held in 3.05 m diameter simulated marsh mesocosms during the weathered oil exposure period, where they were allowed to freely forage under simulated natural bayou conditions. As the goal of the study was to measure sublethal effects of oil on fish behavior, humane endpoints were not used and were not possible during the 10–15 day exposure, as fish were released into turbid mesocosms and unable to be monitored. Moreover, analgesics and anesthetics were not used because of the alterations to behavior that we sought to quantify. During the one-day experiment, fish were held in 19 L plastic buckets filled with 10 L of filtered water with salinity of 7 psu. At the end of the experiment, surviving fish were euthanized humanely using the standard methodology for finfish as outlined in IACUC protocol 201710044-namely, through cold shock immersion in ice slurry followed by immersion in 500 mg/L MS-222 (buffered tricaine methane sulfonate) for 10 min after opercular movement stops.

RESULTS

Shrimp consumption ranged from 18% of shrimp offered to high exposure killifish to 48% of shrimp offered to unexposed control killifish, with low and moderate exposure killifish exhibiting slightly lower overall consumption than control killifish (46% and 42%, respectively). Foraging rates (shrimp consumed fish^{-1} min^{-1}) varied across oil exposure treatments ($Fs_{3,12.9} = 8.2$, $p = 0.0026$), such that rates for killifish from high oil exposure treatments were lower than for killifish from the low and control treatments (Fig. 1 and Table 1). Although average foraging rates of moderate oil exposure killifish were between the averages for low and high exposure treatments, moderate treatment rates showed substantial within-treatment variability (Table 1) that included the two highest foraging rates of the experiment (0.01 and 0.007 shrimp consumed fish^{-1} min^{-1}) as well as four measurements of low rates (ranges between 0.001–0.002 shrimp consumed fish^{-1} min^{-1}) comparable only with high exposure treatment fish (all rates ranged from 0–0.002 shrimp consumed fish^{-1} min^{-1}). No relationship was found between combined fish length per replicate and foraging rate (linear regression: Adj. $r^2 = 0.002$, $F_{1,30} = 1.07$, $p = 0.31$), therefore fish length was not considered as a potential covariate.

Previous exposure to the high oil concentration influenced preference for gravid over non-gravid shrimp, such that high exposure fish consumed a substantially larger proportion of gravid shrimp (0.5) than moderate, low, and control treatment killifish (0.24, 0.12, and 0.24, respectively). This observed proportion of gravid shrimp consumed in high

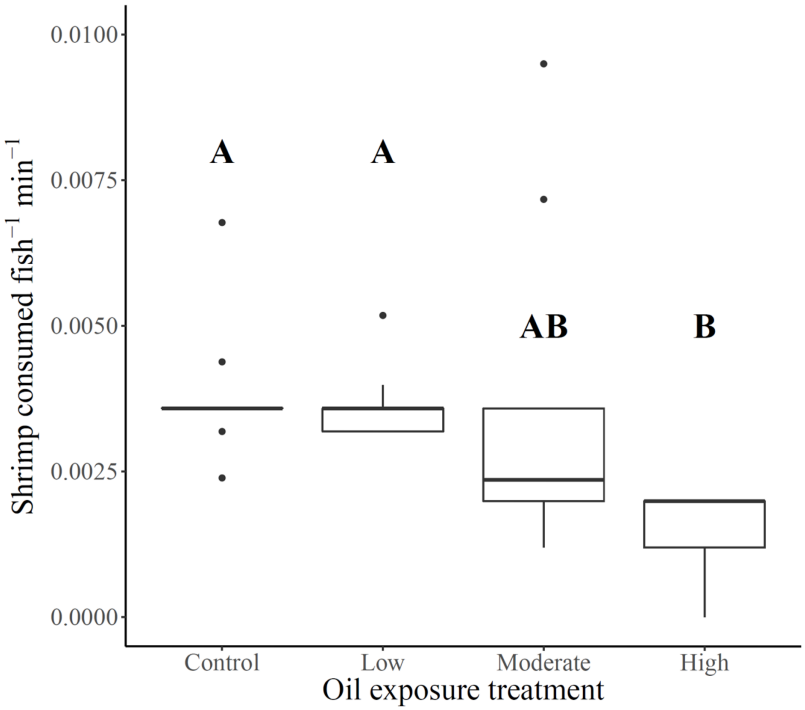

Figure 1 Gulf killifish foraging rates per replicate for each prior oil exposure treatment. Gulf killifish foraging rates (number of shrimp consumed fish^{-1} min^{-1}) per bucket replicate for each prior oil exposure treatment. Solid lines in boxes represent treatment medians and dots are outliers. Different letters indicate treatment differences based on results from Games-Howell post-hoc contrast.

Full-size DOI: 10.7717/peerj.12593/fig-1

Table 1 Basic statistics for Gulf killifish foraging rates at prior oil exposure treatment concentrations.

Oil addition treatment	*N*	Experiment mortality (number of fish)	Mean foraging rate per bucket (shrimp min^{-1})	Standard deviation	Coefficient of variation
Control (0.0 L m^{-2})	9	1	0.003851	0.00121	31.4
Low (0.1 L m^{-2})	9	0	0.00363	0.00064	17.6
Medium (0.5–1.0 L m^{-2})	9	4	0.00359	0.00283	78.8
High (3.0 L m^{-2})	5	1	0.001434	0.00087	60.7

oil treatment fish deviated from the expected high exposure consumption proportion of 0.19 (χ^2 = 10.1, df = 3, p = 0.017; Fig. 2 and Table 2).

DISCUSSION

Our study provides evidence that prior exposure to real-world concentrations of weathered oil (*Lin et al., 2016*) influences foraging of estuarine saltmarsh resident Gulf killifish. Our results reveal a substantial reduction of killifish foraging rates at high oil exposure concentration, a highly variable effect in the moderate concentration, and an absence of effect in the low concentration exposure. Our finding that low and moderate concentration exposures did not substantially influence foraging rate is counter to prior experimental

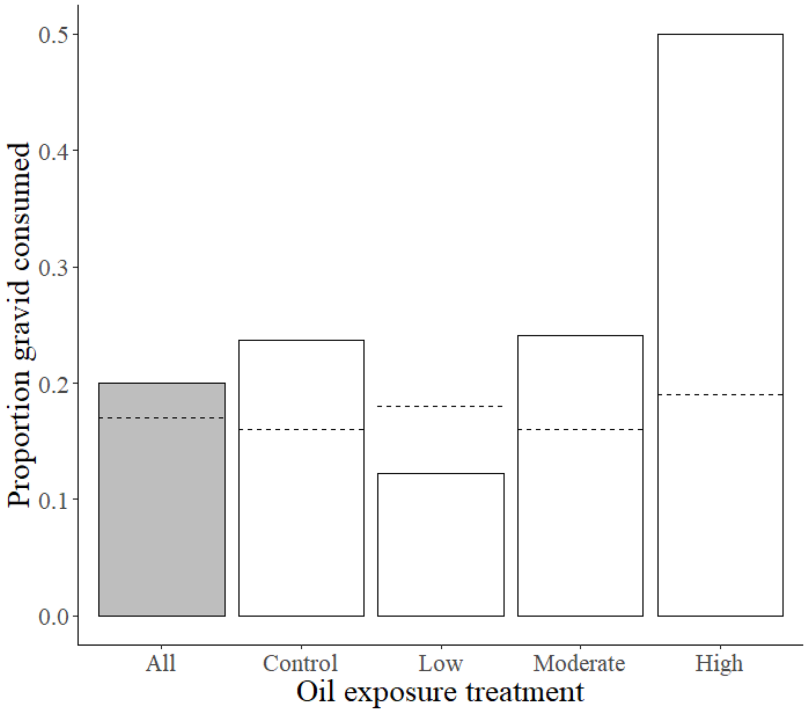

Figure 2 Proportions of gravid shrimp consumption by Gulf killifish. Proportions of observed values of gravid shrimp consumed (out of total shrimp consumed) by Gulf killifish for the entire experiment (grey bar) and at different treatment levels of prior oil exposure, with the calculated expected proportion values represented by dotted lines. Full-size DOI: 10.7717/peerj.12593/fig-2

Table 2 Values to calculate expected *vs* observed outcomes of gravid shrimp consumption for construction of chi square table.

Oil addition treatment	Total shrimp consumed	Proportion of gravid	Expected gravid consumed	Observed gravid consumed
Control (0.0 L m^{-2})	76	0.16	11.8	18
Low (0.1 L m^{-2})	82	0.18	14.8	10
Medium (0.5–1.0 L m^{-2})	29	0.16	4.7	7
High (3.0 L m^{-2})	8	0.19	1.5	4

evidence for killifish behavioral changes at even the lowest previous oil exposure concentration (*Martin et al., 2020b*), and strongly suggest that a threshold of sublethal effects on foraging, and possibly individual-level response plasticity (*Saaristo et al., 2018*), is evident around the crude oil concentrations in the moderate exposure treatment. Our experimental design to test the influence of prior oil exposure on foraging rates was challenged by a reduction in sample sizes caused by mortality of subjects during the exposure period, particularly in the high exposure treatment. However, the foraging behavior responses of surviving killifish from high oil concentration mesocosms were consistently affected by this exposure, providing strong evidence that these sublethal effects are genuine. We also found evidence that fish from the high exposure treatment consumed gravid grass shrimp in a higher proportion than expected, while fish from all other treatments did not exhibit this selectivity, novel evidence of a contamination

exposure-related shift in killifish predatory behavior with potential for ecological repercussions (see *Saaristo et al., 2018* Table S2 for compilation of studies on contaminant effects on predator-prey interactions). These findings indicate prior oil exposure can influence killifish foraging rates and may drive a behavioral shift in prey selection, at least on the spatial and temporal scales used in this study. Despite little field-based evidence of large-scale negative community impacts (*Fodrie et al., 2014*; *Martin et al., 2020a*), the consistent evidence of negative physiological, genomic, and developmental effects on nekton from oil exposure strongly suggests there are key gaps in our understanding of coastal trophic processes that were likely disrupted in part by sublethal effects on nearshore nekton behavior. Our study findings support this inference, as high oil exposure substantially affected Gulf killifish foraging behavior, and moderate oil exposure highlighted the high degree of intraspecific variability for sublethal responses to oil at the thresholds tested.

High inter-individual variability in the moderate treatment foraging rates reveals the potential presence of phenotypic plasticity within this subsample of a local killifish population in response to moderate levels of contamination, a vital feature for enabling species to cope with rapid environmental change (*Chevin, Lande & Mace, 2010*). Yet despite the exceptionally high foraging rates of some individuals, the overall average foraging rate for this treatment was still lower than control and low concentration treatments, suggesting population-level effects on foraging rates at this concentration may have occurred despite high individual-level plasticity. A potential behavioral shift influence on intra-population dynamics relates to our findings that high oil concentration exposure fish selected gravid shrimp at higher proportions than expected if shrimp selection were independent of prior oil exposure. We speculate that this observation could be related to an impairment in prey detection (*Cave & Kajiura, 2018*), as gravid grass shrimp are more visually apparent than non-gravid grass shrimp. Secondly, gravid selection may relate to killifish mobility impairment (*Stieglitz et al., 2016*), as killifish are active predators and gravid grass shrimp may have reduced escape capabilities since swimmerets are occupied with egg masses. However, evidence of the relationship between prior high oil exposure and increased killifish selection of gravid grass shrimp presented here is a preliminary finding due to the limited scale of our foraging experiment design, the potential size difference between gravid and male shrimp (*Alon & Stancyk, 1982*), and the fact that we only exposed the predatory killifish, and not the prey species, to weathered oil.

The reduced predation success of Gulf killifish previously exposed to high concentration of weathered oil measured in this study reflects findings of reduced growth and predation of an Atlantic congeneric, mummichog (*Fundulus heteroclitus*), inhabiting contaminated estuaries (*Weis et al., 2001*). Killifish from contaminated estuaries were found to rely primarily on low nutritional value detrital material for forage, as opposed to higher calorie prey items that constitute a greater dietary proportion in fish from an uncontaminated site (*Weis & Khan, 1991*). Previous foraging experiments suggested contaminated site fish generally could not capture evasive grass shrimp prey, and maintained low activity levels (*Smith et al., 1995*). Grass shrimp are highly abundant and productive estuarine saltmarsh residents (*Nixon & Oviatt, 1973*) that effectively transfer detritus into higher saltmarsh

trophic levels, particularly large killifish, through predator-prey interactions (*Nixon & Oviatt, 1973*; *Welsh, 1975*). The sublethal effect of prior exposure to high concentrations of oil on foraging rates may result in a similar influence on the killifish foraging guild as found in contaminated estuaries (*Weis et al., 2011*). Namely, a depression of predatory foraging wherein killifish diets become dominated by detritus rather than energetically superior grass shrimp which drives a declining efficiency in the transfer of saltmarsh-originated energy to off-marsh systems.

Although our study was not designed to investigate the physiological or genomic impairments that may have caused changes in Gulf killifish foraging behavior due to short term oil exposure, evidence from previous oil and fossil fuel toxicity-related studies on fish suggest numerous physiological impairments that can impact foraging abilities (*Gregg, Fleeger & Carman, 1997*; *Stieglitz et al., 2016*; *Cave & Kajiura, 2018*; *Schlenker et al., 2019*). Field studies that examined adult Gulf killifish genome expression during the oil spill aftermath (*Whitehead et al., 2012*; *Dubansky et al., 2013*) found evidence for damage of gill tissues, an organ that is vital to many functions necessary for physiological resilience of an estuary resident organism. The ecotoxicological effects from exposure to petroleum hydrocarbons can also be compounded by natural abiotic stressors common to estuarine environments, such that energy demands required for fish to compensate for natural stressors are extra costly (*Whitehead, 2013*). Time spent in natural estuarine conditions within various weathered oil exposures of the mesocosms likely impacted energetics budgets of fish used in our experiment, possibly contributing to the pattern of mesocosm mortality and foraging inhibitions during the experiment. Furthermore, evidence of oil ingestion in Gulf killifish four to 5 months after the cessation of the oil spill (*Dubansky et al., 2017*) is a potential pathway for the extended oil exposure influence on these fish linked to their preference for benthic-associated forage (*Rozas & LaSalle, 1990*), as the more viscous weathered oil settles into sediments and remains in the environment longer due to anoxic conditions (*Mendelssohn et al., 2012*).

Despite the noted resilience of this species (*Able et al., 2015*), it is possible that any sublethal impacts driving these behavioral shifts on trophic transfer or food web resilience were highly localized and thus went undetected. Natural avoidance behaviors to oil have been recorded in several fish species (*Martin, 2017*) that in the wild may have somewhat alleviated the more extreme foraging inhibition we measured in high oil exposure treatment fish. However, these avoidance behaviors have been found to degrade over sediments contaminated with weathered oil, as opposed to fresh oil (*Martin, 2017*), and upon the fish having prior exposure to weathered oil at even low levels (0.1 L oil m^{-2}), with some evidence of preference for oiled sediments following exposure to high levels (3.0 L oil m^{-2}) (*Martin et al., 2020b*). The various levels of oiling were patchily distributed across nGoM shorelines such that surveys found ~20% of oiled shorelines were heavily oiled, ~13% were moderately oiled, and ~36% were lightly oiled (*Michel et al., 2013*). These surveys further determined ~53% of total oiled shoreline was marsh habitat, and of that, ~96% of oiled marsh habitat was in Louisiana estuarine environments (*Nixon et al., 2016*). The patchy distribution of oil on diverse saltmarsh subhabitats characterized by spatially heterogenous estuarine saltmarsh nekton communities (*Peterson & Turner, 1994*; *Able et al.,*

2015) that tend to exhibit high site fidelity (Nelson, Sutton & DeVries, 2014; Jensen et al., 2019) suggests that if oil exposure negatively impacted Gulf killifish foraging to the degree that it impacted trophic connectivity, this impact would have been highly spatially variable. High intraspecific redundancy of Gulf killifish combined with high individual-level variability in foraging response to oil exposure, such as that measured in our moderate oil treatment, may have worked to lessen oil exposure impacts on this estuarine nekton species' contributions to saltmarsh food web connectivity.

Our study highlights the need for more experimental and mesocosm-based work to aid with further determinations of what additional sublethal impacts likely occurred in the aftermath of the DwH oil spill, and to help predict how toxic stressors may influence trophic processes in these critical coastal habitats. The extreme variability in killifish foraging responses to moderate oiling suggests that thresholds to negative sublethal effects from oil exposure are highly individualized, but perhaps lower thresholds are within this concentration range, at least at the timeframe of exposure of this experiment. This is potentially the result of intraspecific variability in tolerance to the general "narcosis" effect of unspecific baseline toxicity to organic narcotic compounds (Hsieh, Tsai & Chen, 2006), generally considered a reversable process that causes a variety of responses dependent on the exposure timeframe and affecting compound (Heintz, Short & Rice, 1999; Vines et al., 2000). Additional experimentation at this moderate exposure concentration may provide more insight into whether foraging declines in this treatment were, in fact, a reversible response to the narcosis effect or if high foraging rates may reflect individuals with higher tolerance to this effect. While large-scale resilience of nGoM estuarine saltmarshes to oiling is apparent, continued release of buried oil through marsh erosion and re-oiling of marshes following large storm events may redistribute oil or oil residues for decades (Turner et al., 2019). Thus, sublethal nekton responses to oil exposure may continue to influence trophic connectivity and food web resilience at highly localized scales- making the detection of eroding food web resilience extremely difficult. However, the hearty resilience of a common and dominant nGoM estuarine saltmarsh resident with high intraspecific variability up to the moderate levels of oiling tested here suggests that this near-shore ecosystem has some resilience built into the food web, providing some stability despite a major ecotoxicological perturbation.

CONCLUSIONS

To supplement numerous field sampling studies examining oil spill impacts on GoM shoreline habitats, we tested the hypothesis that prior oil exposure influences foraging behavior of Gulf killifish by conducting feeding trials following exposure to varying levels of oil within an ongoing mesocosm experiment. Our experimental results indicate that previous exposure to weathered oil at moderate to high levels can have highly variable to substantially negative impacts on foraging behavior of this critically resilient saltmarsh resident. The high variability at moderate oiling level, as opposed to no effect at control and low levels and negative effect at high level, suggests this concentration represents a threshold of oil exposure influence on Gulf killifish foraging. High exposure treatment fish exhibited more selective predation behavior than other exposure treatments by consuming

a higher proportion of gravid than expected, suggesting sublethal impacts to foraging abilities. Inefficient predation by killifish has been suggested to directly influence size-frequency distributions of grass shrimp (*Bass et al., 2001*), and therefore this preliminary finding warrants further investigations into the potential selective foraging behaviors of Gulf killifish exposed to weathered oil and how these behaviors may impact local population dynamics of both predator and prey species. Although our findings are limited in scope and based on results of one experimental trial, any discovery of potential sublethal oil exposure effects on organismal behavior is inherently vital. Based on these results, we speculate that trophic transfer of energy from the marsh platform to off-marsh and open water systems may have been impacted by weathered oil, albeit heterogeneously across saltmarsh habitat and on a highly localized scale. Further experimental studies examining oil exposure on ecologically valuable species is warranted to better determine behavioral implications from previous and potential future environmental disasters.

ACKNOWLEDGEMENTS

We thank the staff at Louisiana Universities Marine Consortium for the facilities and logistical support needed to conduct this project and carry out this experiment, particularly members of the Roberts lab for their endeavors with the oiled mesocosm initiation and maintenance (Charles Schutte, Ryann Rossi, Ekaterina Bulygina, Stephanie Plaisance, Caitlin Bauer) and members of the Education and Outreach team (Murt Conover, Aaron Bacala, and Tori Lambert) for assistance in killifish collection and holding. We also thank Placid Refining Company with their contributions to this research by their provision of Louisiana Sweet Crude for use in mesocosm oiling efforts. We further thank the three anonymous reviewers that contributed to the success of this manuscript.

ADDITIONAL INFORMATION AND DECLARATIONS

Funding

This research was made possible by a grant from The Gulf of Mexico Research Initiative to the Coastal Waters Consortium. The funders had no role in the design, execution, or analyses of this project. The funders had no role in study design, data collection and analysis, decision to publish, or preparation of the manuscript.

Grant Disclosures

The following grant information was disclosed by the authors:
The Gulf of Mexico Research Initiative to the Coastal Waters Consortium.

Competing Interests

Guillaume Rieucau is an Academic Editor for PeerJ.

Author Contributions

- Ashley M. McDonald conceived and designed the experiments, performed the experiments, analyzed the data, prepared figures and/or tables, authored or reviewed drafts of the paper, and approved the final draft.

- Charles W. Martin conceived and designed the experiments, performed the experiments, authored or reviewed drafts of the paper, and approved the final draft.
- Guillaume Rieucau conceived and designed the experiments, authored or reviewed drafts of the paper, and approved the final draft.
- Brian J. Roberts conceived and designed the experiments, performed the experiments, authored or reviewed drafts of the paper, and approved the final draft.

Animal Ethics

The following information was supplied relating to ethical approvals (*i.e.*, approving body and any reference numbers):

The use of vertebrate organisms was conducted with IACUC approval and staff training from the University of Florida under protocol 201710044.

Field Study Permissions

The following information was supplied relating to field study approvals (*i.e.*, approving body and any reference numbers):

All field collections were made under Louisiana Department of Wildlife and Fisheries Scientific Collecting Permit #SCP 200.

Data Availability

The following information was supplied regarding data availability:

The data are publicly available through the Gulf of Mexico Research Initiative Information & Data Cooperative (GRIIDC):

Martin, C. W., Roberts, B. J., 2020. Laboratory experiments to determine effects of previous exposure to oil on *Fundulus grandis* avoidance behavior. Distributed by: Gulf of Mexico Research Initiative Information and Data Cooperative (GRIIDC), Harte Research Institute, Texas A&M University–*Corpus* Christi. doi 10.7266/n7-3qjh-2f11.

Supplemental Information

Supplemental information for this article can be found online at http://dx.doi.org/10.7717/peerj.12593#supplemental-information.

REFERENCES

Able KW, López-Duarte PC, Fodrie FJ, Jensen OP, Martin CW, Roberts BJ, Valenti J, O'Connor K, Halbert SC. 2015. Fish assemblages in Louisiana salt marshes: effects of the Macondo oil spill. *Estuaries and Coasts* **38(5)**:1385–1398 DOI 10.1007/s12237-014-9890-6.

Alon NC, Stancyk NE. 1982. Variation in life-history patterns of the grass shrimp Palaemonetes pugio in two South Carolina estuarine systems. *Marine Biology* **68**:265–276.

Alt DC. 2019. An airlifted tidal mesocosm for oil degradation studies. D. Phil. Thesis. Louisiana State University Doctoral Dissertations, 4794.

Atchison GJ, Henry MG, Sandheinrich MB. 1987. Effects of metals on fish behavior: a review. *Environmental Biology of Fishes* **18(1)**:11–25 DOI 10.1007/BF00002324.

Bass CS, Bhan S, Smith GM, Weis JS. 2001. Some factors affecting size distribution and density of grass shrimp (*Palaemonetes pugio*) populations in two New Jersey estuaries. *Hydrobiologia* **450**:231–241 DOI 10.1023/A:1017505229481.

BP Oil Spill Commission. 2011. Deep water–the gulf oil disaster and the future of offshore drilling. Report to the President. Washington, D.C.

Cave EJ, Kajiura SM. 2018. Effect of Deepwater Horizon crude oil water accommodated fraction on olfactory function in the atlantic stingray, *Hypanus sabinus*. *Scientific Reports* **8(1)**:1–8 DOI 10.1038/s41598-018-34140-0.

Chevin LM, Lande R, Mace GM. 2010. Adaptation, plasticity, and extinction in a changing environment: towards a predictive theory. *PLOS Biology* **8(4)**:e1000357 DOI 10.1371/journal.pbio.1000357.

Costanza R, Kemp WM, Boynton WR. 1993. Predictability, scale, and biodiversity in coastal and estuarine ecosystems: implications for management. *Ambio* **22**:88–96.

Crowe KM, Newton JC, Kaltenboeck B, Johnson C. 2014. Oxidative stress responses of gulf killifish exposed to hydrocarbons from the Deepwater Horizon oil spill: potential implications for aquatic food resources. *Environmental Toxicology and Chemistry* **33(2)**:370–374 DOI 10.1002/etc.2427.

Day JW, Hall CAS, Kemp WM, Yanez-Arancibia A. 1989. *Estuarine ecology*. New York: Wiley.

Dubansky B, Rice CD, Barrois LF, Galvez F. 2017. Biomarkers of aryl-hydrocarbon receptor activity in gulf killifish (*Fundulus grandis*) from northern Gulf of Mexico marshes following the Deepwater Horizon oil spill. *Archives of Environmental Contamination and Toxicology* **73(1)**:63–75 DOI 10.1007/s00244-017-0417-6.

Dubansky B, Whitehead A, Miller J, Rice CD, Galvez F. 2013. Multi-tissue molecular, genomic, and developmental effects of the Deepwater Horizon oil spill on resident Gulf killifish (*Fundulus grandis*). *Environmental Science Technology* **47**:5074–5082 DOI 10.1021/es400458p.Multi-tissue.

Elliott M, Whitfield AK. 2011. Challenging paradigms in estuarine ecology and management. *Estuarine, Coastal and Shelf Science* **94(4)**:306–314 DOI 10.1016/j.ecss.2011.06.016.

Fleeger JW. 2020. How do indirect effects of contaminants inform ecotoxicology? A review. *Processes* **8(12)**:1–18 DOI 10.3390/pr8121659.

Fodrie FJ, Able KW, Galvez F, Heck KL, Jensen OP, LÓpez-Duarte PC, Martin CW, Turner RE, Whitehead A. 2014. Integrating organismal and population responses of estuarine fishes in Macondo spill research. *BioScience* **64(9)**:778–788 DOI 10.1093/biosci/biu123.

Garcia TI, Shen Y, Crawford D, Oleksiak MF, Whitehead A, Walter RB. 2012. RNA-seq reveals complex genetic response to Deepwater Horizon oil release in *Fundulus grandis*. *BMC Genomics* **13(1)**:1–9 DOI 10.1186/1471-2164-13-474.

Gregg JC, Fleeger JW, Carman KR. 1997. Effects of suspended, diesel-contaminated sediment on feeding rate in the darter goby, *Gobionellus boleosoma* (Teleostei: Gobiidae). *Marine Pollution Bulletin* **34**:269–275 DOI 10.1016/S0025-326X(97)00129-X.

Harrington RW, Harrington ES. 1961. Food selection among fishes invading a high subtropical salt marsh: from onset of flooding through the progress of a mosquito brood. *Ecology* **42**:646–666 DOI 10.2307/1933496.

Heck KL, Thoman TA. 1981. Experiments on predator-prey interactions in vegetated aquatic habitats. *Journal of Experimental Marine Biology and Ecology* **53**:125–134 DOI 10.1016/0022-0981(81)90014-9.

Heintz RA, Short JW, Rice SD. 1999. Sensitivity of fish embryos to weathered crude oil: part II. increased mortality of pink salmon (*Oncorhynchus gorbuscha*) embryos incubating downstream from weathered Exxon Valdez crude oil. *Environmental Toxicology and Chemistry* **18**:494–503 DOI 10.1897/1551-5028(1999)018<0494:SOFETW>2.3.CO;2.

Holling CS. 1973. Resilience and stability of ecological systems. *Annual Review of Ecology and Systematics* **4(1)**:1–23 DOI 10.1146/annurev.es.04.110173.000245.

Hsieh S-H, Tsai K-P, Chen C-Y. 2006. The combined toxic effects of nonpolar narcotic chemicals to *Pseudokirchneriella subcapitata*. *Water Research* **40(10)**:1957–1964 DOI 10.1016/j.watres.2006.03.026.

Jensen OP, Martin CW, Oken KL, Fodrie FJ, López-Duarte PC, Able KW, Roberts BJ. 2019. Simultaneous estimation of dispersal and survival of the gulf killifish *Fundulus grandis* from a batch-tagging experiment. *Marine Ecology Progress Series* **624**:183–194 DOI 10.3354/meps13040.

Kneib RT. 1987. Predation risk and use of intertidal habitats by young fishes and shrimp. *Ecology* **68(2)**:379–386 DOI 10.2307/1939269.

Kneib RT. 1988. Testing for indirect effects of predation in an intertidal soft-bottom community. *Ecology* **69(6)**:1795–1805 DOI 10.2307/1941158.

Kneib RT. 2000. Salt marsh ecoscapes and production transfers by estuarine nekton in the southeastern United States. In: Weinstein M, Kreeger D, eds. *Concepts and Controversies in Tidal Marsh Ecology*. Dordrecht: Kluwer Academic Publishers, 267–291.

Lin Q, Mendelssohn IA, Graham SA, Hou A, Fleeger JW, Deis DR. 2016. Response of salt marshes to oiling from the Deepwater Horizon spill: implications for plant growth, soil surface-erosion, and shoreline stability. *Science of the Total Environment* **557–558(7)**:369–377 DOI 10.1016/j.scitotenv.2016.03.049.

Little EE, Archeski RD, Flerov BA, Kozlovskaya VI. 1990. Behavioral indicators of sublethal toxicity in rainbow trout. *Archives of Environmental Contamination and Toxicology* **19(3)**:380–385 DOI 10.1007/BF01054982.

MacArthur R. 1955. Fluctuations of animal populations and a measure of community stability. *Ecology* **36(3)**:533 DOI 10.2307/1929601.

Martin CW. 2017. Avoidance of oil contaminated sediments by estuarine fishes. *Marine Ecology Progress Series* **576**:125–134 DOI 10.3354/meps12084.

Martin CW, Lewis KA, McDonald AM, Spearman TP, Alford SB, Christian RC, Valentine JF. 2020a. Disturbance-driven changes to northern Gulf of Mexico nekton communities following the Deepwater Horizon oil spill. *Marine Pollution Bulletin* **155(5)**:111098 DOI 10.1016/j.marpolbul.2020.111098.

Martin C, McDonald A, Rieucau G, Roberts B. 2020b. Previous oil exposure alters oil avoidance behavior in a common marsh fish, the Gulf Killifish *Fundulus grandis*. *PeerJ* **8(5)**:e10587 DOI 10.7717/peerj.10587.

Matich P, Moore KB, Plumlee JD. 2020. Effects of Hurricane Harvey on the trophic status of juvenile sport fishes (*Cynoscion nebulosus, Sciaenops ocellatus*) in an estuarine nursery. *Estuaries and Coasts* **43(5)**:997–1012 DOI 10.1007/s12237-020-00723-2.

McCann MJ, Able KW, Christian RR, Fodrie FJ, Jensen OP, Johnson JJ, López-Duarte PC, Martin CW, Olin JA, Polito MJ, Roberts BJ, Ziegler SL. 2017. Key taxa in food web responses to stressors: the Deepwater Horizon oil spill. *Frontiers in Ecology and the Environment* **15(3)**:142–149 DOI 10.1002/fee.1474.

McNutt MK, Camilli R, Crone TJ, Guthrie GD, Hsieh PA, Ryerson TB, Savas O, Shaffer F. 2012. Review of flow rate estimates of the Deepwater Horizon oil spill. *Proceedings of the National Academy of Sciences of the United States of America* **109(50)**:20260–20267 DOI 10.1073/pnas.1112139108.

Mendelssohn IA, Andersen GL, Baltz DM, Caffey RH, Carman KR, Fleeger JW, Joye SB, Lin Q, Maltby E, Overton EB, Rozas LP. 2012. Oil impacts on coastal wetlands: implications for the

Mississippi River delta ecosystem after the Deepwater Horizon oil spill. *BioScience* **62(6)**:562–574 DOI 10.1525/bio.2012.62.6.7.

Michel J, Owens EH, Zengel S, Graham A, Nixon Z, Allard T, Holton W, Reimer PD, Lamarche A, White M, Rutherford N, Childs C, Mauseth G, Challenger G, Taylor E. 2013. Extent and degree of shoreline oiling: Deepwater Horizon oil spill, Gulf of Mexico, USA. *PLOS ONE* **8(6)**:1–9 DOI 10.1371/journal.pone.0065087.

Moder K. 2010. Alternatives to F-Test in one way ANOVA in case of heterogeneity of variances (a simulation study). *Psychological Test and Assessment Modeling* **52(2)**:343–353 DOI 10.1353/abr.2017.0007.

Moody RM, Cebrian J, Heck KL. 2013. Interannual recruitment dynamics for resident and transient marsh species: evidence for a lack of impact by the Macondo oil spill. *PLOS ONE* **8(3)**:1–11 DOI 10.1371/journal.pone.0058376.

Nelson TR, Sutton D, DeVries DR. 2014. Summer movements of the Gulf Killifish (*Fundulus grandis*) in a northern Gulf of Mexico salt marsh. *Estuaries and Coasts* **37(5)**:1295–1300 DOI 10.1007/s12237-013-9762-5.

Nixon SW, Oviatt CA. 1973. Ecology of a New England salt marsh. *Ecological Monographs* **43(4)**:463–498 DOI 10.2307/1942303.

Nixon Z, Zengel S, Baker M, Steinhoff M, Fricano G, Rouhani S, Michel J. 2016. Shoreline oiling from the Deepwater Horizon oil spill. *Marine Pollution Bulletin* **107(1)**:170–178 DOI 10.1016/j.marpolbul.2016.04.003.

Passow U, Overton EB. 2021. The complexity of spills: the fate of the Deepwater Horizon oil. *Annual Reviews* **13**:109–136 DOI 10.1146/annurev-marine-032320-095153.

Peterson GW, Turner RE. 1994. The value of salt marsh edge vs interior as a habitat for fish and decapod crustaceans in a Louisiana tidal marsh. *Estuaries* **17(1)**:235–262 DOI 10.2307/1352573.

Roberts BJ, Rossi R, Schutte CA, Bernhard AE, Giblin AE, Overton EB, Rabalais NN. 2020. Oiling impacts on salt marsh ecosystem processes: insights from a large-scale marsh mesocosm experiment. In: *Gulf of Mexico Oil Spill and Ecosystem Science (GoMOSES) Conference*, Tampa, FL3–6.

Roberts BJ, Schutte CA, Rossi R, Bernhard AE, Giblin AE. 2019. Oiling impacts on salt marsh nitrogen cycling rates: insights from a large-scale marsh mesocosm experiment. In: *Presented at American Geophysical Union (AGU) Fall meeting, Abstract 622092*. 9–13.

Rozas LP, LaSalle MW. 1990. A comparison of the diets of Gulf killifish, *Fundulus grandis* (Baird and Girard), entering and leaving a Mississippi brackish marsh. *Estuaries* **13(3)**:332–336 DOI 10.2307/1351924.

Saaristo M, Brodin T, Balshine S, Bertram MG, Brooks BW, Ehlman SM, McCallum ES, Sih A, Sundin J, Wong BBM, Arnold KE. 2018. Direct and indirect effects of chemical contaminants on the behaviour, ecology and evolution of wildlife. *Proceedings of the Royal Society B: Biological Sciences* **285**:20181297 DOI 10.1098/rspb.2018.1297.

Schaefer J, Frazier N, Barr J. 2016. Dynamics of near-coastal fish assemblages following the Deepwater Horizon oil spill in the northern Gulf of Mexico. *Transactions of the American Fisheries Society* **145(1)**:108–119 DOI 10.1080/00028487.2015.1111253.

Schlenker LS, Welch MJ, Meredith TL, Mager EM, Lari E, Babcock EA, Pyle GG, Munday PL, Grosell M. 2019. Damsels in distress: oil exposure modifies behavior and olfaction in bicolor damselfish (*Stegastes partitus*). *Environmental Science and Technology* **53(18)**:10993–11001 DOI 10.1021/acs.est.9b03915.

Smith GM, Khan AT, Weis JS, Weis P. 1995. Behavior and brain chemistry correlates in mummichogs (*Fundulus heteroclitus*) from polluted and unpolluted environments. *Marine Environmental Research* **39(1–4)**:329–333 DOI 10.1016/0141-1136(94)00070-6.

Stieglitz JD, Mager EM, Hoenig RH, Benetti DD, Grosell M. 2016. Impacts of Deepwater Horizon crude oil exposure on adult mahi-mahi (*Coryphaena hippurus*) swim performance. *Environmental Toxicology and Chemistry* **35(10)**:2613–2622 DOI 10.1002/etc.3436.

Subrahmanyam C, Drake S. 1975. Studies on the animal communities in two North Florida salt marshes Part I. fish communities. *Bulletin of Marine Science* **25**:445–465.

Tett P, Gowen RJ, Painting SJ, Elliott M, Forster R, Mills DK, Bresnan E, Capuzzo E, Fernandes TF, Foden J, Geider RJ, Gilpin LC, Huxham M, McQuatters-Gollop AL, Malcolm SJ, Saux-Picart S, Platt T, Racault MF, Sathyendranath S, Van Der Molen J, Wilkinson M. 2013. Framework for understanding marine ecosystem health. *Marine Ecology Progress Series* **494**:1–27 DOI 10.3354/meps10539.

Turner RE, Rabalais NN, Overton EB, Meyer BM, McClenachan G, Swenson EM, Besonen M, Parsons ML, Zingre J. 2019. Oiling of the continental shelf and coastal marshes over eight years after the 2010 Deepwater Horizon oil spill. *Environmental Pollution* **252(4)**:1367–1376 DOI 10.1016/j.envpol.2019.05.134.

Upton HF. 2011. *The Deepwater Horizon oil spill and the Gulf of Mexico fishing industry*. Washington, D.C.: Congressional Research Service.

Vastano AR, Able KW, Jensen OP, López-Duarte PC, Martin CW, Roberts BJ. 2017. Age validation and seasonal growth patterns of a subtropical marsh fish: the Gulf Killifish, *Fundulus grandis*. *Environmental Biology of Fishes* **100(10)**:1315–1327 DOI 10.1007/s10641-017-0645-7.

Vernberg FJ. 1993. Salt-marsh processes: a review. *Environmental Toxicology and Chemistry* **12(12)**:2167–2195 DOI 10.1002/etc.5620121203.

Vince S, Valiela I, Backus N, Teal JM. 1976. Predation by the salt marsh killifish *Fundulus heteroclitus* (L.) in relation to prey size and habitat structure: consequences for prey distribution and abundance. *Journal of Experimental Marine Biology and Ecology* **23**:255–266 DOI 10.1016/0022-0981(76)90024-1.

Vines C, Robbins T, Griffin FJ, Cherr GN. 2000. The effects of diffusible creosote-derived compounds on development in Pacific herring (*Clupea pallasi*). *Aquatic Toxicology* **51**:225–239 DOI 10.1016/S0166-445X(00)00107-7.

Weis JS, Bergey L, Reichmuth J, Candelmo A. 2011. Living in a contaminated estuary: behavioral changes and ecological consequences for five species. *BioScience* **61**:375–385 DOI 10.1525/bio.2011.61.5.6.

Weis JS, Khan AA. 1991. Notes: reduction in prey capture ability and condition of mummichogs from a polluted habitat. *Transactions of the American Fisheries Society* **120**:127–129 DOI 10.1577/1548-8659(1991)120<0127:NRIPCA>2.3.CO;2.

Weis JS, Smith G, Zhou T, Santiago-Bass C, Weis P. 2001. Effects of contaminants on behavior: biochemical mechanisms and ecological consequences. *BioScience* **51**:209–217 DOI 10.1641/0006-3568(2001)051[0209:EOCOBB]2.0.CO;2.

Welsh BL. 1975. The role of grass shrimp, *Palaemonetes pugio*, in a tidal marsh ecosystem. *Ecology* **56(3)**:513–530 DOI 10.2307/1935488.

Whitehead A. 2013. Interactions between oil-spill pollutants and natural stressors can compound ecotoxicological effects. *Integrative and Comparative Biology* **53(4)**:635–647 DOI 10.1093/icb/ict080.

Whitehead A, Dubansky B, Bodinier C, Garcia T, Miles S, Pilley C, Raghunathan V, Roach JL, Walker N, Walter RB, Rice CD, Galvez F. 2012. Genomic and physiological footprint of the Deepwater Horizon oil spill on resident marsh fishes. *Proceedings of The National Academy of Sciences* **109(50)**:20298–20302 DOI 10.1073/pnas.1118844109.

Whitfield AK. 1994. Fish species diversity in southern African estuarine systems: an evolutionary perspective. *Environmental Biology of Fishes* **40(1)**:37–48 DOI 10.1007/BF00002181.

View publication stats

Marine Structures 23 (2010) 274–287

Contents lists available at ScienceDirect

Marine Structures

journal homepage: www.elsevier.com/locate/marstruc

Statistical characterization of surfaces of corroded steel plates

R.E. Melchers*, M. Ahammed, R. Jeffrey, G. Simundic

Centre for Infrastructure Performance and Reliability, The University of Newcastle, University Drive, Newcastle, NSW 2308, Australia

ARTICLE INFO

Article history:
Received 29 September 2009
Accepted 26 July 2010

Keywords:
Marine
Corrosion
Steel
Plates
Statistics

ABSTRACT

The statistical characteristics of corroded steel plate surfaces exposed to marine environments are of interest for assessing longer term structural safety and integrity using probabilistic methods. This requires information about the variability of corrosion loss and pitting over surfaces. The present paper reports on the observed statistical character of the surfaces of 10 large (1.2 m × 0.8 m × 3 mm thick) steel plates exposed in temperate climate marine immersion, tidal and splash zones for 2.5 years. For the analysis the plates were cut into smaller segments that were mechanically scanned to obtain digitised surface topographies. These were then analysed to estimate the correlation structure and the standard deviation of the surface topography. Considerable differences were found for these and for the mean corrosion loss between different exposure zones. For any one segment the surface topography was found to be highly statistically dependent, implying that smaller coupon sizes can provide adequate estimates of corrosion loss. From this it may be inferred that the deepest pits are not statistically independent as commonly assumed in extreme value statistical representations.

© 2010 Elsevier Ltd. All rights reserved.

1. Introduction

Marine infrastructure, including sheet piling, bridges, jetties, pipelines, off-shore structures and ships as well as nuclear containment systems exposed to saline ground waters, makes very extensive use of structural grade steels. Usually the exposed steel surfaces are protected using one or more of

* Corresponding author. Tel.: +61 2 4921 6044.
E-mail address: rob.melchers@newcastle.edu.au (R.E. Melchers).

0951-8339/$ – see front matter © 2010 Elsevier Ltd. All rights reserved.
doi:10.1016/j.marstruc.2010.07.002

protective coatings (paints), sacrificial coatings (galvanizing) and impressed current or sacrificial cathodic protection. However, there is widespread evidence that such systems are not always effective, particularly over long-term exposures, under less than perfect maintenance regimes and under severe exposure conditions. For this reason it is common practice in the design of steel structures particularly those operating in the marine environment to make some (sacrificial) allowance for future corrosion. Three questions arise from this for engineers (i) for an existing structure how much corrosion can be expected in the future, (ii) for new designs what is a reasonable corrosion allowance, and (iii) what interpretation can be placed on reported corrosion loss results since these invariably have been obtained for small-scale corrosion coupons when in practice much larger constructions are of interest?

There is an extensive corrosion literature but it does not always provide information the type of information required by structural engineers concerned with major physical infrastructure. The corrosion science literature that deals with fundamental understanding of the corrosion process for a variety of metals (and other materials) typically exposed in the laboratory for short-term durations (seconds, hours, sometimes days) under a range of artificial exposure conditions and often under anodic polarization to artificially accelerate the corrosion process. Care must be exercised in translating the results obtained to field conditions.

The second category of corrosion information deals with empirical field exposure studies, with the results often quoted as corrosion rates, giving the misleading impression that corrosion is a linear process in time. For atmospheric corrosion in particular the empirical research literature provides relatively simple nonlinear models often based on curve-fitting to data with little reference back to corrosion science fundamentals. This situation is changing, particularly for corrosion of steels in the immersion, tidal and costal zones [1]. An intensive research program currently is addressing questions (i) and (ii) above for a variety of exposure conditions (immersion, tidal, marine atmospheric) in terms useful for structural engineers. The question of central interest in the present paper is the third – namely the relationship between corrosion loss results and pit depth characteristics for larger steel surfaces compared with results typical for small-scale coupons in conventional empirical corrosion trials.

Only mild or structural steel exposed to marine immersion, tidal and splash conditions is considered in this paper. Field testing is used rather than laboratory experimentation, despite the much better control that can be achieved in the laboratory. The main reason for this is the difficulty in replicating bacterial, biological and marine growth characteristics of real seawater [2]. Increasingly, these are recognized as key components in the corrosion behaviour of steels (and other metals) in seawater.

The next section describes previous relevant investigations of the variation of surface profile of steel strips and plates in the marine immersion and tidal environments. This is followed by a description of the test program on steel plates, the analysis of their surfaces after recovery at various times and the mathematical and statistical characterization of these surfaces. Conclusions about variability of plate surface corrosion are then given. These results are compared to earlier results obtained for small coupons.

2. Previous investigations

Estimates of the rate of 'uniform' corrosion may be obtained most directly from differences in mass-loss measurements, usually converted to a rate of material loss expressed in mm/year or equivalent. For practical applications the mass-loss measurements are obtained for small coupons of steel exposed in-situ, generally over a period of at least one year and sometimes (much) longer, with periodic coupon recoveries for the longer term programs. Size of coupon employed varies widely, from 300 mm square down to 50 $\times$ 100 mm with metal thickness kept small to reduce errors due to high surface energies and hence higher corrosion at the edges. Larger coupons are preferable for greater accuracy in mass loss determinations but practicalities favour smaller coupons. This is particularly the case for coupon recovery of racks of coupons when there is much biofouling since lifting such racks can be a major logistic issue. On the other hand, where water or exposure conditions change quickly smaller coupons may be preferred to capture variability. Conversely, for structures straddling more than one exposure zone only larger coupons or test pieces can capture the corrosion effect of differential aeration such as caused by differences in wetting and oxygen access in the tidal zone [3]. Conventionally only 2 or 3

coupons are exposed for any given time period, although for variability studies multiple coupons must be used. There are international and national Standards describing the processes involved in surface preparation, cleaning, exposure, recovery and cleaning and weighing coupons, including the use of blanks. The conventional wisdom is that data from coupons are essentially the same as that which would be expected from larger steel surfaces. This has been investigated previously for coupons in the immersion zone varying in size from 50 × 100 mm to 100 × 200 mm and 50 × 400 mm and for coupons of different geometries including circles, squares and rectangles [4]. Only negligible differences were found for the effect of shape and of surface area.

For strips of mild steel and for continuous steel sheet piling it has been found that there are distinct vertical corrosion profiles related to the various exposure zones. These are similar to those for electrically connected coupons but all are distinctly different from the results obtained for electrically isolated coupons [5–8] and for shorter isolated strips [9]. These results show that the importance of differential aeration for exposure straddling different corrosion zones. This effect appears not to have been investigated for larger steel surfaces.

The mathematical or statistical analysis of corroded surfaces has had relatively little attention. Yamamoto et al. [10] used a Fast Fourier Transform (FFT) approach to characterize the surfaces of mild steel plates 100 × 100 mm exposed for one year in various marine environments. They found that for these relatively small plates the auto-correlation function, estimated from the FFT results, suggested the average distance between the cathodic and anodic regions. However they made no conclusions about the effect of coupon size. Sumi and Rahbar-Ranji [11] used a two-dimensional discrete spectrum to analyze the effect of the form of the corroded surface on the stress analysis of a steel plate. They applied techniques derived from modelling of surface roughness and contact mechanics [12,13]. These are applied also in the analysis below. A similar approach was used in preliminary results for small steel plates recovered from shipyards [14].

3. Experimental methods

Commercial low carbon mild steel plates 1200 mm × 600 mm × 3 mm thick were exposed in two locations at the NSW Fisheries complex at Taylors Beach, a protected inlet that is part of Nelson Bay on the east coast of Australia about 200 km north of Sydney. The waters at this location are closely similar to Pacific Ocean coastal seawater. Table 1 summarizes the water quality at the site. Five plates were suspended with nylon ropes from a piled rig located mid-estuary at a site previously used for corrosion testing and exposed sufficiently deep to ensure immersion conditions throughout the year. Another 5 plates were suspended vertically under a local timber jetty (Fig. 1). Two holes were drilled in each to enable suspension. Practicalities dictated that all plates were exposed in the 'as received' condition.

Plates were recovered at 6, 12, 18, 24 and 30 months from first immersion. Fig. 2 shows three of the plates suspended from the jetty, at low tide and immediately before recovery after 6 months exposure. Evidently, the rusts at this time give a uniform pattern over the corroded surface. Fig. 3 shows one of

Table 1
Typical water quality at Taylors Beach.

Parameter	Units	Typical value
Ammonia	ppm	0.017–0.080
Nitrate	ppm	0.017–0.050
Nitrite	ppm	< 0.003–0.011
Sulphate	ppm	1600–2750
Total P	ppm	0.003–0.07
Ca	ppm	374–392
Cl	ppm	21,000
Alkalinity	ppm $CaCO_3$	409–419
Salinity	ppt	25.7–31.3
pH		8.1
DO	%	90
Water temperature (annual mean)	°C	20

Fig. 1. Steel plates immediately after being suspended under jetty at Taylors Beach. [SCAN0039a.jpg.

the fully immersed plates immediately after recovery at 12 months exposure. Evidently this plate had tilted from the horizontal as evident from the black area (lower right) corresponding to where the plate had buried into the mud. All plates were washed to remove marine growth and loose rusts before the plates were taken back to the laboratory. Fig. 4 shows the plate in Fig. 3 after washing with a high-pressure hose. This revealed that the majority of the surfaces had a rather regular undulating surface texture. For the plates that were exposed for more than one year, some areas of bright steel surface that began to tarnish almost immediately upon exposure to air were noted.

Fig. 2. Corroded surfaces of steel plates under jetty after 6 months splash and tidal zone exposure showing uniform nature of external rust layer. [SCAN0042a.jpg.

Fig. 3. Plate recovered from mid-estuary at 12 months exposure, showing that it inclined into the mud (at lower right). Note the distinctly different external rusts. [SCAN0044a.

In the laboratory the plates were cleaned initially by electrolysis in a dedicated tank. They were then dried and guillotined into 3 equal strips along the length and into 4 equal pieces along each strip. This gave twelve 300 × 200 mm pieces that could be handled for final cleaning using standard chemical techniques (ASTM G3) [15]. The plates were then weighed. They were stored in a dessicator while awaiting digitization of each side of each plate. Digitization was done using a mechanical 3D scanner (Picza PIX–30) set to a 2 mm square sampling grid. The scanning process was slow (but relatively inexpensive) and it took many months to process all the plate pieces. The digitised scan results were then transferred to a computer for further processing. Fig. 6 shows a typical result with expanded vertical scale (*z*-axis). A contour map of the same piece of plate with 0.5 mm (relative) contours is shown in Fig. 6. In neither case was it possible to fix an absolute origin vertically since the plates had to be propped in the scanner. This also means that the slope of the plate pieces in the × and *y* directions as shown in Figs. 5 and 6 is arbitrary.

Fig. 4. The same plate as in Fig. 3 immediately after washing with high-pressure water. Note the appearance of some bright metal in the region of the transition zones between mud and tidal and tidal and splash zones. [SCAN0045a.

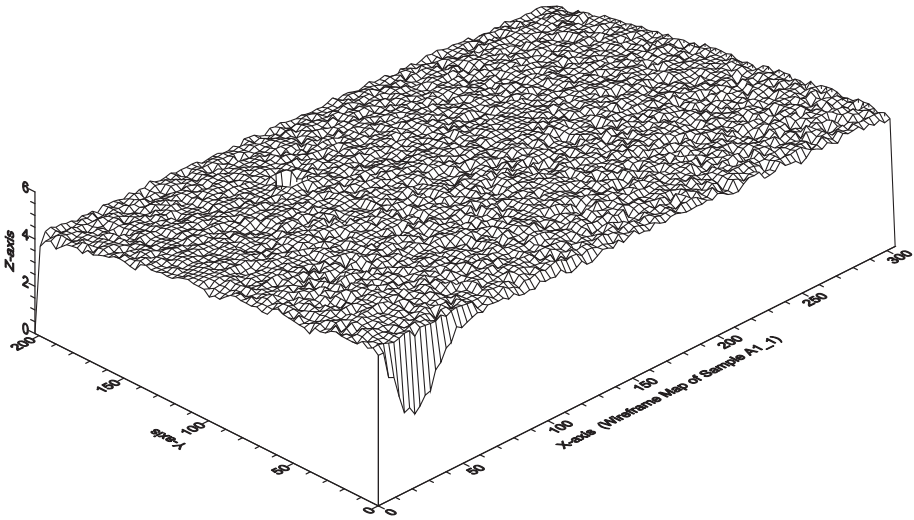

Fig. 5. Wire frame map of the surface geometry of part of plate A, exposed in the splash zone for 6 months. The sample shown was at the top left corner of the plate. Note the fixing hole at top left.

Because of the difficulty in orienting the plate pieces in an absolute orientation for digitization, the loss of plate thickness and hence an estimate for 'uniform' corrosion loss, was obtained by weighing each plate piece and subtracting from this the initial mass estimated from the original plate size and original thickness and steel density. The results, grouped into the splash, tidal and immersion zones, are shown in Fig. 7.

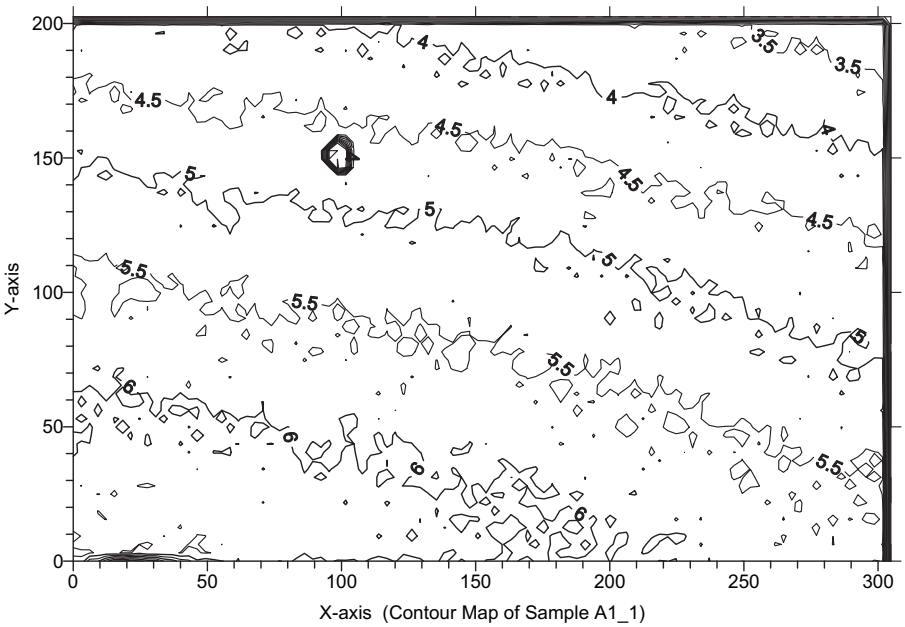

Fig. 6. Relative contours at 0.5 mm interval of the surface shown in Fig. 5. Note the fixing hole at top left.

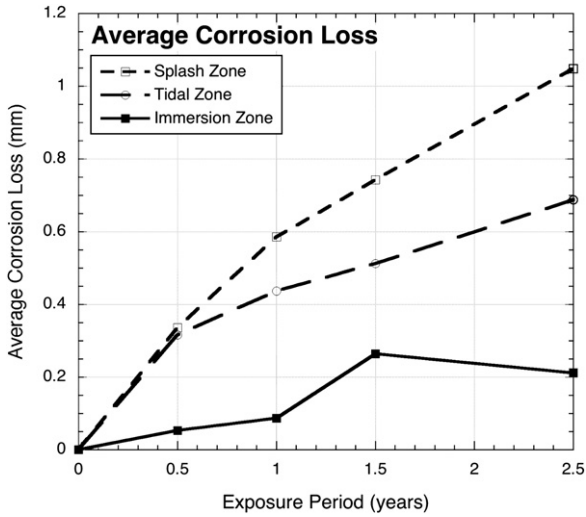

Fig. 7. Average uniform corrosion loss as a function of exposure period for plate pieces exposed in the splash, tidal and immersion zone.

4. Analysis of corroson variability

4.1. Spectral analysis

Fig. 7 provides information about the average corrosion loss and its change with continued exposure period. To consider the effect of plate size on corrosion, and for structural reliability procedures [16], estimates are needed also of the variability of the corrosion loss. This can be done simply by estimating the standard deviation of the amount of corrosion over a small area and comparing it with similar estimates at other locations or for other plates or coupons. A more complex but more informative analysis considers the (auto-) correlation structure of a plate surface or, equivalently, its relative frequency distribution, determined through what is known as a spectral analysis to produce a so-called power spectrum [17]. It will be helpful to review the basics of this analysis applied to two-dimensional surfaces before presenting the results.

Although the profile of a corroded surface is a function of two orthogonal distances, it can be represented as function of frequency using a Fourier transformation. The result is a spectrum of the surface profile, that is, it is re-interpreted as the set of frequency components contained within the profile of the original surface. Thus a power spectrum represents the randomness of the surface in the frequency domain. In particular it is a measure of the frequency distribution of the mean squared value of the corrosion depths (or 'power') at different frequencies.

Let the corrosion depth be defined as $z(k_x,k_y)$ measured at the grid point (k_x,k_y) of a two-dimensional grid defining the surface region (x,y) of interest. Here k_x is the grid number in the x-direction and k_y is the grid number in the y direction. Let the spacing of the grid points in the x-direction be denoted Δ_x and the spacing in the y direction be Δ_y. Thus

$$z(k_x, k_y) \equiv z(l_x, l_y) \tag{1}$$

where l_x and l_y are respectively the x and y co-ordinates of the grid point (k_x,k_y). The relationships between (k_x,k_y) and (l_x,l_y) are given by

$$l_x = k_x \cdot \Delta_x \quad k_x = 0, 1, 2, \ldots.., N_x - 1 \tag{2a}$$

$$l_y = k_y \cdot \Delta_y \quad k_y = 0, 1, 2, \ldots.., N_y - 1 \tag{2b}$$

where N_x and N_y are respectively the total number of grid points in the x and y directions. The mean value of the $z(k_x,k_y)$ over the area defined by (l_x,l_y) is given by

$$\bar{z} = \frac{\sum_{k_y=0}^{N_y-1}\sum_{k_x=0}^{N_x-1} z(k_x,k_y)}{N_x N_y} \tag{3}$$

Evidently, there will exist a surface with exactly corresponding characteristics but with a zero mean value. It is given by

$$h(k_x,k_y) = z(k_x,k_y) - \bar{z} \tag{4}$$

This now allows the corresponding two-dimensional discrete spectrum to be defined as [11,12]:

$$\begin{aligned} S(f_1,f_2) &= \frac{4\Delta_x\Delta_y}{N_x\cdot N_y}\cdot\left[\sum_{k_y=0}^{N_y-1}\sum_{k_x=0}^{N_x-1} h(k_x,k_y)\cdot\exp\left(\frac{i2\pi\cdot k_x n_1}{N_x}\right)\cdot\exp\left(\frac{i2\pi\cdot k_y n_2}{N_y}\right)\right]^2 \\ &= \frac{4\Delta_x\Delta_y}{N_x\cdot N_y}\cdot\left[\sum_{k_y=0}^{N_y-1}\sum_{k_x=0}^{N_x-1} h(k_x,k_y)\cdot\exp\left\{i\left(\frac{2\pi\cdot k_x n_1}{N_x}+\frac{2\pi\cdot k_y n_2}{N_y}\right)\right\}\right]^2 \end{aligned} \tag{5}$$

where, the variations of n_1 and n_2 are given by

$$n_1 = 0,1,2,\ldots\ldots,N_x/2 \tag{6a}$$

$$n_2 = 0,1,2,\ldots\ldots,N_y/2 \tag{6b}$$

and the cyclic frequencies f_1 and f_2 are defined by

$$f_1 = \frac{n_1}{N_x\Delta_x} \tag{7a}$$

$$f_2 = \frac{n_2}{N_y\Delta_y} \tag{7b}$$

If the corrosion depths $h(k_x,k_y)$ exhibit some (perhaps just approximate) repetition on frequencies (f_1,f_2) the spectrum at or near (f_1,f_2) would show a local peak. This local peak indicates an elevated relative occurrence of the frequencies (i.e. the surface characteristics) involved.

Theoretically the upper values of the frequencies f_1 and f_2 are restricted to $1/(2\Delta_x)$ and $1/(2\Delta_y)$, respectively, because no valuable information regarding the spectrum $S(f_1,f_2)$ is obtained for frequencies higher than these values. These cut-off frequencies are known as Nyquist frequencies [17]. Evidently, it is better, if possible, to choose a sufficiently small grid spacing (Δ_x and Δ_y) so as to reduce this effect, which can cause some distortion of results in the frequency domain. It might be noted that another way to estimate the spectrum is via auto-correlation. In this case, the auto-correlations of the corrosion depths for two points separated by a constant distance are evaluated. This process is repeated and the spectrum is calculated from the Fourier transform of the derived auto-correlations. This procedure was not employed herein.

Figs. 8–10 show examples of the power spectra for the splash zone, tidal zone and immersion zones as obtained using Eqs (3) and (4) after the data was normalized in each case to zero means. In each case it is clear that the frequency content is very restricted, with in each case the frequencies (along the two horizontal axes f_1 and f_2) highly localized around 0.1 cycles/mm, with only minor effects elsewhere. This means that in each case there is a high degree of uniformity or regularity in the profile of the surface, with the power spectra, and hence the surface displays a high degree of regularity, concentrated in the lower frequencies. There is little high frequency variation in the form of

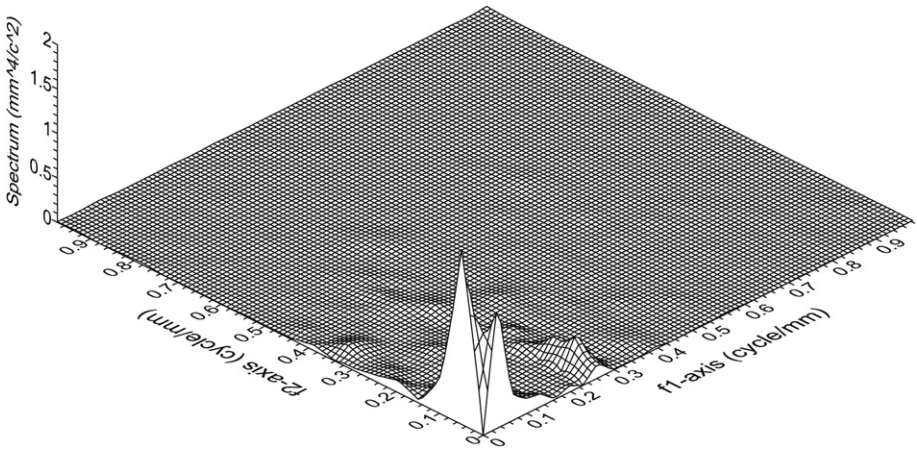

Fig. 8. Power spectrum for sample plate piece A1(side 1) exposed in the splash zone. The axis of the spectrum height, perpendicular to both frequency axes, has units of $mm^4/cycle^2$.

the corroded surfaces. Since this was the case for all pieces of plate exposed to uniform (or near-uniform) exposure conditions, this means that there is negligible or at worst very little effect of surface area in the characteristic pattern of the corroded surface. This was found to be the case throughout the complete exposure period of 2.5 years. It means that for any exposure condition small areas or (relatively) small samples can be taken as representative of the form of the corroded surface and hence of its variability.

4.2. Variability

As a result of the above observations, it is sufficient for representation of the variability of a corroded surface at different exposure periods to consider simply the standard deviation or the coefficient of variation rather than the complete power spectrum or the auto-correlation function. This can be done using only a relatively small area – sufficiently large, however, to capture the statistical characteristics

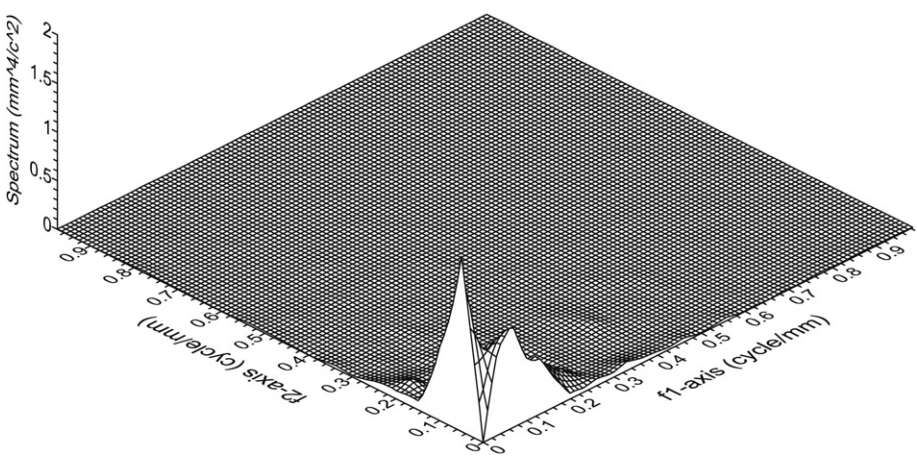

Fig. 9. Power spectrum for sample plate piece A7(side 1) exposed in the tidal zone. The axis of the spectrum height, perpendicular to both frequency axes, has units of $mm^4/cycle^2$.

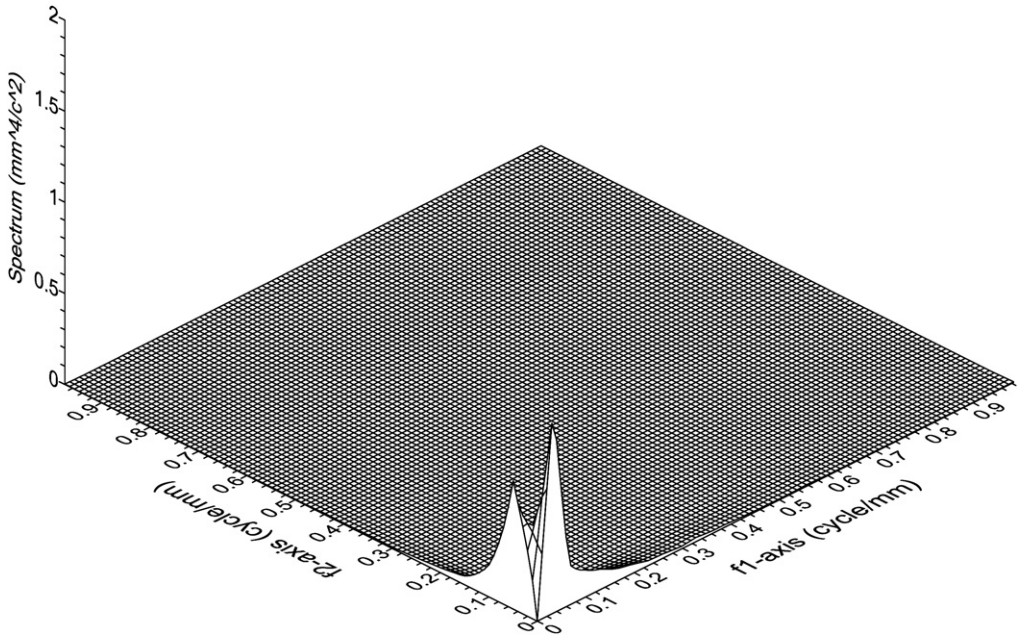

Fig. 10. Power spectrum for sample plate piece B1(side 1) exposed in the immersion zone. The axis of the spectrum height, perpendicular to both frequency axes, has units of $mm^4/cycle^2$.

of the surface. An estimate of the minimum size is as follows. From Figs. 8–10 the number of cycles per millimetre is around 0.2 for those most commonly occurring in the plate surface. This means that to capture at least one complete cycle requires at least 5 mm. This would be the smallest possible size, although in practice it would be desirable to have considerably more. An alternative approach is to note that for random sampling it is common to assume that at least 30 independent samples are required. With sampling at 0.5 mm spacing, this means 15 mm sample size at least. But at this spacing of surface sampling the samples are not completely independent owing to the regularity of corroded surfaces [18]. A bound based on the notion of asymptotic independence can be made as follows. If it is assumed that the main surface characteristic is represented by 0.2 cycles/mm (Figs. 8–10), then the data points within this range can be considered a cluster [19]. It is then reasonable to assume that, asymptotically, one independent sample is given within a spacing of one cycle (5 mm). In this case the minimum required size is around $30 \times 5 = 150$ mm. Considering the assumption of clustering and of independence between clusters, this is a conservative estimate.

The estimation of standard deviations usually is based on the assumption that the underlying distribution can be taken as Normal, at least in the limit for large numbers of (independent) observations. To estimate the standard deviations, small sections 30 mm $\times$ 20 mm were selected for each plate surface such that they could be considered to be representative of the topography of each surface. Profile measurements were made at 0.5 mm spacing in both directions. From these the means μ_z and the standard deviations σ_z were calculated using the standard formulae:

$$\mu_z = \frac{1}{n} \cdot \sum_{i=1}^{n} z_i \tag{8a}$$

$$\sigma_z^2 = \frac{1}{n} \cdot \sum_{i=1}^{n} (z_i - \mu_z)^2 \tag{8b}$$

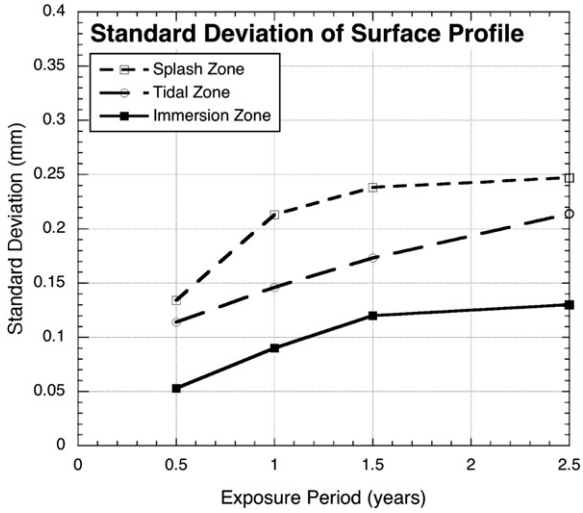

Fig. 11. Standard deviation estimates for corrosion profiles as a function of exposure period for each of the three exposure zones.

where n is the total number of samples. The results are summarized in Fig. 11. The coefficients of variation (COV) defined as μ_Z/σ_Z are shown in Fig. 12.

5. Discussion

The plots for the average corrosion loss as a function of period of exposure (Fig. 8) are in general agreement with those found earlier for much smaller coupons, with a change in trend evident after an early period during which the rate of corrosion gradually decreases. For the immersion curve there is a distinct change soon after one year of exposure, consistent with the results for small coupons at this site [20]. The change in trend occurs less obviously and later in time for the tidal and the splash zones, again consistent with results for tidal and atmospheric corrosion [21].

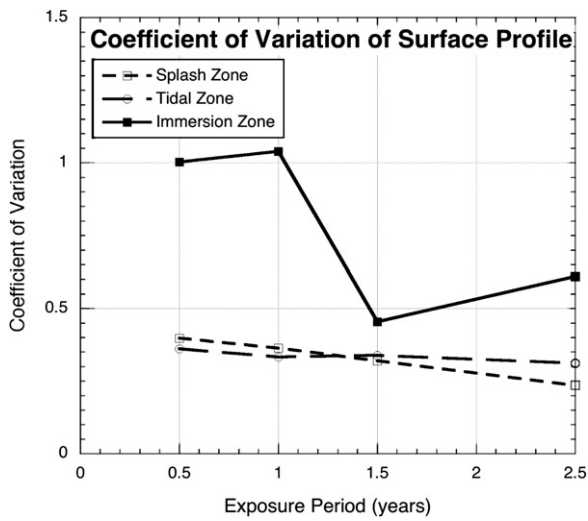

Fig. 12. Coefficients of Variation as a function of exposure period for each of the three exposure zones.

The standard deviations (SD) estimated according to Eq (8) are plotted in Fig. 11. They all show an increase in standard deviation but the rate of increase declines after about one year exposure, significantly so for the splash zone and less so for the tidal zone. Interpretation of these results is not straight-forward but could be related to differences in the rate of corrosion on various parts of the overall plates, captured in the segments that were cut off. It is unlikely to be the result of errors with the digitizing as this would have been detected during the processing of the results. Previously the increase in standard deviation for the immersion zone after about one year exposure has been attributed to the effect of microbiological influences on corrosion since this is known to be related to the highly variable settlement and growth of marine biological agents [22]. From an engineering perspective the most important results are those for the Coefficients of Variation (COV), shown in Fig. 12. These show a gradual decline in COV for the splash and the tidal zone, reflecting the increasing mean corrosion levels to year 2.5. Importantly, the COV estimated from the present experiments is much lower than estimates made from spot thickness measurements of ship corrosion [23] that show COV values exceeding unity in some cases, even for parts that are not continually immersed. Similarly it is of interest that while the COV for the immersed plates was initially quite high, reflecting the low early corrosion loss and higher standard deviation, the eventual COV is roughly similar to the COV values in the splash and tidal zones.

The values for the standard deviations and the coefficients of variation are rather different from those reported earlier as estimated for small coupons [24]. The reason for the difference lies in the way the measurements were made and what was actually considered. In the present case the form of the corroded surface is considered in the estimates for SD and COV. In the earlier work the mass losses for the individual coupons were used instead, and actually represent the SD and COV of the average corrosion loss as derived from mass losses. Since the mass losses are for each coupon, they represent average values and thus the SD and COV derived from them also are averages in this sense. In contrast, the present results refer to the variation of the surface profile and are therefore a measure of the surface undulation. They should not be applied where the average properties are of interest, for example for a steel member in tension.

The spectra of reach of the individual plate segments, such as typical examples shown in Figs. 8–10, all show that the frequency content of the corroded surfaces is closely bounded and of a wavelength much smaller than the plate segments. As argued above, this shows that coupons of considerably smaller size than the present plates or their segments can be used to obtain the characteristic features of the corroded surface, including the mean mass loss and the standard deviation of mass loss. Intuitively this observation should not to be surprising. Fundamental ideas in corrosion mechanics supports the notion that for wet corrosion the anodic and cathodic regions are closely spaced and that therefore the corrosion current is not much influenced by the conductivity of the immediate surrounding environment [25]. In fact, once some degree of corrosion products have built up on the corroding metal surface for each of the splash, tidal and immersion zone exposures, conditions immediately adjacent to the metal are highly likely to be continuously or semi-continuously wet, permitting both the development of closely spaced anodes and cathodes and high corrosion currents. As is well-known, in these wet conditions the rate limiting step in the corrosion process is the diffusion of oxygen to the cathode, not limitations on corrosion currents. The net result, that relatively small coupons can be used to characterize the corrosion process in the splash, tidal and immersion corrosion zones is of practical importance for corrosion testing. Whether this argument can be extended to the corrosion of steel in the atmosphere remains a matter for investigation.

Some tentative lower bounds were given above for the minimum size of coupon for the splash, tidal and immersion corrosion zones. As noted, these were based on different assumptions, primarily as to the degree of independence between adjacent observations of corrosion loss measured on a surface. The bounds can be sharpened a little by proceeding from the assumption that uniform or near-uniform corroded surfaces are partially if not wholly the result of multiple pits. Although a rather high degree of correlation appears to be the case for the depth of adjacent pits in the early period of exposure, the correlation appears to reduce with increased exposure. This can be seen informally through microscope observations of pitted surfaces over one or more years exposure [18]. The implication is that relative to pit size larger surface areas may be necessary for short-term exposures. But since pits grow in surface area (as well as depth) with increased exposure time, the net effect is likely to be that the

actual coupon size can be similar for both early and longer term exposure. On this basis the assumption used above to obtain the larger (150 mm) bounds can now be seen to be rather conservative. The smaller bounds of 15 mm are more likely to be appropriate.

6. Conclusion

The following conclusions may be drawn from the observations reported herein:

1. The corroded surfaces of plates exposed in the splash, tidal and immersion corrosion zones all exhibit a highly regular corroded surface within the one zone. This is evident from visual observations of the corroded surface of large plates and from the spectra extracted from the digitised surfaces of component plates.
2. These observations were found by experiment to be valid for exposures up to 2.5 years. However, the data trends suggest that these observations are likely to remain valid for much longer periods of exposure.
3. As a result it corrosion tests within each of the splash, tidal and immersion corrosion zones can employ relatively small corrosion coupons to capture the essential characteristics of the form of the corroded surfaces, including mass loss and pitting.
4. For the corrosion environment investigated herein, it was estimated that the minimum coupon size should be no less than about 15 mm square or closely similar. A conservative estimate suggests that minimum coupon size of around 150 mm.

Acknowledgement

The work reported herein is part of a project on structural reliability assessment of deteriorating structures supported financially by the Australian Research Council. The authors gratefully acknowledge the continued cooperation of Fisheries NSW in providing access to the Taylors Beach testing facility. The assistance of Ian Jeans and Michael Goodwin with the experimental work is much appreciated.

References

[1] Melchers RE. Development of new applied models for steel corrosion in marine applications including shipping. Ships and Offshore Structures 2008;3(2):135–44.
[2] Lee JS, Ray RI, Little BJ. The influence of experimental conditions on the outcome of laboratory investigations using natural coastal seawaters. Corrosion 2010;66(1). 105001-1- 6. doi:10.5006/1.3318279.
[3] Evans UR. The corrosion and oxidation of metals: scientific principles and practical applications. London: Edward Arnold (Publishers) Ltd; 1960.
[4] Jeffrey R, Melchers RE. Shape and size effects for marine immersion coupons. British Corrosion Journal 2002;37(2):99–104.
[5] Humble AA. The cathodic protection of steel piling in sea water. Corrosion 1949;5(9):292–302.
[6] LaQue FL. Corrosion testing. Proc ASTM 1951;51:495–582 [Edgar Marburg Lecture].
[7] Larrabee CA. Corrosion-resistant experimental steels for marine applications. Corrosion (NACE) 1958;14(11):21–4.
[8] Li Y, Hou B, Li H, Zhang J. Corrosion behaviour of steel in the Chengdao offshore oil exploration area. Materials and Corrosion 2004;55(4):305–9.
[9] Jeffrey R, Melchers RE. Corrosion of vertical mild steel strips in seawater. Corrosion Science 2009;51(10):2291–7.
[10] Yamamoto M, Hirosawa N, Yoshida K, Kato C, Hada T. Characterization of surface texture of corroded steel plates exposed in marine environment. Zairyo to Kankyo (Materials and Environment) 1992;41:803–8 [in Japanese].
[11] Sumi Y, Rahbar-Ranji A. Stress analysis of a randomly undulated plate due to corrosion in marine structure. Japan: Department of Naval Architecture and Ocean Engineering, Yokohama National University; 2001.
[12] Press WH, Teukolsky SA, Vetterling WT, Flannery BP. Numerical recipes in fortran 77. 2nd ed. Cambridge University Press; 1992.
[13] Majumdar A, Bhushan B. "Characterization and modeling of surface roughness and contact mechanics". In: Bhushan B, editor. Handbook of micro/nanotribology. Boca Raton [Florida]: CRC Press LLC; 1999.
[14] Melchers RE, Ahammed M. Characterization of corroded steel plate surfaces, Proc. Aust. Conf. Mech. Struct. And materials. In: Deeks AJ, Hao Hong, editors. Developments in mechanics of structures and materials. Perth: Balkema; 2004. pp. 637–41.
[15] ASTM Standard G3-89. Standard practice for conventions applicable to electrochemical measurements in corrosion testing. West Conshohocken, PA: ASTM International; 2004. doi:10.1520/G0003-89R04.
[16] Melchers RE. The effect of corrosion on the structural reliability of steel offshore structures. Corrosion Science 2005;47(10):2391–410.
[17] de Silva CW. Vibration: fundamental and practice. Boca Raton, FL: CRC Press LLC; 2000.

[18] Jeffrey R, Melchers RE. The changing topography of corroding mild steel surfaces in seawater. Corrosion Science 2007;49: 2270–88.
[19] Galambos J. The asymptotic theory of extreme order statistics. 2nd ed. Malabar, FL: Krieger; 1987.
[20] Melchers RE. Modeling of marine immersion corrosion for mild and low alloy steels - part 1: phenomenological model. Corrosion (NACE) 2003;59(4):319–34.
[21] Melchers RE. The transition from marine immersion to coastal atmospheric corrosion for structural steels. Corrosion (NACE) 2007;63(6):500–14.
[22] Sanders PF, Maxwell S. Microfouling, macrofouling and corrosion of metal test specimens in seawater. In: Microbial corrosion. London: The Metals Society; 1983. pp. 74–83.
[23] Paik J, Lee J, Hwang J, Park Y. A time-dependent corrosion wastage model for the structures of single and double hull tankers and FSOs and FPSOs. Marine Technology 2003;40:201–17.
[24] Melchers RE. Modeling of marine immersion corrosion for mild and low alloy steels – part 2: uncertainty estimation. Corrosion (NACE) 2003;59(4):335–44.
[25] Mikhailovsky YN. Theoretical and engineering principles of atmospheric corrosion of metals. In: Ailor WH, editor. Atmospheric corrosion. New York: John Wiley; 1983. pp. 85–105.

Corrosion Science 67 (2013) 130–141

Contents lists available at SciVerse ScienceDirect

Corrosion Science

journal homepage: www.elsevier.com/locate/corsci

Investigation of the corrosion progress characteristics of offshore subsea oil well tubes

M. Hairil Mohd [a,b], Jeom Kee Paik [a,*]

[a] The Ship and Offshore Research Institute, The Lloyd's Register Educational Trust Research Centre of Excellence, Pusan National University, Busan, Republic of Korea
[b] Maritime Technology Department, Faculty of Marine Science and Maritime Studies, Universiti Malaysia Terengganu, Terengganu, Malaysia

ARTICLE INFO

Article history:
Received 7 May 2012
Accepted 14 October 2012
Available online 2 November 2012

Keywords:
A. Mild steel
B. Modelling studies
B. Weight loss
C. Pitting corrosion

ABSTRACT

One of the most challenging issues in the offshore oil and gas industry is corrosion assessment and management in subsea structures or equipment. The aim of this study was to investigate the corrosion progress characteristics of offshore oil well tubes used in the production of oil in deep water. A direct measurement database of corrosion damage in terms of pit depth with age (time) in offshore oil well tubes was collated. The corrosion data were statistically analysed to identify the probability density distribution of corrosion damage with time. An empirical formula to predict time-dependent corrosion damage in offshore oil well tubes is suggested based on the results of the statistical analysis. Given that there are few corrosion measurement databases of subsea equipment used for offshore oil and gas production in the literature, this study should prove useful for assessing and managing corrosion damage in deep water offshore oil well tubes, which are key pieces of equipment in offshore oil and gas production systems.

© 2012 Elsevier Ltd. All rights reserved.

1. Introduction

Offshore oil and natural gas have long been used to meet the sustained and increasing demand for energy. In recent years, the hydrocarbon resources in shallow waters and reasonably benign environments have been largely depleted, and the oil and gas industries have been compelled to move into more challenging environments such as deeper waters and harsher metocean conditions. These industries will continue to explore and exploit deeper waters as long as the demand for oil and gas continues to increase.

Most of the equipment currently used in the offshore oil and gas industry is approaching the end of its useful life, and the possibility of equipment failing without significant warning is high. Recent oil spills and equipment failures have demonstrated this danger. Various factors contribute to these incidents, including human error, lack of advanced knowledge and corrosion effects.

Generally, ageing is a dominant life-limiting factor for any structure, and corrosion is one is of the most serious features of ageing [1]. It is well known that corrosion is a very complex process, particularly in marine environments where it is significantly affected by many environmental and material factors [2–4]. Corrosion problems occur in numerous subsystems within the offshore oil and gas production system, including oil well tubes. It is essential to ensure that oil well tube structures are running in a safe and controlled environment. Structures such as ships can be repaired and maintained in a variety of ways, and usually have dry docking procedures for maintenance and inspection. There are no such procedures for the maintenance and repair of oil well tube structures at subsea levels. Corrosion tolerance must thus be carefully considered in the design of these structures. A schematic figure of a subsea system with oil well tubes is shown in Fig. 1.

The aim of this study was to investigate the corrosion progress characteristics of offshore oil well tubes in deep water and to suggest an empirical formula for predicting the time-dependent corrosion wastage of these tubes.

Several relevant studies can be found in the literature. Fu et al. [5] noted that the main factors contributing to oil tube corrosion are sweet corrosion and erosion gas fluids. They used the grey relational method to determine the extent of the correlation between the various factors in a system with uncertain information. Ren et al. [6] used X-ray diffraction, scanning electron microscopy, and electrochemical measurement to investigate the corrosion behaviour of N80 steel tubes in a static solution containing carbon dioxide (CO_2) and hydrogen sulphide (H_2S). Migahed et al. [7] studied the use of a newly synthesised compound as a corrosion inhibitor during the acidisation process in petroleum production operations.

In studying the effect of flexure on the corrosion mechanism, Melchers and Paik [8] concluded that the corrosion rate increases by 10–15% when a structure is near or beyond the elastic limit of

* Corresponding author. Tel.: +82 51 510 2429; fax: +82 51 512 8836.
E-mail address: jeompaik@pusan.ac.kr (J.K. Paik).

0010-938X/$ - see front matter © 2012 Elsevier Ltd. All rights reserved.
http://dx.doi.org/10.1016/j.corsci.2012.10.008

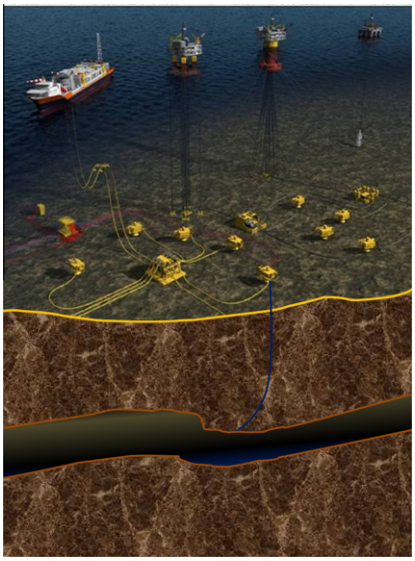

Fig. 1. Illustration of an offshore subsea oil and gas production system.

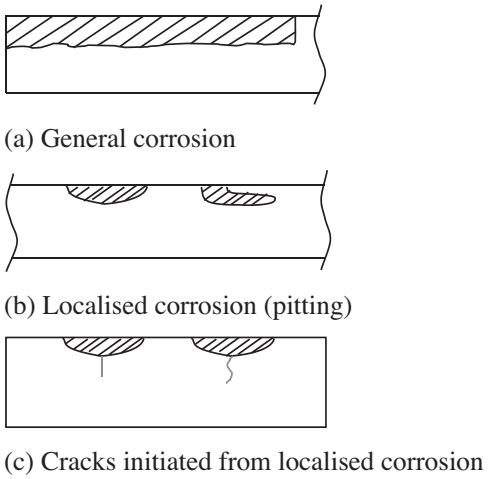

Fig. 2. Typical types of corrosion of marine steel structures [2].

steel. Paik and Tayamballi [9] emphasised that corrosion is one of the factors that may affect the ultimate strength behaviour of steel plate and that careful assessment needs to take into consideration when to accommodate this effect. Many studies have been conducted on the corrosion of pipeline structures, especially pipeline pitting corrosion [10,11], failure pressure prediction for corroded pipelines [12–14] and a general overview of pipeline corrosion [15].

Research has also been conducted on corrosion modelling. Paik et al. [16–19] developed time-dependent corrosion wastage models for ship structures. By statistically analysing corrosion data, they proposed a mathematical function that defines a time-dependent corrosion wastage model. Recently, Paik and Kim [20] developed an advanced method for developing a time-dependent empirical corrosion wastage model that applies the probability density parameter technique to the age of a structure. Melchers et al. [21] statistically characterised corroded steel surfaces exposed to marine environments, and found that the considerable differences in corrosion loss between different exposure zones are statistically dependent on the surface topography. Melchers also reviewed the research on physical corrosion modelling in marine environments [22–27]. Chernov [28] and Chernov and Ponomarenko [29] developed a corrosion model that takes account of the effect of the environment on corrosion. Numerous other empirical models of ship corrosion wastage have been developed [16–19,30–32].

Najjar et al. [33] and Jarrah et al. [34] both suggested an advanced method that efficiently predicts the maximum corrosion pit depth using a combination of two statistical methods. In these papers, generalised lambda distributions together with a computer-based bootstrap method were used to determine a model of distribution fitting and to generate simulated distributions that were equivalent to the experimental case. Chowdhury [35] attempted to derive accurate empirical relationships between the mean and standard deviation of any given midship section as simple functions of corrosion loss. He observed that all geometric properties are linear functions of the total corrosion loss, and that there is a single constant relevant to the section that specifies the property completely.

However, all of this previous research on corrosion wastage models is limited to ships and floating structures. To the best of

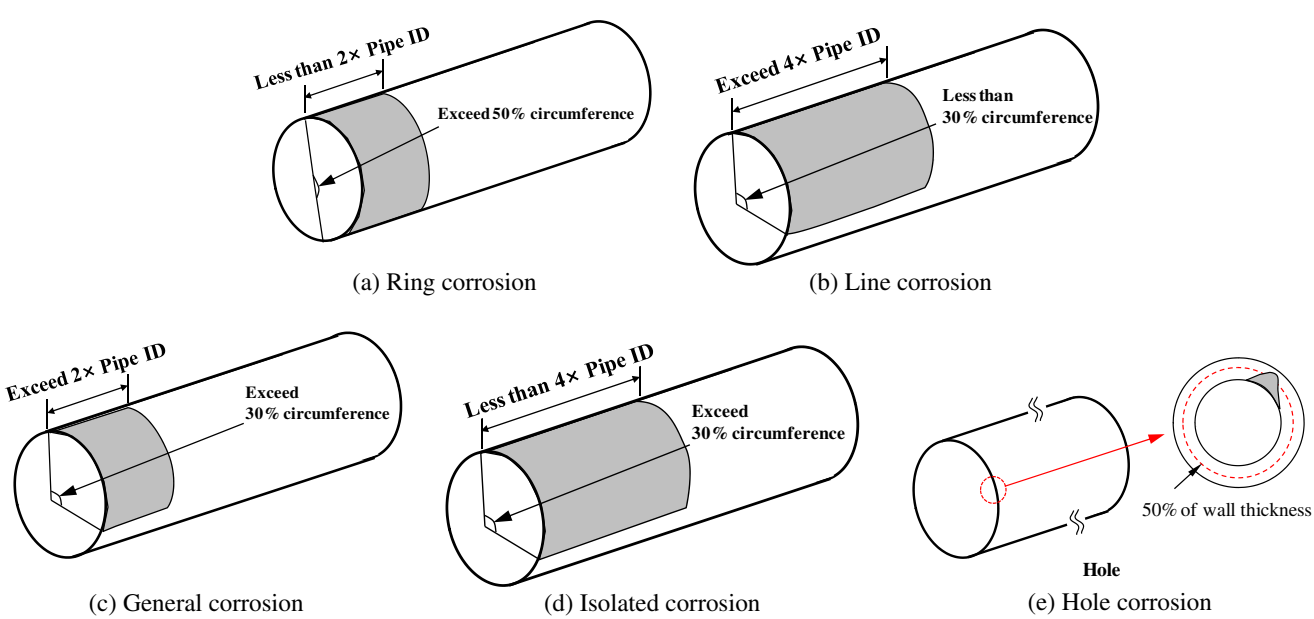

Fig. 3. Corrosion classification (internal corrosion) for oil well tube structures [36].

Table 1
Measurements of the thickness reduction of oil well tubes.

Target oil well tube	Age (years)	Water depth (m)	Number of measurements	Grade	Tube wall thickness (mm)
A	5.1	1349.4	174	L-80	6.45
B	5.8	2610.1	287	L-80	6.45
C	9.1	1320.4	149	N-80	6.45
D	11.7	1419.0	197	AMS-28	5.51
E	15.3	2254.7	246	N-80	6.45
F	18.2	1364.6	184	N-80	6.45
G	22.8	1941.4	200	N-80	5.51

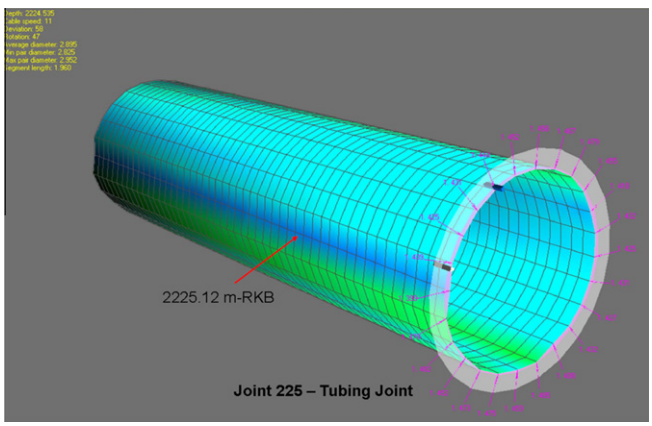

Fig. 4. Principal view of an oil well tube under consideration [36].

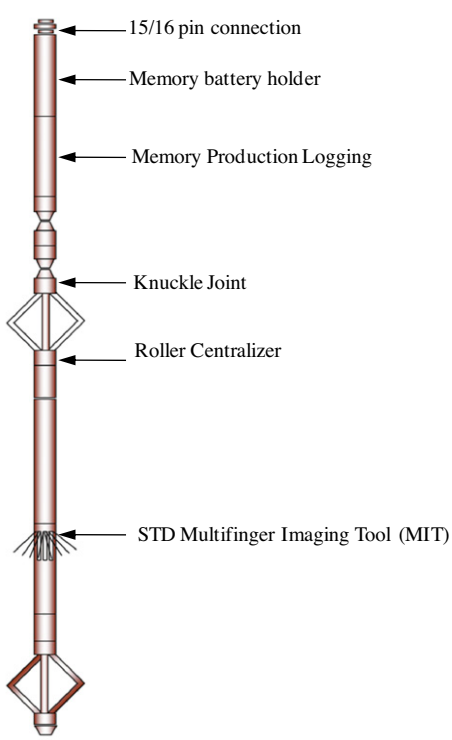

Fig. 5. Schematic view of the Multifinger Imaging Tool (MIT) system [36].

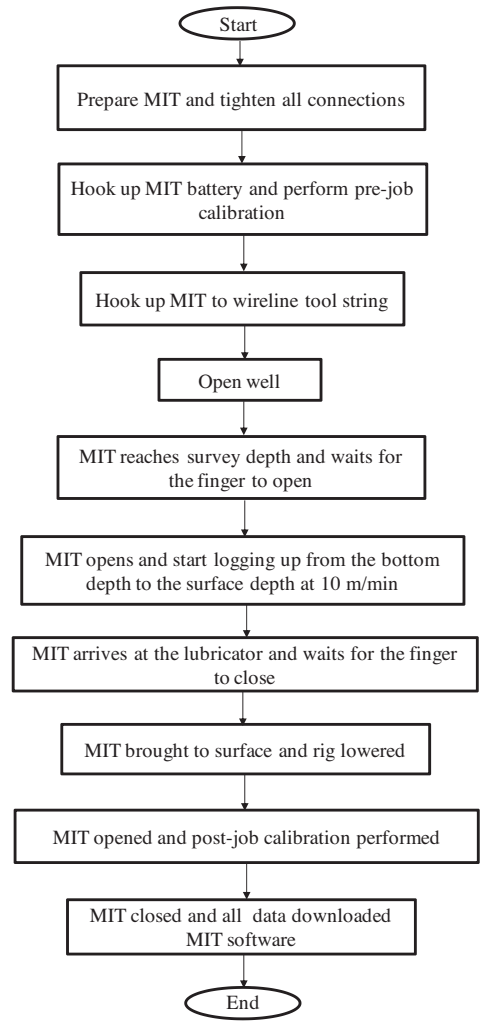

Fig. 6. Procedure for corrosion detection using the Multifinger Imaging Tool (MIT) system [36].

the authors' knowledge, there are no corrosion wastage models for subsea oil well tube structures. This study aimed to fill that gap by contributing to the characterisation of corrosion progress in offshore oil well tubes. With the help of an offshore oil and gas production company, a direct measurement database of corrosion damage in terms of pit depth with time (age) in offshore oil well tubes was collated. The method of Paik and Kim [20] was then used to derive an empirical formula to predict the time-dependent corrosion damage of the tubes.

2. Classification of oil well tube corrosion

In general, several types of corrosion are relevant to offshore steel structures, as shown in Fig. 2 [2]. However, the corrosion classification schemes for subsea oil well tube structures are slightly different. There are five types: ring, line, general, isolated and hole corrosion [34]. This corrosion classification is illustrated in Fig. 3.

3. Collation of the corrosion measurement database for offshore subsea oil well tubes

With the help of an offshore oil and gas production company, a direct measurement database of corrosion damage in offshore

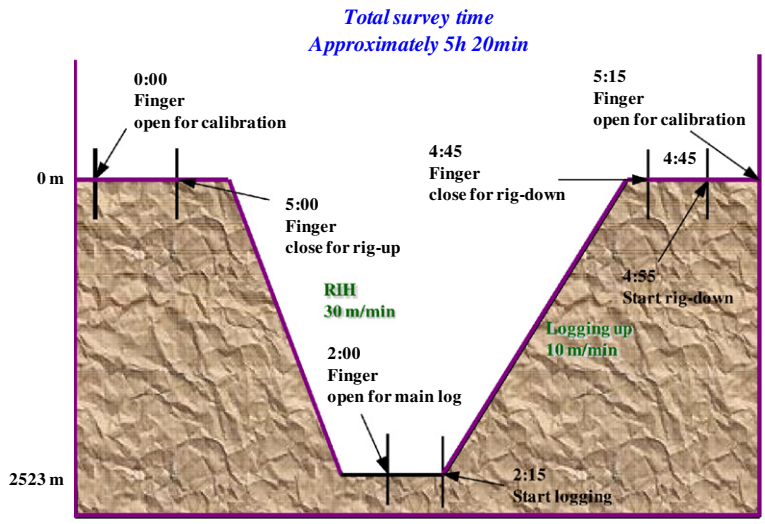

Fig. 7. Schematic view of the MIT running sheet [36].

Table 2
Frequency of wall thickness reduction (pit depth) due to corrosion in the oil well tubes.

Pit depth interval (mm)	Age (years)						
	5.1	5.8	9.1	11.7	15.3	18.2	22.8
0.0–0.2	69	162	24	27	8	0	45
0.2–0.4	55	54	78	72	76	23	68
0.4–0.6	39	38	36	72	82	76	26
0.6–0.8	10	20	9	13	64	37	10
0.8–1.0	1	10	2	7	13	24	5
1.0–1.2	0	3	0	4	3	10	1
1.2–1.4	0	0	0	0	0	7	3
1.4–1.6	0	0	0	0	0	3	3
1.6–1.8	0	0	0	1	0	4	0
1.8–2.0	0	0	0	0	0	0	2
2.0–2.2	0	0	0	0	0	0	6
2.2–2.4	0	0	0	0	0	0	12
2.4–2.6	0	0	0	0	0	0	6
2.6–2.8	0	0	0	0	0	0	3
2.8–3.0	0	0	0	0	0	0	1
3.0–3.2	0	0	0	0	0	0	2
3.2–3.4	0	0	0	0	0	0	5
3.4–3.6	0	0	0	0	0	0	1
3.6–3.8	0	0	0	0	0	0	0
3.8–4.0	0	0	0	0	0	0	0
4.0–4.2	0	0	0	0	0	0	1

subsea oil well tubes was collated. Corrosion measurements for seven oil well tubes with an age range of 5.1–22.8 years were obtained. Details of the corrosion measurements for each oil well tube are given in Table 1. Fig. 4 shows the principal view of an oil well tube. Table 1 shows that the greater the water depth of an oil well tube, the larger the number of measurements taken.

It is not straightforward to detect corrosion damage in offshore subsea oil well tubes. In this study, corrosion detection was performed using a Multifinger Imaging Tool (MIT), and the detected corrosion data were analysed using three-dimensional MIT software. Fig. 5 shows a schematic view of the MIT system [36]. Fig. 6 shows the procedure for corrosion detection in offshore subsea oil well tubes. Before the corrosion detection commenced, the well tube was cleaned using a 70.6 mm drift and tagged XN-nipple at 1500–2000 m. A sinker bar was run after the 70.6 mm drift to below the XN-nipple. The MIT was logged at 3 m below the XN-nipple and set to surface at a speed of 10 m/min. [36]. Fig. 7 illustrates a schematic view of the MIT running sheet.

The measurements of the instances and pit depth of the corrosion on the inner side of the oil well tube were obtained for seven operating oil well tubes to give a total of 1437 pit measurements, as shown in Table 1. The amount of corrosion damage loss (reduced wall thickness or pit depth) relative to the immersion time is summarised in Table 2.

The internal surface of an oil well tube is normally well coated, and corrosion does not occur until the coating has become ineffective. The internal surface coating is thus an important part of oil well tube corrosion protection, as the breakdown of the coating

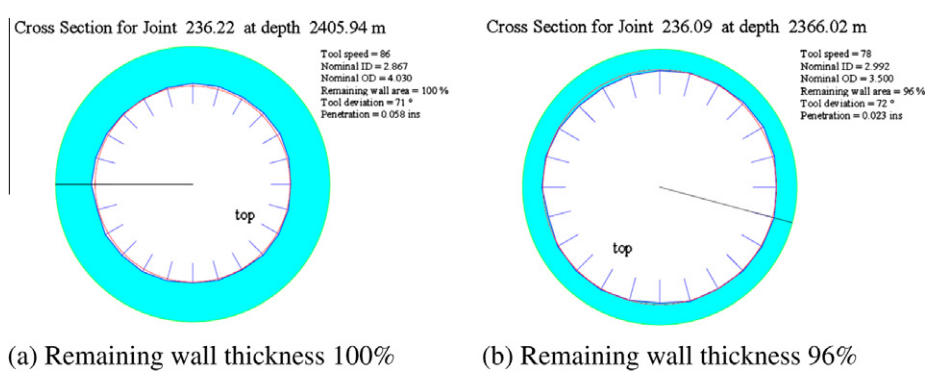

Fig. 8. Typical view of the cross section of a corroded oil well tube [36].

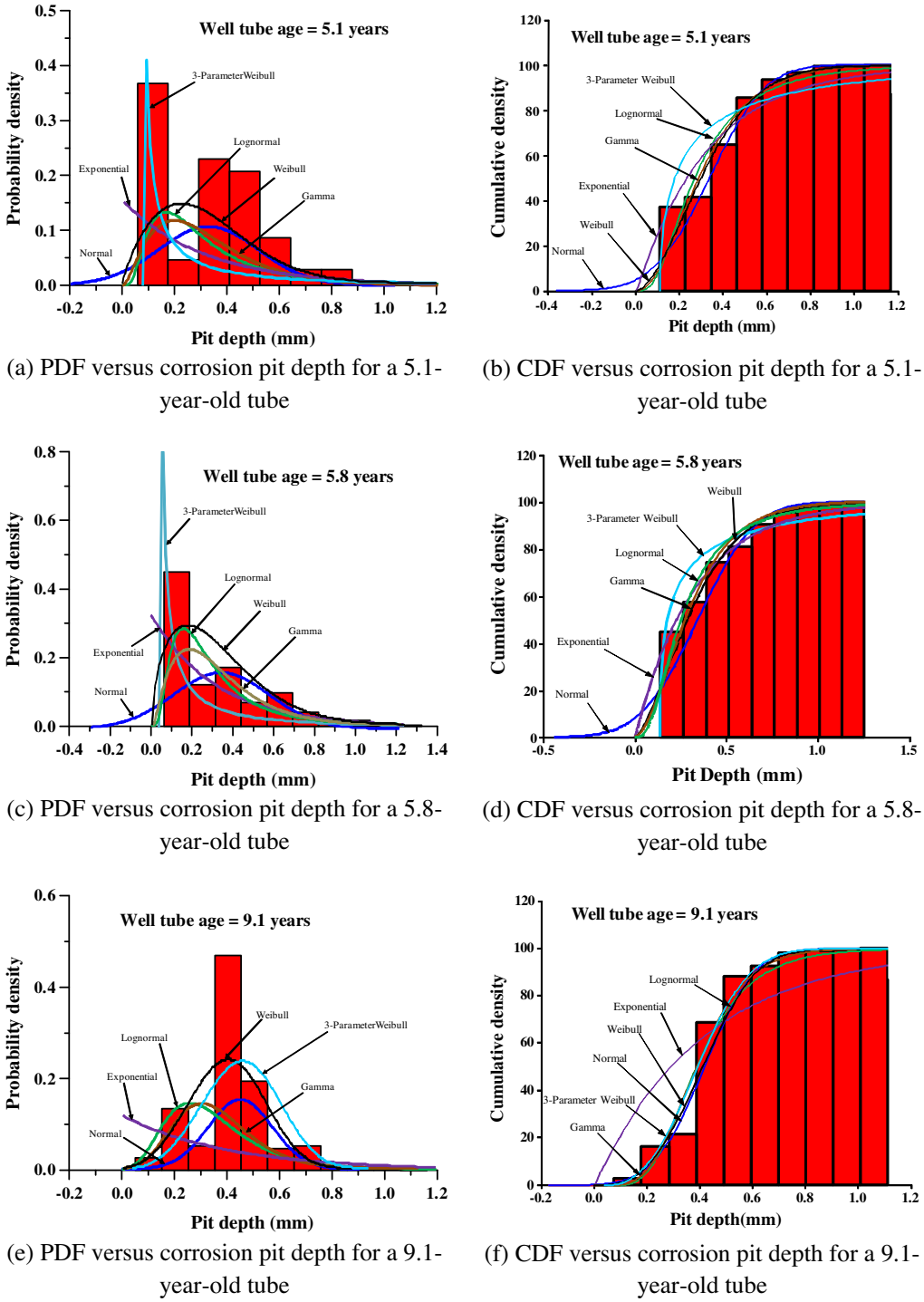

(a) PDF versus corrosion pit depth for a 5.1-year-old tube

(b) CDF versus corrosion pit depth for a 5.1-year-old tube

(c) PDF versus corrosion pit depth for a 5.8-year-old tube

(d) CDF versus corrosion pit depth for a 5.8-year-old tube

(e) PDF versus corrosion pit depth for a 9.1-year-old tube

(f) CDF versus corrosion pit depth for a 9.1-year-old tube

Fig. 9. Probability density distribution (PDF) and cumulative density distribution (CDF) versus pit depth for various ages of oil well tubes.

triggers the start of corrosion. A sample view of corrosion taken with the MIT 3-dimensional software is illustrated in Fig. 8.

4. Analysis of the corrosion progress characteristics of offshore subsea oil well tubes

4.1. Probabilistic characteristics of corrosion damage

The corrosion measurements in the database were statistically analysed. Fig. 9 shows the probability density distribution (PDF) and cumulative density distribution (CDF) versus pit depth for various ages of oil well tubes. Fig. 9 also compares possible representations of the various probability density functions to the corrosion database.

The probability density function that best represents the corrosion database was determined by a goodness of fit test. The Anderson–Darling [37] test statistic was used to quantify how well the database follows a particular distribution. The better the distribution fits the data, the smaller the statistic. Tables 3(a) and 3(b) summarise the results of the Anderson–Darling goodness of fit test

Table 3(a)
Goodness of fit test (Anderson–Darling) for various probability distribution functions.

Distribution function	Goodness of fit test (Anderson–Darling)							
	Age (years)							
	5.1	5.8	9.1	11.7	15.3	18.2	22.8	Average
Normal	4.51	15.59	4.74	5.21	2.54	7.59	23.91	9.16
Lognormal	12.14	7.36	12.24	9.91	1.89	1.73	4.06	7.05
Exponential	7.63	5.37	24.32	23.72	43.42	30.43	9.75	20.66
2-Parameter Weibull	8.46	5.88	6.16	4.82	1.86	5.52	6.12	5.55
3-Parameter Weibull	21.39	17.09	5.53	4.80	1.56	2.21	6.00	8.37
Gamma	8.24	6.11	8.68	5.67	1.31	3.19	7.12	5.76

Table 3(b)
Goodness of fit test ratio (Anderson–Darling) for various probability distribution functions.

Distribution function	Goodness of fit test ratio (Anderson–Darling)							
	Age (years)							
	5.1	5.8	9.1	11.7	15.3	18.2	22.8	Average
Normal	0.21	1.00	0.19	0.22	0.06	0.25	1.00	0.367
Lognormal	0.57	0.47	0.50	0.42	0.04	0.06	0.17	0.279
Exponential	0.36	0.34	1.00	1.00	1.00	1.00	0.41	0.639
2-Parameter Weibull	0.40	0.38	0.25	0.20	0.04	0.18	0.26	0.214
3-Parameter Weibull	1.00	1.10	0.23	0.20	0.04	0.07	0.25	0.361
Gamma	0.39	0.39	0.36	0.24	0.03	0.10	0.30	0.226

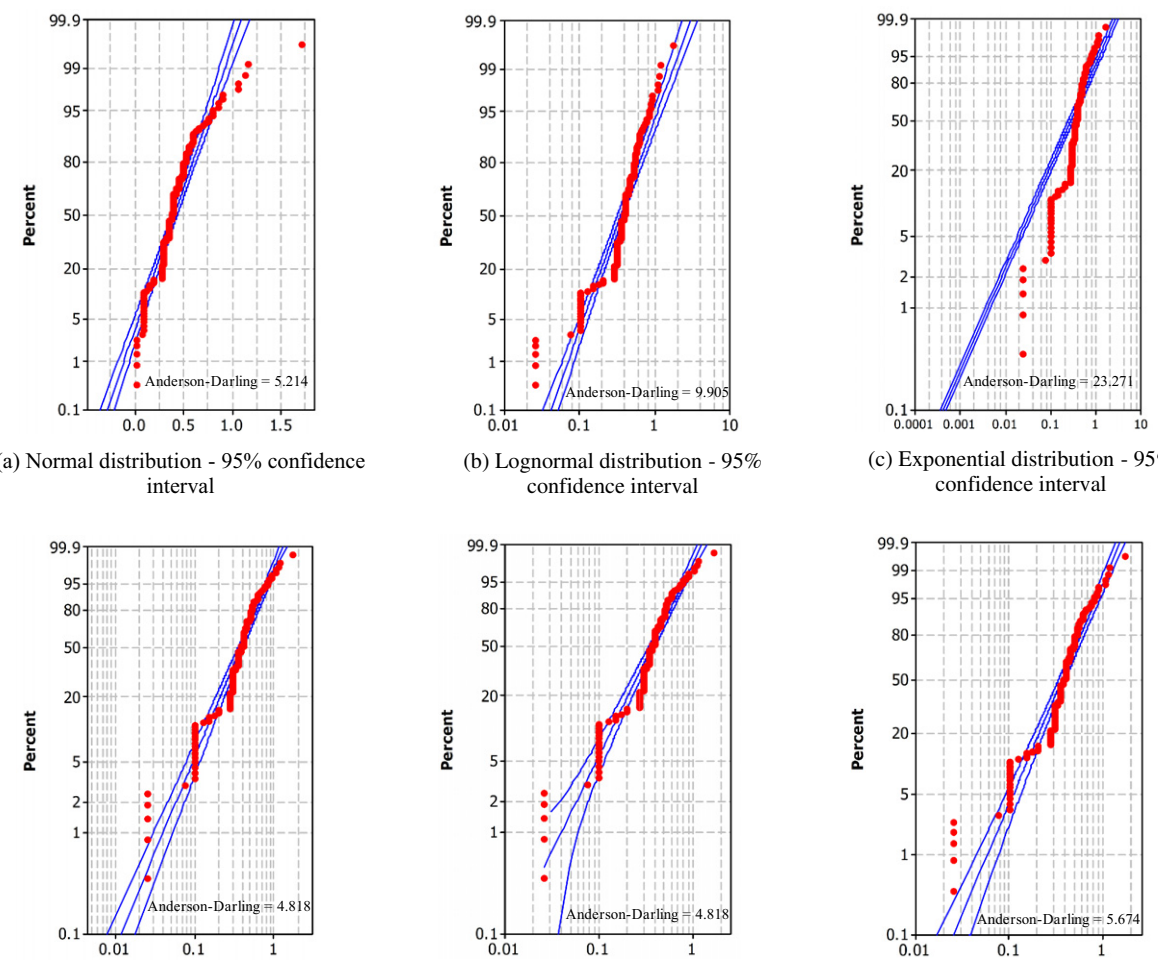

(a) Normal distribution - 95% confidence interval

(b) Lognormal distribution - 95% confidence interval

(c) Exponential distribution - 95% confidence interval

(d) Weibull distribution - 95% confidence interval

(e) 3-Parameter Weibull distribution95% confidence interval

(f) Gamma distribution - 95% confidence interval

Fig. 10. Goodness of fit test (Anderson–Darling) for various probability density functions for an 11.7-year-old tube.

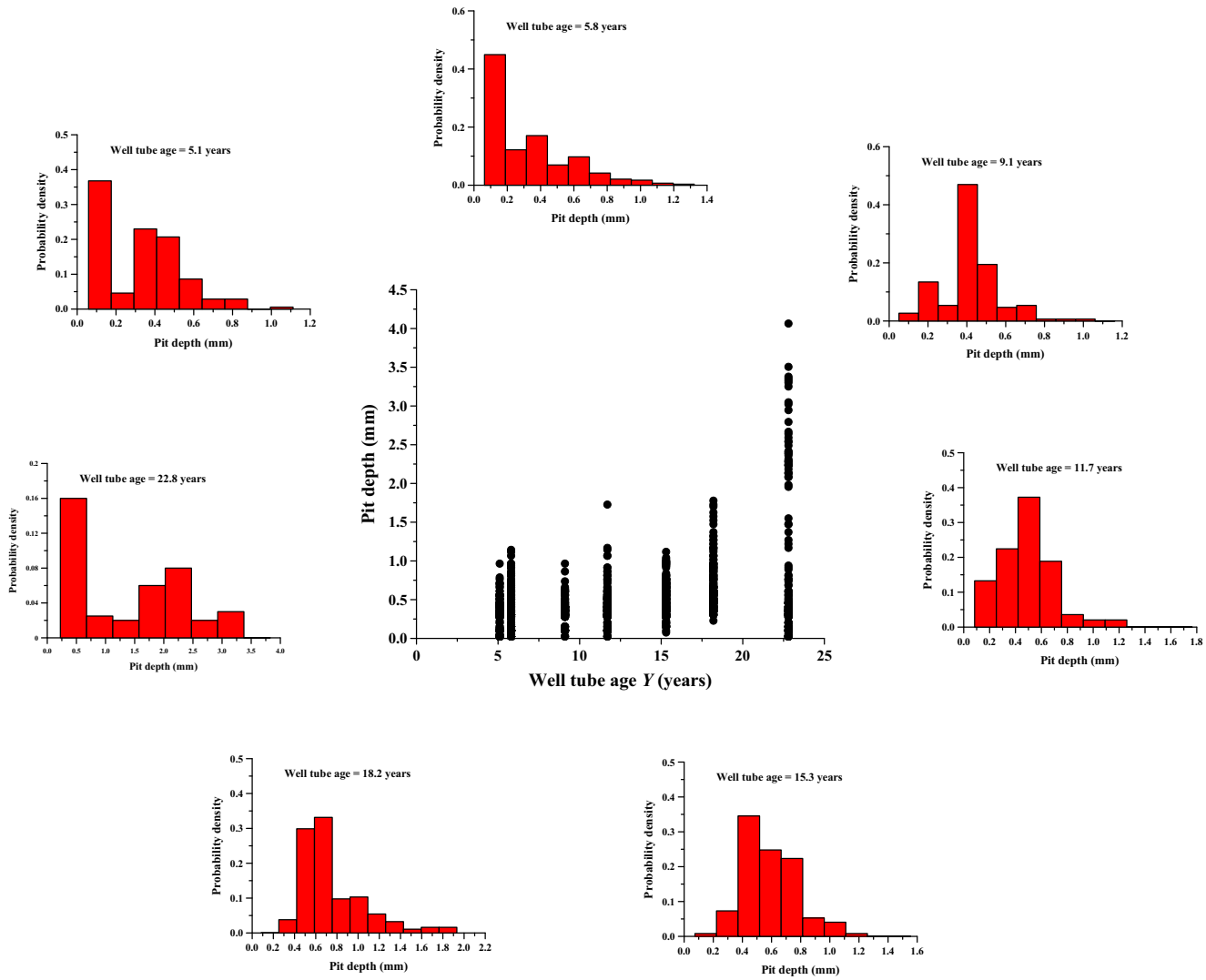

Fig. 11a. Pit depth versus oil well tube age.

and its ratio, respectively. Fig. 10(a–f) show the typical goodness of fit test (Anderson–Darling) for an 11.7-year-old oil well tube. The results of the goodness of fit test indicate that the 2-parameter Weibull function best represents the corrosion progress characteristics of offshore subsea oil well tubes.

4.2. Modelling of time-dependent pit depth

Based on the foregoing statistical analysis, the 2-parameter Weibull function was selected to represent the corrosion characteristics of subsea oil well tubes. The time-dependent pit depth was then modelled using the method of Paik and Kim [20].

Fig. 11(a) shows the corrosion damage (pit depth) as a function of time (oil well tube age) and its relative frequency for each year. The figure shows the distribution of the relative frequency of corrosion loss (pit depth) to be very scattered. As discussed in Section 4.1, however, the relative frequency (probability) distribution of the corrosion damage tends to follow a Weibull distribution. Fig. 11(b) shows the probabilistic characteristics of pit depth as a function of age. It is evident from Fig. 11(b) that the statistical characteristics of the corrosion progress differ with age.

In the statistical modelling of a random variable the effect of the histogram interval (or bin width) is usually significant. The bin width that gives the largest mean value and the smallest coefficient of variation (COV) should be selected [16]. The Doane

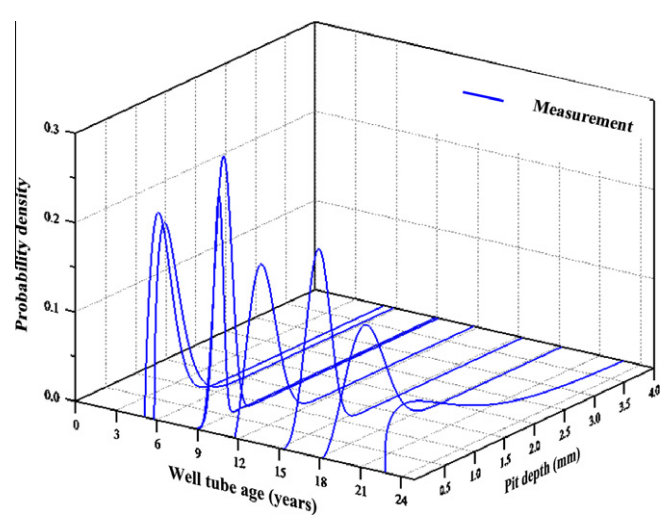

Fig. 11b. Variation in the probability density distribution of pit depth for tubes of different ages.

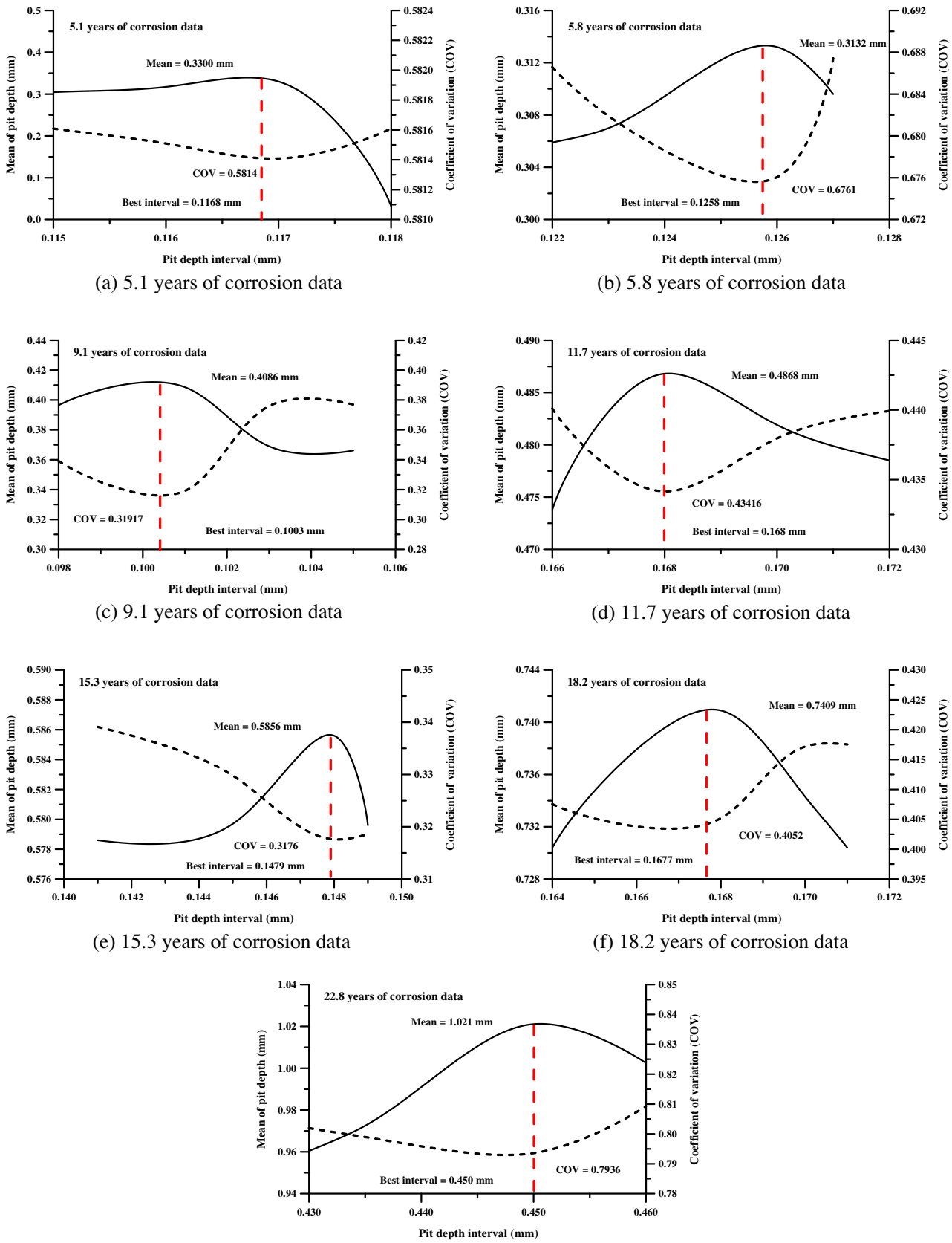

(a) 5.1 years of corrosion data (b) 5.8 years of corrosion data (c) 9.1 years of corrosion data (d) 11.7 years of corrosion data (e) 15.3 years of corrosion data (f) 18.2 years of corrosion data (g) 22.8 years of corrosion data

Fig. 12. Effect of histogram interval (bin width) on the mean and COV of pit depth (the solid lines represent the mean value and the dotted lines represent the COV).

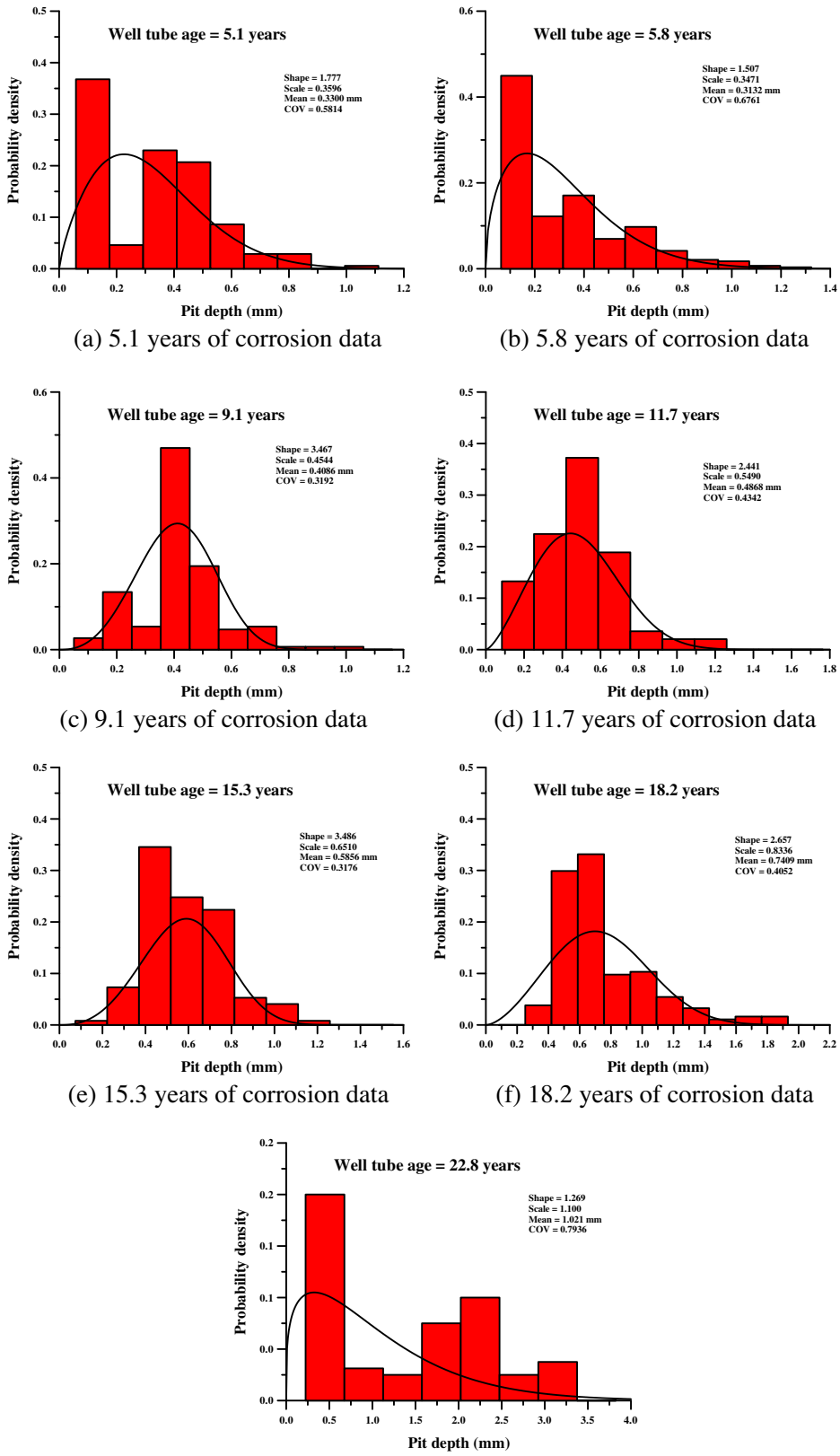

(a) 5.1 years of corrosion data (b) 5.8 years of corrosion data

(c) 9.1 years of corrosion data (d) 11.7 years of corrosion data

(e) 15.3 years of corrosion data (f) 18.2 years of corrosion data

(g) 22.8 years of corrosion data

Fig. 13. Probability density distribution of pit depth and best fit using the 2-parameter Weibull function.

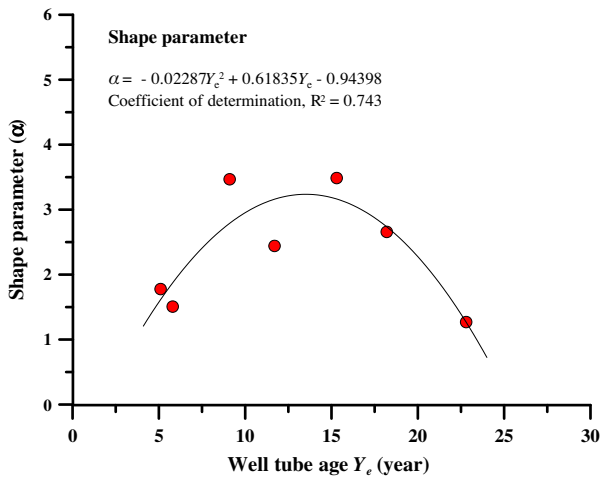

Fig. 14a. Approximation of the shape parameter with the 2-parameter Weibull function.

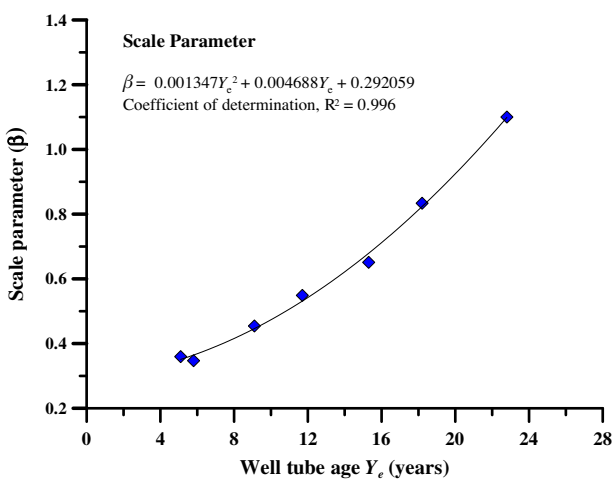

Fig. 14b. Approximation of the scale parameter with the 2-parameter Weibull function.

Table 4
Mean and COV of pit depth for the various oil well tubes.

Target oil well tube	Age (years)	Pit depth mean (mm)	S.D. (mm)	COV
A	5.1	0.3300	0.1861	0.5814
B	5.8	0.3132	0.21	0.6761
C	9.1	0.4086	0.1304	0.3192
D	11.7	0.4868	0.2128	0.4342
E	15.3	0.5856	0.186	0.3176
F	18.2	0.7409	0.3002	0.4052
G	22.8	1.0210	0.8103	0.7936

Note: S.D. = standard deviation, COV = coefficient of variation.

formula [38] is useful for determining the best bin width value. Fig. 12 shows the effect of bin width on the mean and COV of pit depth at different ages, and indicates the bin width value that gives the largest mean value and the lowest COV value.

Table 5
Comparison of the mean and standard deviation of pit depth derived from the measurements and Eq. (4).

Age (years)	Measurements				Eq. (4)			
	α	β	Mean (mm)	S.D (mm)	α	β	Mean (mm)	S.D (mm)
5.1	1.777	0.3596	0.3300	0.1861	1.615	0.3510	0.3144	0.1995
5.8	1.507	0.3471	0.3132	0.21	1.873	0.3646	0.3237	0.1795
9.1	3.467	0.4544	0.4086	0.1304	2.789	0.4462	0.3973	0.1541
11.7	2.441	0.5490	0.4868	0.2128	3.160	0.5313	0.4756	0.165
15.3	3.486	0.6510	0.5856	0.186	3.164	0.6791	0.6079	0.2106
18.2	2.657	0.8336	0.7409	0.3002	2.735	0.8235	0.7327	0.2893
22.8	1.269	1.1000	1.0210	0.8103	1.267	1.0991	1.0206	0.8111

Note: α = shape parameter, β = scale parameter, S.D. = standard deviation.

The 3-parameter Weibull function is given as follows:

$$f(x) = \frac{\alpha}{\beta}\left(\frac{x-\gamma}{\beta}\right)^{\alpha-1} \cdot \exp\left[-\left(\frac{x-\gamma}{\beta}\right)^{\alpha}\right], \tag{1}$$

where, α = shape parameter, β = scale parameter and γ = location parameter.

Because the 2-parameter Weibull function gave the best representation of the corrosion progress of the offshore subsea oil well tubes, $\gamma = 0$ is applied. Eq. (1) can then be rewritten as follows:

$$f_c = \frac{\alpha}{\beta}\left(\frac{Y_e}{\beta}\right)^{\alpha-1} \cdot \exp\left[-\left(\frac{Y_e}{\beta}\right)^{\alpha}\right], \tag{2}$$

where f_c is a function of the corrosion damage depth (pit depth); Y_e is the age of the well tube in years after the breakdown of the coating, which can be given as $Y_e = Y - Y_c$; Y_c is the coating life and Y is the age of the oil well tube structure. Here, the coating life is unknown and is presumed to be zero.

Fig. 13 shows the probability density distribution of pit depth and the best fit with the measured corrosion progress data using the 2-parameter Weibull function. The two parameters α and β can be approximated by the following continuous formula.

$$\alpha = -0.02287Y_e^2 + 0.61835Y_e - 0.94398 \tag{3.a}$$

$$\beta = 0.001347Y_e^2 + 0.004688Y_e + 0.292059 \tag{3.b}$$

Figs. 14(a) and 14(b) confirms the accuracy of Eq. (3).

The following formula is suggested to predict the time-dependent pit depth of offshore subsea oil well tubes:

$$f_c = \frac{\alpha}{\beta}\left(\frac{Y_e}{\beta}\right)^{\alpha-1} \cdot \exp\left[-\left(\frac{Y_e}{\beta}\right)^{\alpha}\right], \tag{4}$$

where, $\alpha = -0.02287Y_e^2 + 0.61835Y_e - 0.94398$, and $\beta = 0.001347Y_e^2 + 0.004688Y_e + 0.292059$.

Eq. (4) can also be used to calculate the corrosion rate at any given time (age) by differentiating the pit depth with respect to the age of the oil well tube Y. Table 4 summarises the mean value and COV of pit depth for the various ages of oil well tube considered.

Table 5 and Figs. 15–17(a) and 17(b) compare the pit depth progress characteristics of offshore oil well tubes as derived from the measurements and Eq. (4). Eq. (4) is in good agreement with the direct measurements of pit depth. The results show that the corrosion rate of offshore subsea oil well tubes tends to speed up once the tubes reach 15 years of age.

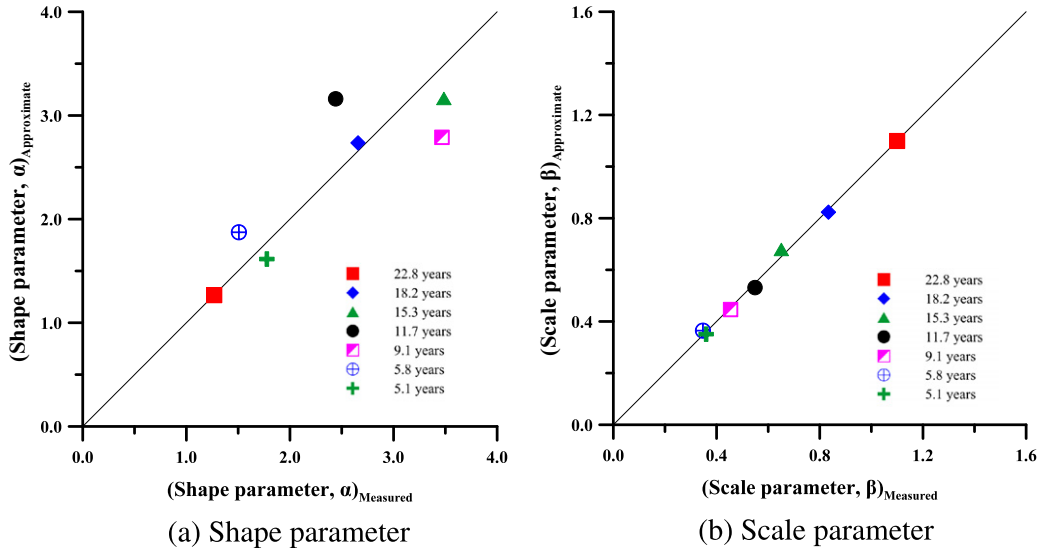

Fig. 15. Comparison of the shape and scale parameter values derived from the measurements and Eq. (4).

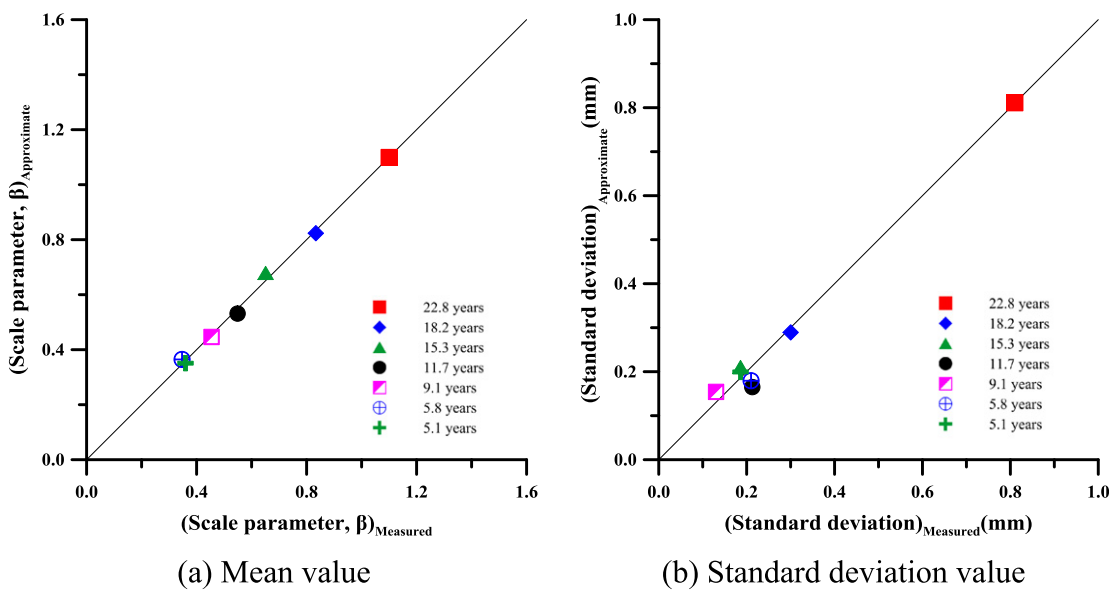

Fig. 16. Comparison of the mean and standard deviation (S.D.) of pit depth derived from the measurements and Eq. (4).

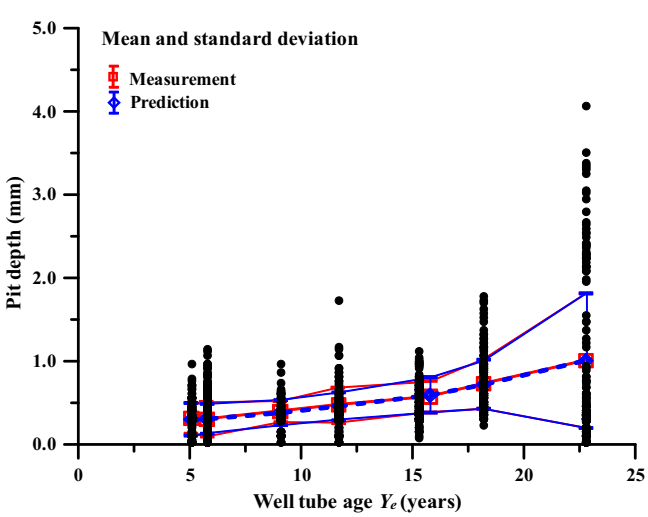

Fig. 17a. Comparison of the mean values of time-dependent pit depth derived from the measurements and Eq. (4).

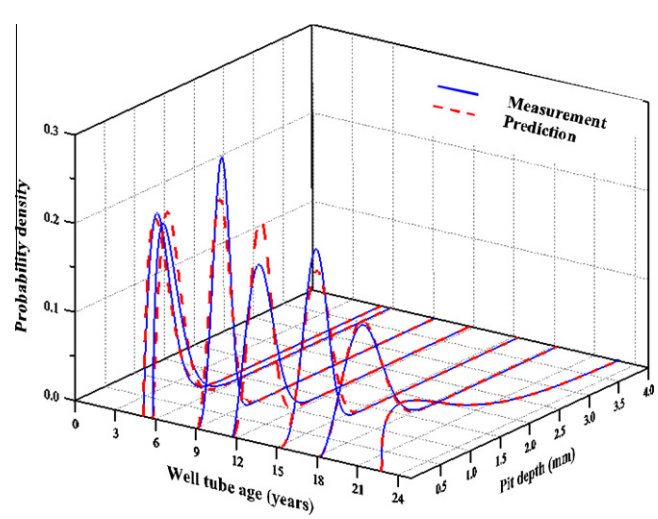

Fig. 17b. Comparison of the probability density distribution of pit depth with time derived from the measurements and Eq. (4).

5. Concluding remarks

The aim of this study was to investigate the progress characteristics of corrosion in offshore subsea oil well tubes and develop an empirical formula for the prediction of the time-dependent corrosion pit depth. The following conclusions are drawn from the findings.

(1) Although it is very hard to obtain direct measurements of offshore subsea oil well tubes, the MIT (Multifinger Imaging Tool) system proves useful in this regard.
(2) The probability density distribution of corrosion pit depth in offshore subsea oil well tubes tends to follow the 2-parameter Weibull function.
(3) The effect of histogram interval (bin width) on the mean and COV values of pit depth is significant in the statistical modelling process. The bin width that gives the largest mean value and the smallest COV value should be selected.
(4) The probability density distribution of pit depth differs with age.
(5) Eq. (4) is in very good agreement with the direct measurements of pit depth with time in offshore subsea oil well tubes.

Acknowledgements

This research was supported by the Basic Science Research Program through the National Research Foundation of Korea (NRF) funded by the Ministry of Education, Science and Technology (Grant No.: K20903002030-11E0100-04610). The study was undertaken at The Lloyd's Register Educational Trust (LRET) Research Centre of Excellence (Ship and Offshore Research Institute) at Pusan National University, Korea. The LRET funds education, training and research programmes in transportation, science, engineering, technology and the safety of life, worldwide, for the benefit of all. The authors are very pleased to acknowledge the help of the anonymous oil and gas company that provided the pit depth measurement database. Thanks are also due to Mr. D.K. Kim, a Ph.D. student for his help in statistical analyses.

References

[1] T. Nakai, N. Yamamoto, Corroded structures and residual strength, in: J.K. Paik, R.E. Melchers (Eds.), Condition Assessment of Aged Structures, CRC Press, New York, 2008 (Chapter 7).
[2] J.K. Paik, A.K. Thayambali, Marine corrosion mechanisms, in: Ship-shaped Offshore Installations Design, Building and Operation, Cambridge University Press, Cambridge, 2007 (Chapter 10).
[3] B.J. Little, J.S. Lee, Microbiologically Influenced Corrosion, Hoboken, John Wiley & Sons, New Jersey, 2007.
[4] A.C. Palmer, R.A. King, Subsea Pipeline Engineering, PennWell Corporation, Oklahoma, 2008.
[5] C. Fu, J. Zheng, J. Zhao, W. Xu, Application of grey rational analysis for corrosion failure of oil tubes, Corros. Sci. 43 (2001) 881–889.
[6] C. Ren, D. Liu, Z. Bai, T. Li, Corrosion behavior of oil tube steel in simulant solution with hydrogen sulfide and carbon dioxide, Mater. Chem. Phys. 93 (2005) 305–309.
[7] M.A. Migahed, I.F. Nassar, Corrosion inhibition of tubing steel during acidization of oil and gas wells, Electrochim. Acta 53 (2008) 2877–2882.
[8] A. Igor, R.E. Melchers, Pitting corrosion in pipeline steel weld zones, Corros. Sci. 53 (12) (2011) 4026–4032.
[9] R.E. Melchers, J.K. Paik, Effect of flexure on rusting of ship's steel plating, Ships Offshore Struct. 5 (1) (2010) 25–31.
[10] J.K. Paik, A.K. Thayamballi, Some recent developments on ultimate limit state design technology for ships and offshore structures, Ships Offshore Struct. 1 (2) (2006) 99–116.
[11] F. Caleyo, J.C. Velázquez, A. Valor, J.M. Hallen, Probability distribution of pitting corrosion depth and rate in underground pipelines: a Monte Carlo study, Corros. Sci. 51 (12) (2009) 1925–1934.
[12] L.Y. Xu, Y.F. Cheng, Reliability and failure pressure prediction of various grades of pipeline steel in the presence of corrosion defects and pre-strain, Int. J. Press. Vessels Pip. 89 (2012) 75–84.
[13] D.D. Leon, O.F. Macías, Effect of spatial correlation on the failure probability of pipelines under corrosion, Int. J. Press. Vessels Pip. 82 (2005) 123–128.
[14] E.S. Meresht, T.S. Farahani, J. Neshati, Failure analysis of stress corrosion cracking occurred in a gas transmission steel pipeline, Eng. Fail. Anal. 18 (2011) 963–970.
[15] Y. Bai, Q. Bai, Subsea Engineering Handbook, Gulf Professional Publishing, Amsterdam, Netherlands, 2010.
[16] J.K. Paik, A.K. Thayamballi, Y.I. Park, J.S. Hwang, A time-dependent corrosion wastage model for seawater ballast tank structures of ships, Corros. Sci. 46 (2004) 471–486.
[17] J.K. Paik, S.K. Kim, S.K. Lee, Probabilistic corrosion rate estimation model for longitudinal strength members of bulk carriers, Ocean Eng. 25 (1) (1998) 837–860.
[18] J.K. Paik, A.K. Thayamballi, Y.I. Park, J.S. Hwang, A time-dependent corrosion wastage model for bulk carrier structures, Int. J. Marit. Eng. 145 (A2) (2003) 61–87.
[19] J.K. Paik, J.M. Lee, J.S. Hwang, Y.I. Park, A time-dependent corrosion wastage model for the structures of single/double hull tankers and FSOs/FPSOs, Mar. Technol. 40 (3) (2003) 201–217.
[20] J.K. Paik, D.K. Kim, An advanced method for the development of an empirical model to predict time-dependent corrosion wastage, Corros. Sci. 63 (2012) 51–58.
[21] R.E. Melchers, M. Ahammed, R. Jeffrey, G. Simundic, Statistical characterization of surfaces of corroded, Mar. Struct. 23 (2010) 274–287.
[22] R.E. Melchers, Probabilistic modelling of immersion corrosion of steels in marine waters, in: Proceedings of the Offshore Mechanics and Arctic Engineering Conference, Rio de Janeiro, 3–8 June 2011.
[23] R.E. Melchers, Corrosion wastage in aged structures, in: J.K. Paik, R.E. Melchers (Eds.), Condition Assessment of Aged Structures, CRC Press, New York, 2008 (Chapter 4).
[24] R.E. Melchers, Modelling of corrosion of steel specimens, in: R.M. Kain, W.T. Young (Eds.), Corrosion Testing in Natural Waters, ASTM STP 1300, American Society for Testing and Materials, Philadelphia, PA, 1997, pp. 20–33.
[25] R.E. Melchers, Mathematical modelling of the diffusion controlled phase in marine immersion corrosion of mild steel, Corros. Sci. 45 (5) (2003) 923–940.
[26] R.E. Melchers, Modeling of marine immersion corrosion for mild and low alloy steels – Part 1: phenomenological model, Corrosion (NACE) 59 (4) (2003) 319–334.
[27] R.E. Melchers, Development of new applied models for steel corrosion in marine applications including shipping, Ships Offshore Struct. 3 (2) (2008) 135–144.
[28] B.B. Chernov, Predicting the corrosion of steel in seawater from its physiochemical characteristics, Prot. Met 26 (2) (1990) 238–241.
[29] B.B. Chernov, S.A. Ponomarenko, Physiochemical modelling of metal corrosion in seawater, Prot. Met 27 (5) (1991) 612–615.
[30] N. Yamamoto, K. Ikegami, A study on the degradation of coating and corrosion of ship's hull based on the probabilistic approach, J. Offshore Mech. Arct. Eng. 120 (3) (1998) 121–128.
[31] C. Guedes Soares, Y. Garbatov, A. Zayed, G. Wang, Non-linear corrosion model for immersed steel plates accounting for environmental factors, Trans. SNAME 111 (2006) 194–211.
[32] S. Qin, W. Cui, Effect of corrosion models on the time-dependent reliability of steel plated structures, Mar. Struct. 15 (2002) 15–34.
[33] D. Najjar, M. Bigerelle, C. Lefebvre, A. Iost, A new approach to predict the pit depth extreme value of a localized corrosion process, ISIJ Int. 43 (2003) 720–725.
[34] A. Jarrah, M. Bigerelle, G. Guillemot, D. Najjar, A. Iost, J.-M. Nianga, A generic statistical methodology to predict the maximum pit depth of a localized corrosion process, Corros. Sci. 53 (2011) 2453–2467.
[35] M. Chowdhury, The changes in mean and variance of midship section properties due to uniform corrosion wear, Ships Offshore Struct. 3 (1) (2008) 67–77.
[36] MIT Survey Report, Petroliam Nasional Berhad (Petronas), Kuala Lumpur, Malaysia, 2011.
[37] T.W. Anderson, D.A. Darling, A test of goodness-of-fit, J. Am. Stat. Assoc. 49 (1954) 765–769.
[38] D.P. Doane, Aesthetic frequency classifications, Am. Stat. 30 (4) (1976) 181–183.

PHILOSOPHICAL TRANSACTIONS OF THE ROYAL SOCIETY A

rsta.royalsocietypublishing.org

Review

Cite this article: Muggeridge A, Cockin A, Webb K, Frampton H, Collins I, Moulds T, Salino P. 2014 Recovery rates, enhanced oil recovery and technological limits. *Phil. Trans. R. Soc. A* **372**: 20120320.
http://dx.doi.org/10.1098/rsta.2012.0320

One contribution of 13 to a Theme Issue 'The future of oil supply'.

Subject Areas:
energy

Keywords:
enhanced oil recovery, crude oil recovery, water injection, miscible gas, water alternating gas, chemical flooding

Author for correspondence:
Ann Muggeridge
e-mail: a.muggeridge@imperial.ac.uk

Recovery rates, enhanced oil recovery and technological limits

Ann Muggeridge[1], Andrew Cockin[2], Kevin Webb[2], Harry Frampton[2], Ian Collins[2], Tim Moulds[3] and Peter Salino[2]

[1]Department of Earth Science and Engineering, Imperial College, London SW7 2AZ, UK
[2]BP Exploration and Production, Sunbury-on-Thames TW16 7LN, UK
[3]BP Exploration Operating Company Ltd, Aberdeen AB21 7PB, UK

Enhanced oil recovery (EOR) techniques can significantly extend global oil reserves once oil prices are high enough to make these techniques economic. Given a broad consensus that we have entered a period of supply constraints, operators can at last plan on the assumption that the oil price is likely to remain relatively high. This, coupled with the realization that new giant fields are becoming increasingly difficult to find, is creating the conditions for extensive deployment of EOR. This paper provides a comprehensive overview of the nature, status and prospects for EOR technologies. It explains why the average oil recovery factor worldwide is only between 20% and 40%, describes the factors that contribute to these low recoveries and indicates which of those factors EOR techniques can affect. The paper then summarizes the breadth of EOR processes, the history of their application and their current status. It introduces two new EOR technologies that are beginning to be deployed and which look set to enter mainstream application. Examples of existing EOR projects in the mature oil province of the North Sea are discussed. It concludes by summarizing the future opportunities for the development and deployment of EOR.

© 2013 The Authors. Published by the Royal Society under the terms of the Creative Commons Attribution License http://creativecommons.org/licenses/by/3.0/, which permits unrestricted use, provided the original author and source are credited.

Royal Society Publishing

1. Introduction

The majority of oil companies today are focusing on maximizing the recovery factor (RF) from their oilfields as well as maintaining an economic oil rate. This is because it is becoming increasingly difficult to discover new oilfields. Most of the sedimentary basins that might contain oil have already been explored and new discoveries tend to be small. Those basins that remain unexplored are in remote and environmentally sensitive areas of the world (e.g. the Arctic and the Antarctic). Although there are huge volumes of unconventional hydrocarbons, such as the very viscous oils, oil shales, shale gas and gas hydrates, many of the technologies for exploiting these resources are either very energy intensive (e.g. steam injection into heavy oil), politically or environmentally sensitive (e.g. as seen in recent adverse press coverage of 'fraccing' to recover shale gas) or are not yet ready to be applied at scale.

The average RF from mature oilfields around the world is somewhere between 20% and 40% [1–3]. This contrasts with a typical RF from gas fields of between 80% and 90%. At current production rates existing proven oil reserves will last 54 years [4]. This is probably as good as it has ever been. Improving oil recovery to that typical of gas fields could more than double the time for which oil is available or alternatively allow for increased production rates. This would provide more time for an increasingly energy-hungry world to develop alternative energy sources and technologies.

Crude oil and natural gas are found in large underground deposits (usually termed reservoirs or pools) in sedimentary basins around the world. The largest oil reservoir in the world (the Arab D limestone in Ghawar in Saudi Arabia) is approximately 230 km long and 30 km wide and 90 m thick [5]. While most commercially exploited minerals and ores exist as solid rocks and have to be physically dug out of the ground, oil and gas exist as fluids underground. They occupy the connected pore space (figure 1) within strata of sedimentary rocks (figure 2), typically sandstones or carbonates.

Oil and gas are extracted by creating pressure gradients within the reservoir that cause the oil and/or gas to flow through the interconnected pores to one or more production wells. In most oilfields the pressure gradients are maintained by injecting another fluid (usually water but sometimes gas and termed 'water flooding' or 'gas flooding', respectively) into the reservoir through injection wells. The injected water displaces the oil and occupies the pore space that it originally occupied. By contrast, gas fields are normally exploited simply by reducing the pressure at the production well using compressors. The gas in the reservoir expands as the pressure drops and thus flows to the production well.

Enhanced oil recovery (EOR) involves injecting a fluid into an oil reservoir that increases oil recovery over that which would be achieved from just pressure maintenance by water or gas injection. For lighter oils, these processes include miscible gas injection [6,7], water alternating gas (WAG) injection [8], polymer flooding [9], flow diversion via polymer gels [10] and the use of surfactants [11]. For more viscous (so-called heavy) oils these processes include steam injection and air injection (leading to *in situ* combustion) [12]. The majority of EOR processes used today were first proposed in the early 1970s at a time of relatively high oil prices.

Improved oil recovery (IOR) is a term that is sometimes used synonymously with EOR [13] although it also applies to improvements in oil recovery achieved via better engineering and project management, e.g. identifying volumes of oil that have been bypassed during water injection using seismic surveying and then drilling new wells to access those oil pockets [14,15]. It was first introduced in the late 1980s when the oil price dropped and as a result there was less interest in EOR technologies. At this time there were significant improvements in computer processing speed, computer memory and seismic analysis [16]. Improved computing power enabled engineers to build more complex geological models and thus estimate the effect of reservoir heterogeneity on flow [17–19]. Improved seismic analysis algorithms combined with more powerful computers meant that engineers and geoscientists could use 'four-dimensional' seismic surveying, involving the comparison of seismic data taken at different times, in combination with reservoir simulation to identify bypassed volumes of oil on the scale of

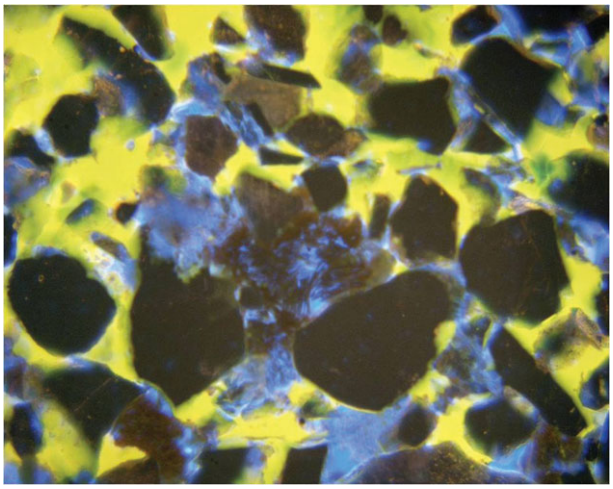

Figure 1. A thin section through an oil-bearing sandstone showing how the oil (dyed blue) and water (dyed yellow) occupy the spaces between the sand grains. The pore space was originally filled with water before oil migrated into the reservoir rock displacing the water.

Figure 2. Photograph of the Bridport sands that are exposed in cliffs near West Bay, UK. These rocks form one of the reservoirs in the Wytch Farm oilfield that is found near Bournemouth, UK. (Online version in colour.)

hundreds of metres horizontally and tens of metres vertically [16]. Developments in measurement while drilling [20] and a new capability to drill deviated, horizontal and multi-lateral wells meant that engineers could target these bypassed accumulations very accurately and drain them.

Using combinations of traditional EOR and IOR technologies it has been possible to achieve RFs of between 50% and 70% [21,22] for some fields but this is still less than the typical RF for a gas field. It is believed that much of this remaining oil is trapped or bypassed in volumes that cannot be accessed by IOR technologies, on lengthscales that cannot be resolved by seismic surveying or accessed by drilling new wells.

New and improved EOR processes are needed to access this remaining oil and improve RFs further while maintaining economic oil production rates. This paper will review existing and emerging EOR technologies, discussing the underlying science, its application and its limitations. In particular, it will focus on recent advances in our understanding of the nature of wettability

in rocks and discuss the opportunities arising from the much wider range of polymers that is now available commercially. These two factors have driven a renewed interest in existing EOR technologies and the development of new methods. We will concentrate primarily on the recovery of conventional, light oil from fields that have already been or are about to be developed. The recovery of heavy and unconventional oils will not be discussed in any detail, nor will we consider the recovery of oil by IOR techniques except in passing.

2. Why is recovery so low?

Water flooding is currently the preferred recovery technique for most reservoirs because of the higher sustained oil production rates, and the overall higher RFs, that are obtained compared with the case if water were not injected. Oil production without injection is often termed primary recovery. This is because the first wells drilled in a field development are typically production wells to enable oil production and thus the start of income from a field. Where reservoir pressure is well above the bubble point, primary production can be continued for some time before additional pressure support is required to prevent gas coming out of solution in the reservoir.

During depletion, oil flows through the production wells to the surface because the pressure at the base of the well exceeds that exerted by the hydrostatic head of the column of oil in the well. Initially, this occurs naturally but over time the oil rate tends to decrease as the reservoir pressure decreases. In the absence of water injection, pumping may be used to maintain oil rate at economic levels. If reservoir pressure falls below the oil bubble point pressure, gas that was initially dissolved in the oil will come out of solution and, because it has a much lower viscosity, will flow preferentially to the production well. At the same time the viscosity of the remaining oil increases, reducing its mobility further. This will reduce the oil production rate further (although it may increase the total (oil plus gas) production rate through reducing the hydrostatic head in the well). Water (or gas) injection is usually applied before this happens so as to maintain reservoir pressure above the bubble point. For this reason, it is sometimes known as secondary recovery.

Water flooding is relatively cheap, especially for offshore fields because of the ready availability of seawater, although care has to be taken to ensure that the injected water does not result in unwanted, adverse reactions in the reservoir. In some cases injected brines may react with the naturally occurring water in the reservoir (termed connate water) to form scale while injecting very pure water rather than brine may result in clay swelling. Both of these may block the rock pores and reduce the rock permeability. The cost of drilling additional wells for injection is more than outweighed by the increased oil rates that result. Re-injection of gas (produced along with the oil) is used when there is no easy, economic way to export it for sale.

The factors affecting RF from water flooding (and gas flooding) can be understood by considering the following approximate relationship [23]:

$$\mathrm{RF} = E_{PS} \times E_S \times E_D \times E_C, \tag{2.1}$$

where (i) RF is the recovery factor which is defined as the volume of oil recovered over the volume of oil initially in place (OIIP), both measured at surface conditions. (ii) E_{PS} is the microscopic displacement efficiency. This describes the fraction of oil displaced from the pores by the injected water, in those pores which are contacted by the water. (iii) E_S is the macroscopic sweep efficiency—the proportion of the connected reservoir volume that is swept by the injected fluid(s). This is principally affected by heterogeneity in rock permeability and by gravitational segregation of the fluids. (iv) E_D is the connected volume factor—the proportion of the total reservoir volume connected to wells. This represents the fact that sealing faults or other low-permeability barriers may result in compartments of oil that are not in pressure communication with the rest of the reservoir. (v) E_C is the economic efficiency factor, representing the physical and commercial constraints on field life such as facilities life, capacity to deal with produced gas and water, reservoir energy (the reservoir pressure may become so low that fluids cannot be produced).

It can even be seen that if each of the efficiency factors is a very respectable 80% then the overall RF is only 41%. Increasing RF therefore requires each of these factors to be increased to close to 100%.

EOR methods are targeted at increasing E_{PS} and E_S while IOR methods also aim to increase E_D and to some extent E_S. Improving E_C is mainly the role of the production and facilities engineers but is also affected by EOR methods if these reduce the amount of water and gas produced alongside the oil, enabling oil to be produced for longer before economic limits are reached.

(a) Factors influencing microscopic displacement efficiency

The typical microscopic displacement efficiency from a water flood is 70% or less. This is mainly because oil ganglia become trapped in the pore space by capillary effects [24,25] but E_{PS} is also affected by the relative permeability characteristics of the rock [26], which control the relative mobility of the oil and water when moving through the pore space.

The importance of pore-scale capillary effects on a displacement can be quantified by the capillary number

$$\mathrm{Ca} = \frac{v\mu}{\gamma}, \tag{2.2}$$

where v is the interstitial velocity, μ is the fluid viscosity and γ is the interfacial tension (IFT) between the displaced and displacing fluid. When $\mathrm{Ca} < 10^{-5}$ flow is dominated by capillary effects and, in particular, capillary trapping is likely to occur. The typical interstitial velocity in an oilfield displacement (distant from the wells) is approximately $10^{-5}\,\mathrm{m\,s^{-1}}$ while the viscosity of a typical light oil is similar to that of water (approx. 10^{-3} Pa s). The IFT between brine and oil is approximately $70\,\mathrm{mN\,m^{-1}}$ so for a typical water flood the capillary number is approximately 2.5×10^{-7}. It is generally not possible to apply a sufficiently large pressure gradient between wells to significantly increase the interstitial velocity or to maintain this velocity while injecting a high-viscosity fluid, thus the only way for a reservoir engineer to increase the capillary number is to reduce the IFT. Based on the above calculations this means that the IFT between the oil and the displacing fluid has to be less than approximately $0.1\,\mathrm{mN\,m^{-1}}$ in order to minimize capillary trapping.

Both capillary and relative permeability effects are also influenced by the wetting behaviour of the rock in which the oil is found. As discussed in the previous paragraph, if the rock is water wet then there is a higher residual oil saturation (the proportion of oil which remains permanently trapped by capillary effects at the pore scale). This is caused by the growth in the water film on the rock surface during water injection, which ultimately leads to water bridging at the pore throats (so-called snap-off [27]; figure 3) trapping droplets of oil within the pores. As a result, little oil is produced after water breakthrough at the production well unless a higher pressure drop is applied (which is impractical in most cases).

If the rock is oil wet, then the proportion of oil trapped by capillary effects is much lower, as oil continuity is maintained over the rock surfaces and through the pore throats, but water breakthrough is earlier and there is a long period of time during which oil and water are produced simultaneously. The net result is that overall recovery is generally higher [28] if the reservoir rock is oil wet but only after a very large throughput of water.

Most oil reservoir rocks are thought to have a heterogeneous wettability, usually termed 'mixed wettability', in that larger pores and throats have both water- and oil-wet surfaces but smaller pores remain mainly water wet [29,30]. It is believed that the reservoir rock changes from an initially water-wet state to this mixed wettability state after the migration of oil into the reservoir [31,32]. Polar compounds in the oil alter the wettability of the rock by a range of interactions including precipitation of asphaltenes, acid–base interactions and ion binding between charged sites on the pore walls and polar hydrocarbon moieties involving higher valency ions in the water that shares the pore space with the oil [31,33–35]. The wettability of reservoir rock thus depends upon its mineralogy, the crude oil composition, the connate water composition and the pore size distribution.

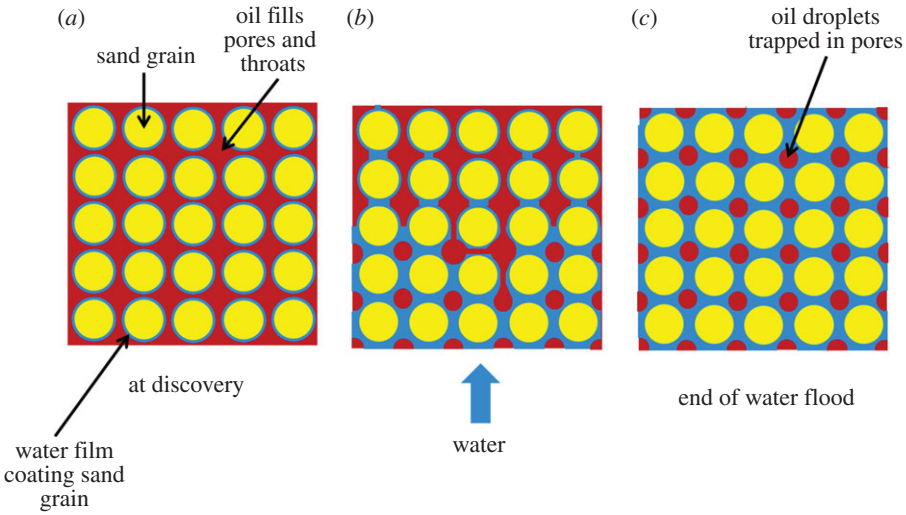

Figure 3. Illustration of oil trapping in a water-wet rock. (*a*) At discovery the sand grains are coated with a thin water film and the pores are filled with oil; (*b*) as water flooding progresses the water films become thicker until (*c*) the water films join and oil continuity is lost.

During water flooding in a mixed wettability rock oil and water drain simultaneously through the pore space, snap-off is reduced as most throats have both oil- and water-wet surfaces and thus there is less capillary trapping of oil. This simultaneous drainage of water and oil through the pore space behind the water front combined with the lower residual oil saturation means that more oil is recovered than when the rock is either water or oil wet [36,37].

Increasing microscopic displacement efficiency depends upon finding ways to (i) reduce capillary effects, by reducing the oil–water (or gas) IFT, and (ii) modify the rock wettability to the optimum mixed wettability state.

(b) Factors influencing macroscopic sweep efficiency

The macroscopic sweep efficiency of a water flood is principally affected by the geological heterogeneity in the reservoir, which controls the spatial distribution of porosity and permeability. Rock permeability is dependent on the number, size and connectivity of the pores in the rock. The permeability of a typical reservoir rock is approximately $10^{-13}\,\mathrm{m}^2$. A very good reservoir rock might have permeability as high as $10^{-11}\,\mathrm{m}^2$ while a permeability of $10^{-15}\,\mathrm{m}^2$ would be considered very poor. It is controlled by the size of the sediment grains from which the rock was formed, their packing and the subsequent diagenesis (chemical alteration) and cementation (mineral deposition) around those grains. The patterns of grains forming a sedimentary rock depend upon the depositional environment in which the original sediments were formed. These result in permeability heterogeneities with lengthscales from millimetres to kilometres (figure 4).

Higher permeability channels or layers (often described as 'thief zones') through the rock are one common, adverse manifestation of geological heterogeneity. The injected water flows preferentially through these zones, bypassing volumes of oil contained in the lower permeability portions of the reservoir. This results in early water production along with the oil and a reduced RF (figure 5).

A particular problem is that the distribution of permeability in a reservoir is usually very uncertain. It is possible to infer the general characteristics of the heterogeneity from the depositional environment and sometimes to correlate specific rock layers between wells, but there is virtually no information about the detailed permeability distribution on smaller lengthscales (e.g. [39,40]). This means that statistical approaches, often based on limited numbers

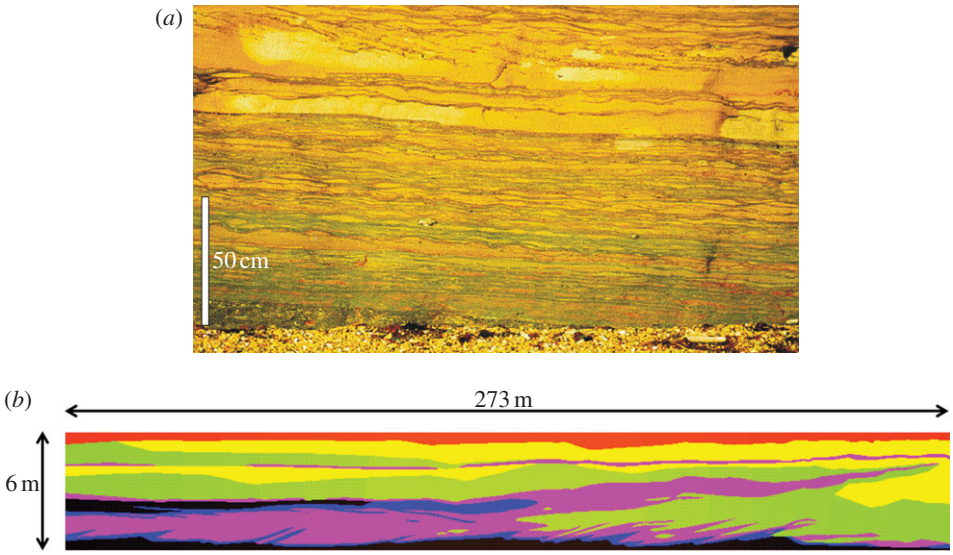

Figure 4. Examples of the types of geological heterogeneities encountered in sandstone oil reservoirs. These examples come from rocks deposited in a deltaic environment. (*a*) Photograph of a heterolithic facies with permeability variations on a centimetre lengthscale vertically and a 10 cm lengthscale horizontally (after Jackson *et al*. [38]). (*b*) Interpreted picture of tidal bar deposits. The lengthscale of these heterogeneities is approximately 100 m. (Online version in colour.)

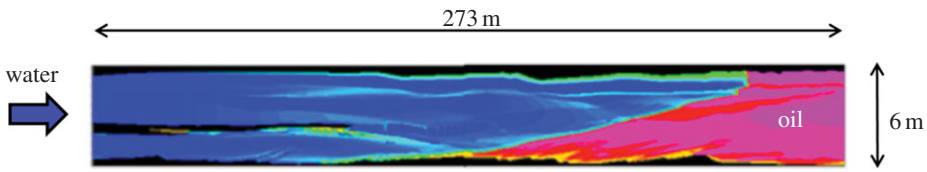

Figure 5. A numerical simulation of a water flood through a heterogeneous reservoir. Flow is from left to right. The oil is coloured red and the water saturation is shown in shades of blue. The water has flowed preferentially through the higher permeability parts of the reservoir, resulting in early water breakthrough at the production well and regions of bypassed oil that will not be recovered.

of realizations of the possible reservoir heterogeneity, are needed when attempting to predict reservoir performance (e.g. [19]).

The effect of geological heterogeneity is exacerbated if the injected fluid has a much lower viscosity than the oil, as is the case when gas is injected instead of water [41–45]. This effect is characterized by the mobility ratio M, which compares the mobility of the saturating (S) and displacing (D) phases in the porous medium

$$M = \frac{\mu_S k_{rD}(S_{or})}{\mu_D k_{rDS}(S_{wc})}, \tag{2.3}$$

where $k_{rD}(S_{or})$ is the relative permeability of the porous medium to the displacing phase at the residual oil saturation S_{or}, $k_{rDS}(S_{wc})$ is the relative permeability of the oil to the displacing phase at the immovable water saturation S_{wc} and μ is the viscosity of the fluid. This is derived from the Darcy equation [46]. The viscosity component of this equation is usually dominant. Even in a homogeneous reservoir, the macroscopic sweep will be reduced when $M > 1$ owing to unstable viscous fingering ([43,47–49]; figure 6), where fingers of the displacing fluid develop along the gas–oil interface, rather than the more efficient even contact zone. A typical oil–water viscosity ratio is about 2 while a typical gas–oil viscosity ratio is about 20 [49]. In most cases, it

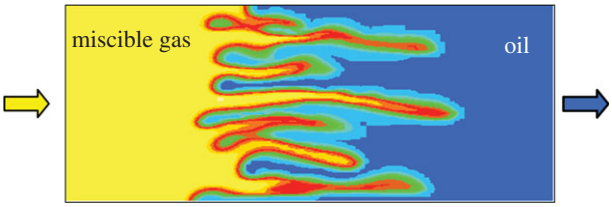

Figure 6. A numerical simulation of viscous fingering seen when low-viscosity gas displaces higher viscosity oil. The viscosity ratio in this simulation is 10. Flow is from left to right. (Online version in colour.)

is channelling caused by the reservoir heterogeneity rather than viscous fingering that dominates macroscopic sweep.

Macroscopic sweep may also be affected by gravitational segregation but this is more often observed in gas–oil rather than water–oil displacements because of the higher density contrast between gas and oil [6]. The gas tends to rise above the oil because of its low density and then flow rapidly along the top of the reservoir in an unstable gravity tongue [50] because of its low viscosity. This can result in very early gas breakthrough and poor vertical sweep efficiency.

Improving the macroscopic sweep efficiency depends upon finding techniques that minimize the impact of geological heterogeneity. This is usually achieved by a mixture of viscosity modification of the injected fluid and/or flow diversion in which the water is diverted from the higher permeability zones in the reservoir into the lower permeability rock still containing displaceable oil. In gas floods, it is also important to minimize gravitational segregation.

3. Overview of conventional enhanced oil recovery processes

As noted above, the purpose of EOR technologies is to improve the microscopic displacement efficiency and/or the macroscopic sweep efficiency over that obtained from water flooding. Traditionally these involved adding chemicals to the injected water to change its viscosity and/or reduce the IFT with oil, or injecting other fluids into the reservoir (such as carbon dioxide, nitrogen or hydrocarbon gases) that have a very low IFT with the oil (less than $0.1\,\mathrm{mN\,m^{-1}}$). Most EOR processes are thus more expensive to implement than a conventional water flood and only become economically attractive for larger oilfields and when the oil price is high.

(a) Miscible gas injection

Miscible gas injection is an EOR process that improves microscopic displacement efficiency by reducing or removing the IFT between the oil and the displacing fluid (the miscible gas). When used after a water flood this has the effect of re-establishing a pathway for the remaining oil to flow through and results in a very low residual oil saturation (2% has been measured in reservoir cores recovered from gas swept zones [51]). The drawback of this process is that the gas is both less viscous and less dense than the oil. As a result, these schemes often have a lower macroscopic sweep efficiency as they are adversely affected by viscous fingering [43,47–49], heterogeneity [42,44] and gravity [49,50].

The injected gas may be hydrocarbon gas, carbon dioxide or nitrogen depending on what is available and the reservoir conditions. CO_2 is miscible with oil at a relatively low pressure and temperature but obviously requires a source of CO_2. Past applications were in fields near natural sources of CO_2 [52,53]. It can result in problems with corrosion of steel pipe unless care is taken in the design of wells, flowlines and facilities [54] as well as provision for the separation of the CO_2 from the hydrocarbon gas when produced. Nitrogen requires a relatively high reservoir pressure for miscibility and involves the use of additional equipment to separate it from the air. As a result, it has not been widely used [53]; the Mexican supergiant Cantarell field is the best

known example [55]. Hydrocarbon gas is usually readily available from the field itself or adjacent fields and is thus most widely used, especially in fields where there is no ready market for the gas [22,51,53,56]. In most cases, however, the produced gas that was originally associated with the oil has to be artificially enriched with heavier components in order to make it miscible or nearly miscible with the oil. It may also have to be supplemented with gas from other sources or water injection (see §3*b*) because the volume of produced gas, when re-injected, may not be sufficient to maintain reservoir pressure above the minimum miscibility pressure (MMP).

It is more usual for the injected hydrocarbon gas to be nearly miscible with the oil rather than miscible on first contact. Miscibility then develops between the fluids through the exchange of components, commonly referred to as multi-contact miscibility, resulting in the gas becoming heavier as it passes through the oil and/or the oil becoming lighter [6,7]. However, even if the gas does not achieve full miscibility with the oil there are likely to be pore-scale displacement benefits compared with a water flood as gas components may dissolve in the oil, causing its volume to increase and its viscosity to reduce. As a result it is possible for an immiscible gas flood to result in a lower residual saturation than a water–oil displacement.

(b) Water alternating gas

WAG injection is an EOR process that was developed to mitigate the technical and economic disadvantages of gas injection. It is the most widely applied and most successful traditional EOR process [8,56].

It involves the injection of slugs of water alternately with gas although sometimes the two fluids are injected simultaneously (termed SWAG). Usually the gas is first contact miscible or multi-contact miscible with the oil but this is not always the case. Injecting water alternately with the gas reduces the volume of gas required to maintain reservoir pressure. It also reduces the tendency for the gas to finger or channel through the oil as the presence of mobile water in the pore space reduces the gas mobility through relative permeability effects [6]. Vertical sweep efficiency is also improved as water, being heavier than oil, tends to slump towards the bottom of the reservoir while the gas, being lighter, rises to the top [8].

Although the majority of WAG applications in the field have been successful, the incremental recovery achieved is generally less than that predicted [8,56]. Early gas breakthrough and a reduced macroscopic sweep, owing to channelling or gravity over-ride, are common. In addition, there are often operational problems. In particular, injectivity can be lower than expected owing to a reduced total fluid mobility near the well as a result of three-phase relative permeability effects and/or a reduced hydrostatic head in the injection well during gas injection.

(c) Chemical flooding

Chemical flooding is a term that is used to describe the addition of chemicals to the water. Depending on the process, these may change the IFT of water with oil (usually surfactants and alkalis) and/or make the water viscosity match that of the oil (polymers). Chemical flooding has been an option for EOR since the mid-1960s [57]. Early projects using polymer alone were soon supplemented by adding surfactants [58] developed to reduce the water–oil IFT and increase the recovery. Soon afterwards alkalis were added to reduce adsorption of the chemicals by the rock and form added surfactants from charged oil molecules in the reservoir [59].

4. Polymer flooding

One means of achieving a more favourable mobility ratio, and thus improve macroscopic sweep, in a water flood is to viscosify the water. This has most often been achieved using high molecular weight water-soluble polymers of 2-propenamide (acrylamide) and 2-propenoic acid (acrylic acid) as the partly neutralized sodium salt in a ratio of about 70 : 30 of polymer to acid by weight [60,61]. The polymers typically have a molecular weight (or relative molecular mass)

of 9–25 million daltons. When dissolved in water, the solutions have a viscosity that depends on the polymer concentration, polymer molecular weight, temperature, water salinity and the concentration of divalent ions. Other polymers, such as xanthan gum [60,61], have been used for the benefit of the improved viscosity yield in more saline water, but these have often been consumed by anaerobic sulfate-reducing bacteria resident in oil reservoirs causing the generation of dissolved hydrogen sulfide (commonly known as known as 'souring').

Polymer flooding can recover a substantial increment of the oil in place, typically 8%, at an additional cost of between US$8 and US$16 per incremental barrel [62], but even after 46 years there are difficulties that limit the use of this technology [61]. Large volumes are needed to make the process work at the field scale. The polymers are most effectively supplied as a dried powder but the equipment needed to dissolve them at suitable rates is bulky and there may not be space for this to be retrofitted on offshore platforms. The resultant solutions are vulnerable to shear damage at high shear rates (over about $1000\,\mathrm{s}^{-1}$) and are particularly damaged by extensional shear. Increasing the viscosity of the injected fluid inevitably makes it more difficult to inject that fluid into the reservoir and, if the polymer solution has not been properly prepared, debris may actually plug the pore space around the well-bore [63]. Once in the reservoir, the polymer molecules are unstable at temperatures above approximately 70°C depending on the water salinity and ionic composition. The mechanisms of thermal degradation are hydrolysis of the amide groups to acid followed by 'salting out' (precipitation, mainly driven by the interaction of the acid groups with calcium ions) of the polymer, or free radical (redox) depolymerization resulting in smaller molecules with a lower viscosity.

These difficulties have not prevented the use of polymer flooding in the industry but have limited its extent, with most of the use being in China [64], initially as the result of government policy requiring oil companies to maximize recovery. The recent rise in oil price has initiated a renaissance of the technique among the international oil companies with applications underway in Angola [65] and Oman [66] as well as many being planned for other regions including the UK North Sea [67].

5. Alkaline surfactant polymer flooding

Alkaline surfactant polymer (ASP) flooding aims to improve microscopic displacement efficiency by reducing the IFT between the water and oil through the addition of a surfactant to the water, while matching the oil and water mobility through the addition of polymer [68]. Alkali is also added to the water to reduce adsorption of the surfactant onto the pore walls and to control the local salinity to ensure minimum IFT. It can also alter the rock wettability [68–70]. Alkali–surfactant mixtures have also been used to improve macroscopic sweep during WAG. In this process, the gas mobility is further reduced by adding alkali and surfactant to the injected water and thus creating a foam within the pore space [68,71,72]

Like polymer flooding, ASP flooding can significantly improve RFs [73–75] with incremental costs quoted to be as low as $2.42 per incremental barrel for an onshore field [76]; however, like polymer flooding, there are a number of difficulties which have limited widespread field application, especially offshore [61]. Operational difficulties include the large volumes of chemicals that have to be transported to remote sites and then stored on platforms where space is limited. Additional produced fluid processing is needed as ASP flooding results in the production of emulsions with droplets as small as $10\,\mu\mathrm{m}$ in diameter. Finally produced fluids (containing the ASP chemicals) need to be disposed of without impacting the environment. Technical difficulties include the fact that the chemical mix needs to be carefully designed for the fluids to be encountered in the field. ASP flooding works best with relatively low-salinity water (often optimal performance is achieved by the use of a salinity gradient during injection of the different stages), but, offshore, seawater is the only source of injection water so desalination or alternative chemicals may be required.

Despite these difficulties, ASP flooding was applied onshore in the early 1980s when the oil price was high. There has been a recent resurgence of interest as oil prices have increased to the

point where the process is once again economic but the only recent large field-scale application outside Daqing [73] in China is in Oman [75].

(a) Flow diversion

The final type of EOR process commonly applied in light oil reservoirs is that of flow diversion. Unlike other EOR processes, flow diversion does not involve displacing the oil with another fluid, from injection to production well. Instead it involves changing the path of the injected water (or gas) through the reservoir so it contacts and displaces more oil. Until recently, this was typically achieved by injecting a polymer solution with a suitable cross-linker into the higher permeability zones of the formation around the injection well. After injection was complete the polymer and cross-linker reacted to form a gel in the near well-bore region which reduced the absolute permeability of that zone and/or its relative permeability to water [76–80]. The most widely applied treatment of this type consisted of polyacrylamide as the polymer and a Cr(III)–carboxylate complex as the cross-linker [78], although other polymers and cross-linkers are used if the reservoir is particularly hot [81] or the water is saline.

The object of the exercise is to reduce the permeability [78,79] and/or relative permeability [80] of a zone or zones in which water or gas is preferentially flowing. After a successful treatment more water (or gas) will flow into adjacent oil-bearing zones, displacing the oil therein.

Using careful target selection and evaluation and, detailed planning, placement and reagent formulation, many treatments have recovered profit above cost and have been declared commercial successes [79,82,83]. At their best the benefits from such treatments can endure for many years [83], e.g. a well in the Prudhoe Bay field continued producing a high proportion of oil compared with water for 5 years after treatment. In many other cases, however, no benefits were observed or died out after weeks or months [77,83].

In order for this type of flow diversion treatment to be successful, the treated zone needs to be physically isolated from adjacent oil-bearing zones by impermeable shales that extend from the injection well to the production well. If this is not the case then (i) gel may also form in the hydrocarbon-bearing zones, reducing oil production and reducing injectivity/productivity, or (ii) water will simply flow around the zone containing the gel and enter the thief zone further into the reservoir (figure 7) [84]. This is a significant limitation as there are not many reservoirs where the shales are in the right place and laterally extensive, and it is difficult to determine whether such a laterally extensive shale is indeed continuous.

6. Enhanced oil recovery deployment

As noted above there are significant practical and economic challenges as well as technical challenges that need to be addressed before EOR technologies can be deployed in the field. Reviewing the development of gas injection as an EOR technology in the North Sea provides insight into the challenges that newer EOR technologies are likely to face in a harsh offshore environment.

We examine a North Sea gas injection EOR scheme that has been in operation for a number of years: the Magnus field in the UK Continental Shelf (UKCS). It is the most northerly producing field in the UK sector of the North Sea. It originally contained approximately 2.4×10^8 m^3 (or 1.5×10^9 barrels) of oil (measured at surface conditions). Like most oilfields, one company operates the field (in this case BP with 85% equity) although it is co-owned by a number of other companies (in this case JX Nippon Exploration & Production (7.5%), Eni (UK) Ltd (5%) and Marubeni North Sea Ltd (2.5%)) [85–88].

The field was initially developed by peripheral water flooding with oil production beginning in 1983. A plateau oil production rate, of 24 000 m^3 at standard conditions per day (sm^3 day^{-1}), was maintained until 1995, when seawater broke through to wells at the crest of the reservoir. At this stage approximately 40% of the OIIP had been recovered. The remaining oil was believed

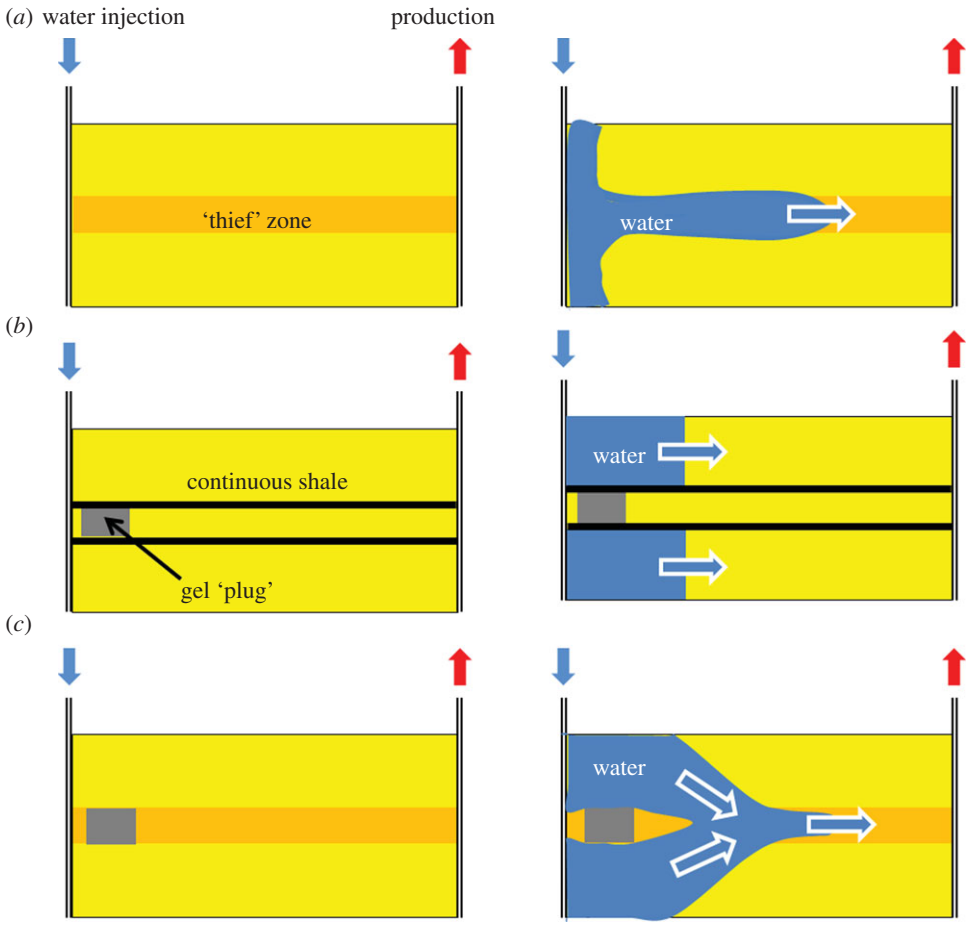

Figure 7. Diagram showing (*a*) how a high-permeability thief zone may result in bypassing of oil in higher permeability zones, (*b*) how a gel plug may successfully divert the water into lower permeability layers if the thief zone has zero permeability shales top and bottom and (*c*) how in the absence of those shales the gel plug will only result in a partial improvement of sweep. The water will flow back into the high-permeability thief zone once the plug has been passed. (Online version in colour.)

to be partly trapped on the pore scale (as residual oil) and partly bypassed owing to reservoir heterogeneity with further oil remaining up-dip of the production wells.

Although the residual oil saturation, trapped within the pores, was relatively low at 25% [86], it still presented a favourable target for EOR because of the large volume of OIIP. Surfactant and polymer flooding were ruled out because of the high reservoir temperature (115°C). The chemicals existing at that time would have degraded rapidly at these conditions. CO_2 injection was also deemed infeasible because of the lack of CO_2 supply and also the costly changes to wells, facilities and pipelines that would have been required to cope with the associated corrosion [55,86]. Nonetheless, the geology of Magnus was felt to create a favourable target for miscible gas injection. The reservoir is formed of repeated layers, in each of which the permeability increases with depth. This increases the tendency of water to sink under gravity towards the bottom of the reservoir, but reduces the tendency of injected gas to segregate upwards, thereby increasing the vertical sweep from the gas.

The injection of hydrocarbon gas was determined to be the best EOR option, as the Magnus oil is sufficiently light and the reservoir pressure sufficiently high for miscibility to be achieved at reservoir conditions with hydrocarbon gas that was relatively lean in heavier components [87,88].

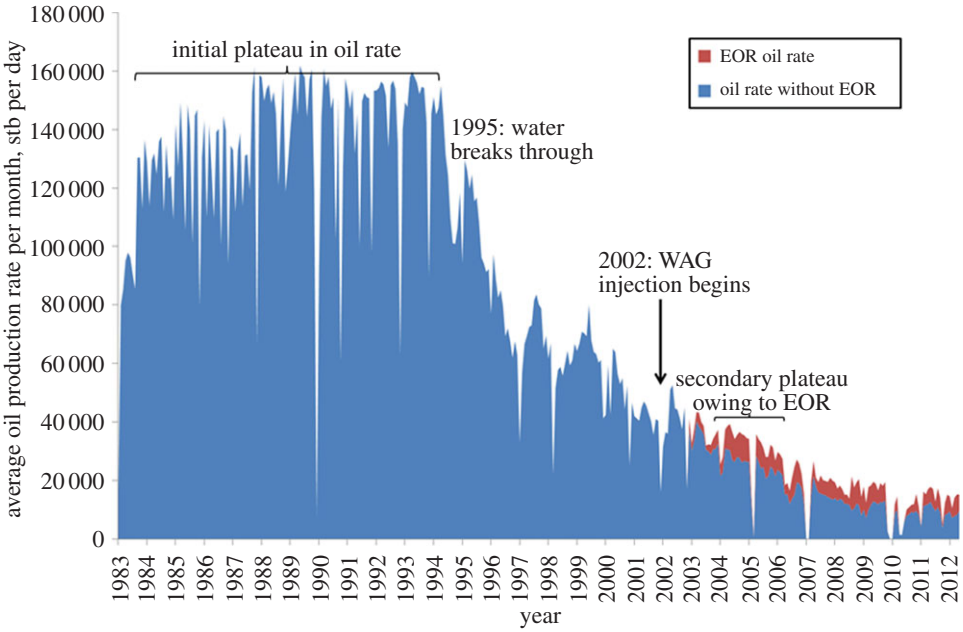

Figure 8. Daily oil production rate (average over a month) from the Magnus field from the start of production in 1983. WAG injection was started in 2002 and by 2005 it was clear that the decline in oil production had been reduced. The oil rate expected without EOR was estimated using numerical simulation. stb, stock tank barrel. (Online version in colour.)

Nonetheless, this option only became reality when suitable gas became available from a number of fields located to the west of the Shetland Islands.

The EOR scheme that was finally implemented in 2002 uses WAG injection. New gas enrichment facilities had to be built at the Sullom Voe Terminal in the Shetland Islands plus over 400 km of new pipeline to transport the gas. The injection rate was maintained as high as possible to limit gravity segregation of the injected gas and water. By 2005, the previous decline in oil rate had been arrested and a secondary plateau in oil production rate was achieved (figure 8). By 2010 some 3.2×10^9 sm^3 of gas had been injected into four gas injection wells yielding 1.8×10^6 sm^3 of incremental oil overall and contributing 40% of the oil production rate in 2010 [88].

Delivering this additional oil required significant changes to both the operation of the field and the way its performance was monitored. This is because operating an EOR WAG injection scheme is inherently more complex than operating a primary recovery process or water injection scheme. Four aspects of this additional operational complexity are described below.

(a) Water alternating gas changeovers

The aim was to operate two wells on gas injection and two wells on water injection at any given time, swapping them between water and gas injection at appropriate intervals. It was intended that equal reservoir volumes of water and gas would be injected during each cycle. The operation to change each well over from water to gas injection, and vice versa, takes 3 days and involves physically removing the injection line for one phase and replacing it with the injection line for the other phase. These changeovers need to be scheduled in advance to fit in with other planned platform activities. Unfortunately, they are perceived by the platform staff as low priority with little associated cost in delaying them, although in reality delaying changeover reduces the benefit of the WAG process by changing the effective WAG ratio. This is illustrated by a combination of events that occurred in late 2008 that resulted in one of the gas injection wells being temporarily shut-in. This caused a change to the effective WAG ratio in the remaining gas injection well. This

in turn resulted in more gas being produced, because the gas mobility was not being reduced by a following slug of injected water, to the extent that the ability of the platform to manage the volume of returned gas was exceeded. Consequently, production from all the EOR production wells was cut back, reducing the oil production rate.

(b) Measurement of gas flow rate

Accurate measurement of gas volumes over time, and allocation to the various injection and production wells, is important to maintain efficient WAG scheduling and thus the overall efficiency of the EOR process. This meant that all wells that inject gas should have individual flow meters. These would not be required for an ordinary water flood. Even retro-fitting flow meters to these wells was challenging as it competed for offshore time against another major project to construct additional drilling slots, and later against drilling activity.

(c) Reservoir pressure management

Average reservoir pressure in those parts of the reservoir subject to the WAG scheme has to be maintained above the MMP of 34.5×10^6 Pa. However, this is also the pressure rating for the EOR production wellheads, which in turn places an upper limit on the reservoir pressure. After allowing for safety margins and worst case conditions in which the production tubing would be full of gas, this combination of MMP target and wellhead pressure rating created a narrow range for the reservoir pressure. As a result, the reservoir pressure must be routinely measured in those parts of the reservoir subject to WAG, which would not be done for an ordinary water flood.

(d) Gas supply

The injected gas is imported from other producing oilfields. Operational issues at these other fields have led to a variable gas supply at Magnus, resulting in a less efficient sweep through the reservoir.

7. Emerging enhanced oil recovery technologies

The traditional EOR technologies (miscible gas/WAG and chemical flooding) for improving microscopic displacement and macroscopic sweep have been around for a long time but significant technical, operational and economic difficulties (such as discussed above) continue to limit their application and the volume of oil recovered when they are implemented at scale.

Several completely new technologies have been developed over recent years that aim to improve recovery using rather different mechanisms from those used by the traditional EOR techniques. They benefit from significantly lower cost per incremental barrel, have broader applicability, are less dependent on detailed characterization of the reservoir rock and fluids and are less complex to implement.

In this section, we examine two of these new processes (low-salinity water flooding and deep reservoir flow diversion), as well as considering the time taken from identification of the process in the laboratory to implementation in the field.

(a) Low-salinity water injection

Low-salinity water injection is a recently developed EOR process that improves microscopic displacement efficiency by modifying the reservoir wettability. As noted above, most oil reservoir rocks have a heterogeneous or 'mixed' wettability. The effect of the low-salinity water is to make these rocks slightly more (but not completely) water wet as it progresses through the reservoir. This has the effect of mobilizing more of the oil behind the displacement front and increasing recovery.

The potential to use wettability alteration as the main recovery mechanism in an EOR process has only recently become a major topic of research. This is despite the fact that it was first recognized in 1959 by Wagner & Leach [69] and tested in the field in 1962 [89]. These workers controlled the wettability through adjusting the pH and sodium content of the injected water. Wettability alteration was recognized as a secondary recovery mechanism in ASP floods (resulting from the addition of the alkali to the chemical mix in the injected water [68]) but developments of these floods focused primarily on minimizing the IFT.

The recovery process involves injecting brine, with a low salinity and that is depleted in divalent cations (compared with the *in situ* brine), into sandstone reservoirs. It should be noted that the salinity should be as low as possible without adversely affecting flow performance. It does not usually involve injecting pure water as this can reduce oil recovery by causing swelling and deflocculation of some types of clay minerals and subsequent blockage of the pore space. After the first laboratory investigations of the effect of water composition on oil recovery in 1959 [65] and 1967 [90], no further systematic laboratory studies of the effect were performed until the 1990s [91–94]. These and other studies performed in BP (1997–2002, unpublished data) resulted in the first field test in a single well in 2004 [95]. Several other such tests [96] led eventually to an inter-well field trial in 2010 [97]. All confirmed that lowering brine salinity increased oil recovery.

All the core flood and field evidence is consistent with the theory that low-salinity water injection progressively modifies the reservoir wettability through multi-component ion exchange [98,99]. As noted in [33], one of the mechanisms causing areas of the pore walls to be oil wet is ion binding between the oil and mineral surface, mediated through multi-valent cations such as Ca^{2+}, Mg^{2+} and Fe^{2+}. Injecting lower salinity water that has a reduced concentration of these divalent cations results in this ion-bound oil being released from the mineral surface (usually, but not exclusively, kaolinite) and that part of the surface becoming water wet. It is important to note that this only has a slight effect on the bulk rock wettability—overall it still has a mixed wettability. It is just slightly more water wet. Recent academic studies are providing support for the proposed mechanism [100–103].

Seventeen years after the publication of initial investigations into the impact of water composition on oil recovery by Jadhunandan & Morrow [92], EOR by low-salinity water injection is about to be deployed in the second phase of the Clair field development, Clair Ridge, in the UKCS. Reservoir condition core flood tests using Clair rock and oil showed significant benefits to secondary low-salinity flooding with a reduction in residual oil saturation of between 5.6% and 7.6% [104].

This long time frame to take preliminary research to deployment is typical. It was a function of the need to confirm the results under realistic reservoir conditions using real reservoir rocks and fluids, and also to develop a sufficient mechanistic understanding to convince business managers and partner companies that the technology was robust. Further time was taken to scale up the technology to field scale including identification of suitable desalination plants that could be operated safely in harsh offshore conditions.

(b) Deep reservoir flow diversion

Deep reservoir flow diversion is a recently developed EOR technique for improving macroscopic sweep efficiency. It was recognized that, while flow diversion by polymer gels in the reservoir adjacent to the injection well could be very successful [79,82,83], in many cases cross-flow in the high-pressure gradient environment near the well meant that the diverted water soon flowed back into the thief zone [84]. It was then realized that chemical treatments placed deep in the reservoir would not be so vulnerable to this, but rather would benefit from the diversion of fluid in the interval between the injection well and the reduced permeability zone [105].

The challenge was to identify a chemical that would only reduce the permeability of the thief zone when it reached the right part of the reservoir. An early attempt involved using a water-soluble polymer mixed with hydrolysed aluminium citrate as the cross-linker [103]. It was

Table 1. Comparison of EOR processes with water flooding in terms of their microscopic displacement efficiency and macroscopic sweep efficiency, together with a summary of their limitations.

EOR process	microscopic displacement efficiency, E_{ps} (compared with water injection)	macroscopic sweep efficiency, E_s (compared with water injection)	limitations
miscible gas injection	+	−	very sensitive to heterogeneity poor vertical sweep owing to large density difference from water reservoir pressure must be greater than minimum miscibility pressure excess gas production
WAG injection	+	+	operationally more complex oil may be trapped in pores by water if too much water injected
polymer flooding	~	+	well injectivity owing to higher viscosity of injected water loss of polymer by adsorption cost due to large volumes of chemical required may not be feasible in hot reservoirs or those with saline water
ASP flooding	+	+	complex to design, requiring analysis of oil, water and rock chemistry as well as geological heterogeneity cost due to large volumes of chemicals required may not be feasible in hot reservoirs, carbonate reservoirs or those with saline water
low-salinity water injection	+	~	mechanism not fully understood possible dilution of injected low-salinity water by *in situ* brine
polymer gel treatments at injection wells	~	+	only works where high-permeability thief zone is isolated from other oil-bearing zones may not be feasible in hot reservoirs, carbonate reservoirs or those with saline water

(*Continued.*)

Table 1. (*Continued.*)

EOR process	microscopic displacement efficiency, E_{ps} (compared with water injection)	macroscopic sweep efficiency, E_s (compared with water injection)	limitations
			potential production of H_2S by sulfate-reducing bacteria in reservoir
deep reservoir flow diversion	~	+	only works for water injection may not be feasible in hot reservoirs, carbonate reservoirs or those with saline water

believed that the cross-linker and polymer would travel together through the reservoir and form a permeability-reducing gel phase on heating, but this proved unreliable, probably because of chromatographic separation of the polymer and cross-linker and/or precipitation of the metal ion [106]. The lesson from this field trial was that the blocking agent had to travel through a large amount of rock and that it should be a single component to prevent deactivation. It was concluded that it should be particulate, inert and compact when travelling through the rock pores to the target location, then when triggered should expand and block the rock pores. The trigger selected was the temperature difference between the injected water (which coming from the surface is initially cooler than the reservoir) and the reservoir. Over prolonged injection, cooled zones are created around the injection well resulting in a thermal gradient between injection and production wells.

A particle system was developed consisting of water-soluble polymer backbones linked together with permanent cross-linker in sufficient quantity to allow them to swell significantly in water. A larger amount of thermally breakable cross-linker was added to lock the particles into their manufactured particle size. This was achieved by polymerizing the monomers as an emulsion in light mineral oil [107,108].

To deploy this system, a surfactant is added to the injection water followed immediately afterwards by the particle dispersion. The natural turbulence in the well-bore is sufficient to cause the oil in the formulation to emulsify and the particles to be individually wetted by water. The dispersion of particles in water continues down the injection well, into and through the pores of the formation rock. The water-particle system travelling down the thief layers is progressively heated by the unswept layers above and below (which do not contain injected water and are thus at the original reservoir temperature). Eventually the water–particle system is heated to the point where the temperature-sensitive cross-links are broken and the particles absorb the water, swell and block the rock pores. The permeability of the rock in the thief zones is reduced and the subsequent water injection is diverted into the oil-bearing lower permeability zones to displace oil towards a producing well.

The technical field trial of the 'temperature-triggered' particles took place in 2001 [109,110] followed by commercial field trials in 2004 through to 2007 [111–113]. Following successful incremental oil production results, the technology deployment started in 2007. The first 19 treatments produced over 200 000 m^3 of incremental oil [114]. To date approximately 80 treatments have been completed with significant incremental oil recovery over the water flood and a success rate in excess of 80%. Pressure fall-off tests suggest that the blockages have been formed in excess of 100 m into the reservoir, which is desirable for maximum flow diversion with minimum decrease in water injectivity [111].

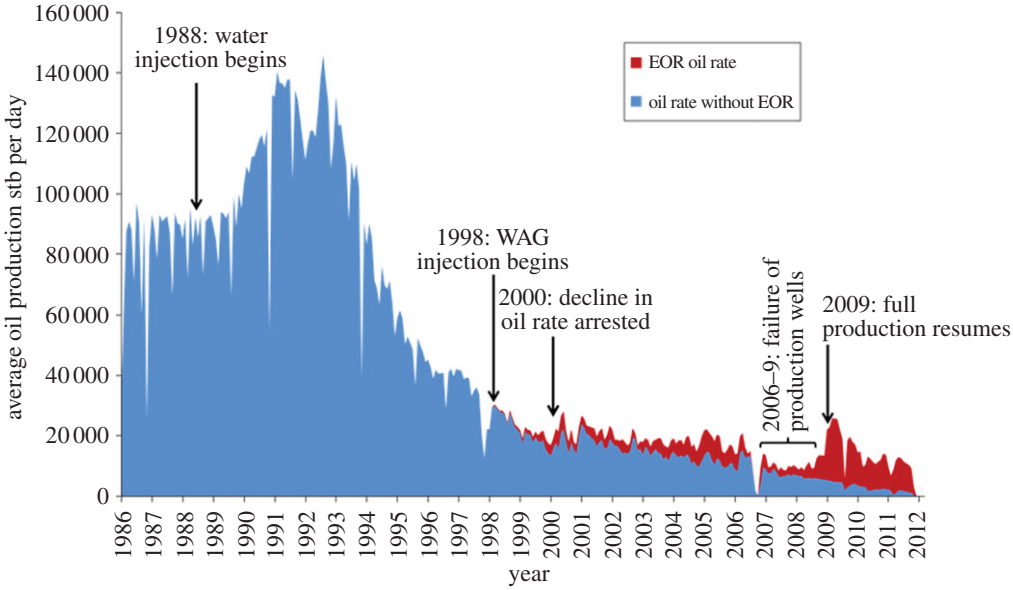

Figure 9. Daily oil production rate (average over a month) from the Ula field from start of production in 1983. WAG injection was started in 1998 and by 2000 it was clear that the decline in oil production had been stopped. Today almost all the oil production is believed to have come from EOR. The oil rate expected without EOR was estimated using numerical simulation. (Online version in colour.)

Other treatments have been proposed based on intra-molecularly cross-linked polymer- [115], salinity- [116] or pH-triggered systems [117] or pre-formed gel particles [118–120]. It is believed for various reasons, though not universally accepted, that the intra-molecularly cross-linked polymer systems do not propagate as far into the reservoir pore systems as the temperature-triggered particles (e.g. [120] and the references therein).

Again it is interesting to note that it took more than 15 years for this technology to be deployed after its initial conception leading to publication in 1992 [105].

8. Discussion and conclusion

Crude oil is expected to supply 20–25% of the world's energy by 2035 [121]. Most of this is expected to come from conventional crude oil [3] and mature fields. This suggests that there will be an increasing application of EOR in order to increase the RF and oil production rate from these fields.

We have seen that traditional EOR technologies can be very effective at improving recovery, especially through increasing microscopic displacement efficiency (table 1). When they are implemented, they can be very successful, e.g. as in Magnus (figure 8) and in the Ula field in the North Sea where almost all the oil produced is believed to come from WAG injection (figure 9). They are, however, often complex to design, develop and operate, as we have seen through the summary of WAG deployment in the Magnus field. Furthermore, in many mature fields offshore (such as in the UKCS) it is impossible to implement EOR because of the lack of space on the platforms for the additional equipment needed to inject different fluids and/or process the produced fluids. The response to the application of these techniques, in terms of increased oil production rate, is usually slow, typically months or years after the process is initiated. These issues, combined with the use of large quantities of expensive chemicals or valuable hydrocarbon gases, means that they are only economical when the oil price is high.

Traditional miscible gas EOR techniques are very sensitive to geological heterogeneity and so additional work must be performed to evaluate the reservoir description before development

proceeds. Chemical flooding techniques also require a good understanding of the chemical behaviour of the rock and may need careful selection of chemical(s) that are robust to the temperature conditions in the reservoir.

New EOR technologies are needed that are easier to design, require less specialist equipment and produce a quicker response in terms of oil rate. This is particularly the case for mature offshore fields where there is little space for additional equipment on platforms. This also suggests that companies should be planning the deployment of both new and existing EOR technologies at the beginning of field development to ensure that there will be facilities and space to implement EOR in due course. In many cases, maximum oil recovery is only achieved if EOR is deployed as soon as production begins. The traditional approach of only moving to EOR after oil rates from a water flood drop results in significant volumes of oil being bypassed.

A major challenge remains the time delay between the deployment of a given EOR process in a field, often involving considerable extra capital and operational costs, and the response in terms of additional oil production. The benefits from drilling additional water injection wells are usually seen within months while it may take a year or more before incremental oil resulting from an EOR scheme reaches the production wells.

We have discussed two emerging EOR technologies (low-salinity water injection and deep reservoir flow diversion) that remedy some of the drawbacks of traditional EOR processes. Low-salinity water injection is simple to plan and deploy as it is very similar to conventional water flooding. There are no additional chemicals required or additional processing after production. The main additional cost (and limiting factor on existing platforms) is the need for desalination equipment. Deep reservoir flow diversion has proved to be more successful than traditional near-well gel treatments because it is less sensitive to the nature of the geological heterogeneity in the reservoir. It therefore requires less reservoir characterization and few reservoir simulation studies before implementation. In addition, it does not require any upfront capital investment.

It is probable that there will be further developments in enhancing water flooding. We have described how low-salinity water injection improves oil recovery in sandstone reservoirs by making the rock more water wet. A similar change in wettability has been observed in chalk when seawater enriched in Ca^{2+}, Mg^{2+} and SO_4^{2-} is injected [122], although other workers suggest that viscosity alteration and formation of a microemulsion between oil and water may also improve oil recovery [123].

Further developments are probable in EOR technologies that improve macroscopic sweep. The deep reservoir flow diversion technique described above is designed for water flooding. Similar technologies are required for gas flooding, especially if CO_2 injection for EOR and geological sequestration of the CO_2 is to succeed.

Increasing or even maintaining crude oil production to help supply the world's energy demand is likely to adversely affect climate change unless it is associated with geological carbon sequestration. Oil reservoirs are ideal candidates for secure storage of anthropogenic CO_2 because they are known to have trapped oil for millions of years. CO_2 injection is also able to significantly improve oil recovery [124], although in this case there is still a net increase in CO_2 emissions, i.e. more CO_2 is produced from burning the additional oil than is stored in the reservoir by injection [125]. To achieve this will require the development of technologies to improve the macroscopic sweep efficiency of this process in order to maximize the trapping of CO_2 in the reservoir while maximizing oil recovery and production rate. It will also require additional political and financial support to put in place the carbon capture facilities at power stations, the pipelines for distributing the CO_2 to the oilfields and new pipelines and facilities that are resistant to corrosion in existing oilfields [126].

Another EOR technology that we have not discussed in any detail is that of microbial EOR. This uses native or introduced microbes to improve oil recovery via a variety of mechanisms including flow diversion, *in situ* upgrading, wettability modification and generation of biosurfactants within the reservoir [127]. Although it was first proposed by Zobell [128] in 1947 and has been the subject of much research since then [127–130], it has not been widely applied. This is probably because it has proved to be difficult to predict performance in the field. With

recent advances in the biological sciences and the modelling of biological processes, it is possible that microbial EOR or methanogenesis [129] may yet be more widely applied in the future.

EOR projects are going to become increasingly common worldwide in the future, despite concerns about greenhouse gas emissions, as demand for oil will continue to increase [3] while at the same time it becomes harder to find new oilfields. We have not yet achieved the technological limit in terms of the RF that can be obtained using these processes. At present, their deployment is controlled by economic factors and operational constraints. Research continues to try and mitigate these factors and constraints, as well as to develop more advanced and effective recovery processes, but the challenge in all cases is to move these technologies more rapidly from the laboratory to the field.

Acknowledgements. BP and its partners are thanked for permission to publish this material. A.C., K.W., H.F., I.C., T.M. and P.S. are either current or former employees of BP Exploration & Operating Company or its affiliates which hold patents or patent applications relating to some of the technologies described in this paper. A.M. acts as a consultant to BP in a personal capacity. All authors declare that they have no competing interest in relation to this paper.

References

1. Sandrea I, Sandrea R. 2007 Recovery factors leave vast target for EOR technologies. *Oil Gas J.* **105**, 44–47.
2. Advanced Resources International. 2006 Undeveloped domestic oil resources: the foundation for increased oil production and a viable domestic oil industry. US Department of Energy, Office of Fossil Energy—Office of Oil and Natural Gas. See http://www.fossil.energy.gov/programs/oilgas/publications/eor_co2/Undeveloped_Oil_Document.pdf.
3. International Energy Agency. 2008 *World energy outlook 2008*. Paris, France: OECD/IEA. See http://www.iea.org/textbase/nppdf/free/2008/weo2008.pdf.
4. BP. 2012 *BP statistical review of world energy 2012*. London, UK: BP. See www.bp.com/statisticalreview.
5. Durham LS. 2005 The elephant of all elephants. *AAPG Explorer*, January. See http://www.aapg.org/explorer/2005/01jan/ghawar.cfm.
6. Stalkup FI. 1983 Status of miscible displacement. *J. Petrol. Technol.* **35**, 815–826. (doi:10.2118/9992-PA)
7. Orr FJ Jr. 2007 *Theory of gas injection processes*. Copenhagen, Denmark: Tie-Line Publications.
8. Christensen JR, Stenby EH, Skauge A. 2001 Review of WAG field experience. *SPE Reservoir Eval. Eng.* **4**, 97–106. (doi:10.2118/71203-PA)
9. Willhite GP, Seright RS. 2011 *Polymer flooding*. Digital edition. Tulsa, OK: Society of Petroleum Engineers.
10. Liang J-T, Lee RL, Seright RS. 1993 Gel placement in production wells. *SPE Prod. Facilities* **8**, 276–284. (doi:10.2118/20211-PA)
11. Green DW, Hirasaki G, Pope GA, Willhite GP. 2011 *Surfactant flooding*. Digital edition. Tulsa, OK: Society of Petroleum Engineers.
12. Ambastha A. 2008 *Heavy oil recovery*. SPE Reprint Series no. 61. Tulsa, OK: Society of Petroleum Engineers.
13. Hite JR, Stosur G, Carnaham NF, Miller K. 2003 Guest editorial. IOR and EOR: effective communication requires a definition of terms. *J. Petrol. Technol.* **55**, 16.
14. Sneider RM, Sneider JS. 2002 New oil in old places: the value of mature field redevelopment. In *Petroleum provinces of the twenty-first century* (eds MW Downey, JC Threet, WA Morgan), pp. 63–84. AAPG Memoirs 74. Tulsa, OK: American Association of Petroleum Geologists.
15. Lumley DE. 2001 Time-lapse seismic reservoir monitoring. *Geophysics* **66**, 50–53. (doi:10.1190/1.1444921)
16. Heming RF. 1996 Impact of information technology on the earth sciences. *Technol. Soc.* **18**, 297–319. (doi:10.1016/0160-791X(96))
17. Journel AG, Alabert FG. 1990 New method for reservoir mapping. *J. Petrol. Technol.* **42**, 212–218. (doi:10.2118/18324-PA)

18. Fayers FJ, Hewett TA. 1992 A review of current trends in petroleum reservoir description and assessment of their impacts on oil-recovery. *Adv. Water Resour.* **15**, 341–265. (doi:10.1016/0309-1708(92)90002-J)
19. Deutsch CV, Hewett TA. 1996 Challenges in reservoir forecasting. *Math. Geol.* **28**, 829–842. (doi:10.1007/BF02066003)
20. Gravley W. 1983 Review of downhole measurement-while-drilling systems. *J. Petrol. Technol.* **35**, 1439–1445. (doi:10.2118/10036-PA)
21. Toole ST, Grist DM. 2003 Oil and gas recovery behaviour in the UKCS basins. In *Proc. Offshore Europe Conf., Aberdeen, UK, 2–5 September 2003*. Tulsa, OK: Society of Petroleum Engineers. (doi:10.2118/83982-MS)
22. McGuire PL, Spence AP, Redman RS. 2001 Performance evaluation of a mature miscible gasflood at Prudhoe Bay. *SPE Reservoir Eval. Eng.* **4**, 318–326. (doi:10.2118/59326-MS)
23. Smalley PC, Ross B, Brown CE, Moulds TP, Smith MJ. 2009 Reservoir technical limits: a framework for maximizing recovery from oil fields. *SPE Reservoir Eval. Eng.* **12**, 610–629. (doi:10.2118/109555-PA)
24. Muskat M. 1953 Oil recovery—100 per cent? *Ind. Eng. Chem.* **45**, 1401–1405. (doi:10.1021/ie50523a021)
25. Arriola A, Willhite GP, Green DW. 1983 Trapping of oil drops in a noncircular pore throat and mobilization upon contact with a surfactant. *SPE J.* **23**, 99–114. (doi:10.2118/9404-PA)
26. Buckley SE, Leverett MC. 1942 Mechanism of fluid displacement in sands. *Trans. AIME* **146**, 107–116. (doi:10.2118/942107-G)
27. Roof JG. 1970 Snap-off of oil droplets in water-wet pores. *SPE J.* **10**, 85–90. (doi:10.2118/2504-PA)
28. Anderson WG. 1987 Wettability literature survey—part 6: the effects of wettability on waterflooding. *J. Petrol. Technol.* **39**, 1605–1622. (doi:10.2118/16471-PA)
29. Schmid C. 1964 The wettability of petroleum rocks and results of experiments to study effects of variations in wettability of core samples. *Erdoel Kohle* **17**, 605–609.
30. Brown RJS, Fatt I. 1956 Measurements of fractional wettability of oilfield rocks by nuclear magnetic relaxation method. *Trans. AIME* **207**, 206–264.
31. Buckley JS, Liu Y. 1998 Some mechanisms of crude oil/brine/solid interactions. *J. Petrol. Sci. Eng.* **20**, 155–160. (doi:10.1016/S0920-4105(98)00015-1)
32. Bennett B, Buckman JO, Bowler BJF, Larter SR. 2004 Wettability alteration in petroleum systems: the role of polar hydrocarbons. *Petrol. Geosci.* **10**, 271–277. (doi:10.1144/1354-079303-606)
33. Denekas MO, Mattax CC. 1959 Effects of crude oil components on rock wettability. *Trans. AIME* **216**, 330–333.
34. Anderson WG. 1986 Wettability literature survey—part 1: rock/oil/brine interactions and the effects of core handling on wettability. *J. Petrol. Technol.* **38**, 1125–1144. (doi:10.2118/13932-PA)
35. Drummond C, Israelachvili J. 2004 Fundamental studies of crude oil-surface water interactions and its relationship to reservoir wettability. *J. Petrol. Sci. Eng.* **45**, 61–81. (doi:10.1016/j.petrol.2004.04.007)
36. Salathiel RA. 1973 Oil recovery by surface film drainage in mixed-wettability rocks. *J. Petrol. Technol.* **25**, 1216–1224. (doi:10.2118/4104-PA)
37. Morrow NR. 1990 Wettability and its effect on oil recovery. *J. Petrol. Technol.* **42**, 1476–1484. (doi:10.2118/21621-PA)
38. Jackson MD, Muggeridge AH, Yoshida S, Johnson H. 2003 Upscaling permeability measurements within complex heterolithic tidal sandstones. *Math. Geol.* **35**, 499–520. (doi:10.1023/A:1026236401104)
39. Martinius AW, Ringrose PS, Brostrom C, Elfenbein C, Naess A, Ringas JE. 2005 Reservoir challenges of heterolithic tidal sandstone reservoirs in the Halten Terrace, mid-Norway. *Petrol. Geosci.* **11**, 3–16. (doi:10.1144/1354-079304-629)
40. Kim EB *et al*. 2011 Genome sequencing reveals insights into physiology and longevity of the naked mole rate. *Nature* **479**, 223–227. (doi:10.1038/nature10533)
41. Kuruana AK. 1976 Influence of tidal phenomenon on interpretation of pressure build up and pulse test. *APEA J.* **16**, 99–105.
42. Waggoner JR, Castillo JL, Lake LW. 1992 Simulation of EOR processes in stochastically generated permeable media. *SPE Formation Eval.* **7**, 173–180. (doi:10.2118/21237-PA)

43. Homsy GM. 1987 Viscous fingering in porous media. *Annu. Rev. Fluid Mech.* **19**, 271–311. (doi:10.1146/annurev.fluid.19.1.271)
44. Araktingi UG, Orr FR Jr. 1993 Viscous fingering in heterogeneous porous media. *SPE Adv. Technol. Ser.* **1**, 71–80. (doi:10.2118/18095-PA)
45. Houseworth JE. 1991 Sensitivity of large-scale water/oil displacement behavior to fine-scale permeability heterogeneity and relative permeabilities. In *Proc. SPE Annu. Technical Conf. and Exhibition, Dallas, TX, 10 June 1991*. Tulsa, OK: Society of Petroleum Engineers. (doi:10.2118/22590-MS)
46. Darcy H. 1856 *Les fontaines publiques de la ville de Dijon*. Paris, France: Dalmont.
47. Blackwell RJ, Rayne JR, Terry WM. 1959 Factors influencing the efficiency of miscible displacement. *Trans. AIME* **217**, 1–8.
48. Christie MA, Bond DJ. 1987 Detailed simulation of unstable processes in miscible flooding. *SPE Reservoir Eng.* **2**, 514–522. (doi:10.2118/14896-PA)
49. Claridge EL. 1972 Prediction of recovery in unstable miscible flooding. *SPE J.* **12**, 143–155. (doi:10.2118/2930-PA)
50. Fayers FJ, Muggeridge AH. 1990 Extensions to Dietz theory and behaviour of gravity tongues in slightly tilted reservoirs. *SPE Reservoir Eng.* **5**, 487–494. (doi:10.2118/18438-PA)
51. McGuire PL, Spence AP, Stalkup FI, Cooley MW. 1995 Core acquisition and analysis for optimization of the Prudhoe Bay miscible-gas project. *SPE Reservoir Eng.* **10**, 94–100. (doi:10.2118/27759-PA)
52. Stalkup FI. 1978 Carbon dioxide miscible flooding: past, present and outlook for the future. *J. Petrol. Technol.* **30**, 1102–1112. (doi:10.2118/7042-PA)
53. Alvarado V, Manrique E. 2010 Enhanced oil recovery: an update review. *Energies* **3**, 1529–1575. (doi:10.3390/en3091529)
54. Stone PC, Steinberg BG, Goodson JE. 1989 Completion design for waterfloods and CO_2 floods. *SPE Prod. Eng.* **4**, 365–370. (doi:10.2118/15006-PA)
55. Sánchez JL, Astudillo A, Rodríguez F, Morales J, Rodríguez A. 2005 Nitrogen injection in the Cantarell comples: results after four years of operation. In *Proc. SPE Latin American and Carribean Petroleum Engineering Conf., Rio de Janeiro, Brazil, 20–24 June 2005*. Tulsa, OK: Society of Petroleum Engineers. (doi:10.2118/97385-MS)
56. Awan AR, Teigland R, Kleppe J. 2008 A survey of North Sea enhanced-oil-recovery projects initiated during the years 1975–2005. *SPE Reservoir Eval. Eng.* **11**, 497–512. (doi:10.2118/99546-PA)
57. Sandiford BB. 1964 Laboratory and field studies of water floods using polymer solutions to increase oil recoveries. *J. Petrol. Technol.* **16**, 917–922. (doi:10.2118/844-PA)
58. Gogarty WB, Tosch WC. 1968 Miscible-type waterflooding: oil recovery with micellar solutions. *J. Petrol. Technol.* **20**, 1407–1414. (doi:10.2118/1847–1-PA)
59. Hill HJ, Reisberg J, Stegemeier GL. 1973 Aqueous surfactant systems for oil recovery. *J. Petrol. Technol.* **25**, 186–194. (doi:10.2118/3798-PA)
60. Needham RB, Doe PH. 1987 Polymer flooding review. *J. Petrol. Technol.* **39**, 1503–1507. (doi:10.2118/17140-PA)
61. Raney K, Ayirala S, Chin R, Verbeek P. 2012 Surface and subsurface requirements for successful implementation of offshore chemical enhanced oil recovery. *SPE Prod. Oper.* **27**, 294–305. (doi:10.2118/155116-PA)
62. Alusta G, Mackay E, Fennema J, Armih K, Collins I. 2012 EOR vs. infill well drilling: sensitivity to operational and economic parameters. In *Proc. North Africa Technical Conf. and Exhibition, Cairo, Egypt, 20–22 February 2012*. Tulsa, OK: Society of Petroleum Engineers. (doi:10.2118/150454-MS)
63. Seright RS, Seheult M, Talashek T. 2009 Injectivity characteristics of EOR polymers. *SPE Reservoir Eng. Eval.* **12**, 783–792. (doi:10.2118/115142-PA)
64. Wang D, Dong H, Lu C, Fu X, Nie J. 2009 Review of practical experience by polymer flooding at Daqing. *SPE Reservoir Eval. Eng.* **12**, 270–476. (doi:10.2118/114342-MS)
65. Morel D, Vert M, Gauchet R, Bouger Y. 2012 First polymer injection in deep offshore field Angola: recent advances in the Dalia/Camelia field case. *Oil Gas Facilities* **1**, 43–52. (doi:10.2118/135735-PA)
66. Al-Saadi F, Amri BA, Nofli S, van Wunnik J, Jaspers HF, Harthi S, Shuaili K, Cherukupalli C, Chakravarthi R. 2012 Polymer flooding in a large field in South Oman—initial results and future plans. In *Proc. SP EOR Conf. Oil and Gas West Asia, Muscat, Oman, 16–18 April 2012*. Tulsa, OK: Society of Petroleum Engineers. (doi:10.2118/154665-MS)

67. Spildo K, Skauge A, Aarra MG, Tweheyo MT. 2009 A new polymer application for North Sea reservoirs. *SPE Reservoir Eval. Eng.* **12**, 427–432. (doi:10.2118/113460-PA)
68. Hirasaki GJ, Miller CA, Puerto M. 2011 Recent advances in surfactant EOR. *SPE J.* **16**, 889–907. (doi:10.2118/115386-PA)
69. Wagner OR, Leach RO. 1959 Improving oil displacement efficiency by wettability adjustment. *Trans. AIME* **216**, 65–72.
70. Ehrlich R, Hasiba HH, Raimondi P. 1974 Alkaline waterflooding for wettability alteration—evaluating a potential field application. *J. Petrol. Technol.* **26**, 1335–1343. (doi:10.2118/4905-PA)
71. Bernard GG, Holm LW. 1964 Effect of foam on permeability of porous media to gas. *SPE J.* **4**, 267–274. (doi:10.2118/983-PA)
72. Bernard GG, Holm LW, Harvey CP. 1980 Use of surfactant to reduce CO_2 mobility in oil displacement. *SPE J.* **20**, 281–292. (doi:10.2118/8370-PA)
73. Shutang G, Huabin L, Zhenyu Y, Pitts MJ, Surkalo H, Wyatt K. 1996 Alkaline/surfactant/polymer pilot performance of the west central Saertu, Daqing oil field. *SPE Reservoir Eng.* **11**, 181–188. (doi:10.2118/35383-PA)
74. Vargo J, Turner J, Vergnani B, Pitts MJ, Wyatt K, Surkalo H. 2000 Alkaline-surfactant-polymer flooding of the Cambridge Minnelusa field. *SPE Reservoir Eval. Eng.* **3**, 552–558. (doi:10.2118/68285-PA)
75. Stoll WM, Al Sureqi H, Al-Harthy SAA, Oyemade S, de Kruijif A, van Wunnik J, Arkestijn F, Bouwmeester R, Faber MJ. 2011 Alkaline/surfactant/polymer flood: from the laboratory to the field. *SPE Reservoir Eval. Eng.* **14**, 702–712. (doi:10.2118/129164-PA)
76. Clampitt RL, Hessert JE. 1975 *Method of treating subterranean formations with aqueous gels*. US Patent no. 3908760.
77. Eoff L, Dalrymple D, Everett D, Vasquez J. 2007 Worldwide field applications of a polymeric gel system for conformance applications. *SPE Prod. Oper.* **22**, 231–235. (doi:10.2118/98119-PA)
78. Seright RS, Lane RH, Sydansk RD. 2003 A strategy for attacking excess water production. *SPE Prod. Facilities* **18**, 158–169. (doi:10.2118/84966-PA)
79. Sydansk RD, Southwell GP. 2000 More than 12 years experience with a successful conformance-control polymer–gel technology. *SPE Prod. Facilities* **15**, 270–278. (doi:10.2118/66558-PA)
80. Sydansk RD, Seright RS. 2007 When and where relative permeability modification water-shut-off treatments can be successfully applied. *SPE Prod. Oper.* **22**, 236–247. (doi:10.2118/99371-PA)
81. Moradi-Araghi A. 2000 A review of thermally stable gels for fluid diversion in petroleum production. *J. Petrol. Sci. Eng.* **26**, 1–10. (doi:10.1016/S0920-4105(00)00015-2)
82. Portwood JT, Lackey SH, Abel SW. Selective polymer treatments improve oil recovery in five mature southern Oklahoma waterfloods. In *Proc. SPE Improved Oil Recovery Symposium, Tulsa, OK, 24–28 April 2010*. Tulsa, OK: Society of Petroleum Engineers. (doi:10.2118/129796-MS)
83. Sanders GS, Chambers MJ, Lane RH. 1994 Successful gas shutoff with polymer gel using temperature modelling and selective placement in the Prudhoe Bay field. In *Proc. 69th SPE Annu. Technical Conf. and Exhibition, New Orleans, LA, 25–28 September 1994*. Tulsa, OK: Society of Petroleum Engineers. (doi:10.2118/28502-MS)
84. Sorbie KS, Seright RS. 1992 Gel placement in heterogeneous systems with crossflow. In *Proc. SPE/DOE Enhanced Oil Recovery Symposium, Tulsa, OK, 22–24 April 1992*. Tulsa, OK: Society of Petroleum Engineers. (doi:10.2118/24192-MS)
85. Jayasekera AJ, Goodyear SG. 2002 Improved hydrocarbon recovery in the United Kingdom Continental Shelf: past, present and future. In *Proc. SPE/DOE Improved Oil Recovery Symposium held in Tulsa, OK, 13–17 April 2002*. Tulsa, OK: Society of Petroleum Engineers. (doi:10.2118/75171-MS)
86. Moulds TP, Trussell P, Haseldonckx SA, Carruthers RA. 2005 Magnus field: reservoir management in a mature field combining waterflood, EOR and new area developments. In *Proc. SPE Offshore Europe Conf., Aberdeen, UK, 6–9 September 2005*. Tulsa, OK: Society of Petroleum Engineers. (doi:10.2118/96292-MS)
87. Moulds TP, Trussell P, Erbas D, Cox DJ, Laws ED, Davies C, Strachan N. 2010 Post-plateau reservoir management in the Magnus field. In *Proc. SPE Annu. Technical Conf. and Exhibition, Florence, Italy, 19–22 September 2010*. Tulsa, OK: Society of Petroleum Engineers. (doi:10.2118/134953-MS)

88. Brodie J, Jhaveri B, Moulds T, Mellemstrand Hetland S. 2012 Review of gas injection projects in BP. In *Proc. 18th SPE Improved Oil Recovery Symp., Tulsa, OK, 14–18 April 2012*. Tulsa, OK: Society of Petroleum Engineers.
89. Leach RO, Wagner OR, Wood HW, Harpke CF. 1962 A laboratory and field study of wettability adjustment in water flooding. *J. Petrol. Technol.* **14**, 206–212. (doi:10.2118/119-PA)
90. Bernard GG. 1967 Effect of floodwater salinity on recovery of oil from cores containing clays. In *Proc. SPE Annu. Conf. and Exhibition, Los Angeles, CA, 26–27 October 1967*. Tulsa, OK: Society of Petroleum Engineers. (doi:10.2118/1725-MS)
91. Jadhunandan P. 1990 Effects of brine composition, crude oil and aging conditions on wettability and oil recovery. PhD Thesis, University of Wyoming, Wyoming.
92. Jadhunandan P, Morrow NR. 1995 Effect of wettability on waterflood recovery for crude oil/brine/rock systems. *SPE Reservoir Eval. Eng.* **10**, 40–46. (doi:10.2118/22597-PA)
93. Yildiz HO, Morrow NR. 1996 Effect of brine composition on recovery of Moutray crude oil by waterflooding. *J. Petrol. Sci. Eng.* **14**, 159–168. (doi:10.1016/0920-4105)
94. Tang GQ, Morrow NR. 1999 Salinity, temperature, oil composition and oil recovery by waterflooding. *SPE Reservoir Eng.* **12**, 269–276. (doi:10.2118/36680-PA)
95. Webb KJ, Black CJJ, Al-Ajeel H. 2004 Low salinity oil recovery—log inject log. In *Proc. 14th SPE/DOE Improved Oil Recovery Symposium, Tulsa, OK, 17–21 April 2004*. Tulsa, OK: Society of Petroleum Engineers.
96. McGuire PL, Chatham JR, Paskvan FK, Sommer DM, Carini FH. 2005 Low salinity oil recovery: an exciting new EOR opportunity for Alaska's North Slope. In *Proc. SPE Western Regional Meeting, Irvine, CA, 30 March–1 April 2005*. Tulsa, OK: Society of Petroleum Engineers.
97. Seccombe J, *et al.* 2010 Demonstration of low-salinity EOR at the interwell scale, Endicott field, Alaska. In *Proc. SPE Improved Oil Recovery Symp., Tulsa, OK, 24–28 April 2010*. Tulsa, OK: Society of Petroleum Engineers.
98. Lager A, Webb KJ, Black CJJ, Singleton M, Sorbie KS. 2008 Low salinity oil recovery—an experimental investigation. *Petrophysics* **49**, 28–35.
99. Sorbie KS, Collins I. 2010 A proposed pore-scale mechanism for how low salinity waterflooding works. In *Proc. SPE Improved Oil Recovery Symp., Tulsa, OK, 24–28 April 2010*. Tulsa, OK: Society of Petroleum Engineers.
100. Hassenkam T, Pedersen CS, Dalby K, Austad T, Stipp SLS. 2011 Pore scale observation of low salinity effects on outcrop and oil reservoir sandstone. *Colloids Surf. A* **390**, 179–188. (doi:10.1016/j.colsurfa.2011.09.025)
101. Fogden A. 2012 Removal of crude oil from kaolinite by water flushing at varying salinity and pH. *Colloids Surf. A* **402**, 13–23. (doi:10.1016/j.colsurfa.2012.03.005)
102. Hassenkam T, Mitchell AC, Pedersen CS, Skovbjerg LL, Bovet N, Stipp SLS. 2012. The low salinity effect observed on sandstone model surfaces. *Colloids Surf. A* **403**, 79–86. (doi:10.1016/j.colsurfa.2012.03.058)
103. Lee SY, O'Sullivan M, Routh AF, Clarke SM. 2009 Thin water layers on $CaCO_3$ particles dispersed in oil with added salts. *Langmuir* **25**, 3981–3984. (doi:10.1021/la802616n)
104. Buikema TA, Mair C, Williams D, Mercer D, Webb KJ, Hewson A, Reddick CEA, Robbana E. 2011 Low salinity enhanced oil recovery—laboratory to day one field implementation—LoSal EOR into the Clair Ridge project. In *Proc. EAGE IOR Symp., Cambridge, UK, 12–14 April 2011*. See www.earthdoc.org.
105. Fletcher AJP, Flew S, Forsdyke IN, Morgan JC, Rogers C, Suttles D. 1992 Deep diverting gels for very cost effective waterflood control. *J. Petrol. Sci. Eng.* **7**, 33–43. (doi:10.1016/0920-4105(92)90006-M)
106. Walsh MP, Rouse BA, Senol NN, Pope GA, Lake LW. 1983 Chemical interactions of aluminium citrate solutions with formation minerals. In *Proc. Int. Symp. of Oilfield and Geothermal Chemistry, Denver, CO, 1–3 June 1983*. (doi:10.2118/11799-MS)
107. Chang KT, Frampton H. Morgan JC. *Method of recovering hydrocarbon fluids from a subterranean reservoir*. US Patent no. 6454003.
108. Chang K-T, Frampton H, Morgan JC. *Composition and method of recovering hydrocarbon fluids from a subterranean reservoir*. US Patent no. 6729402.
109. Pritchett J, Frampton H, Brinkman J, Cheung S, Morgan JC, Chang KT, Williams D, Goodgame J. 2003 Field application of a new in-depth waterflood conformance improvement tool. In *Proc. SPE Int. Improved Oil Recovery Conf. in Asia Pacific, Kuala Lumpur, Malaysia, 20–21 October 2003*. Tulsa, OK: Society of Petroleum Engineers. (doi:10.2118/84897-MS)

110. Frampton H, Morgan JC, Cheung SK, Munson L, Chang KT, Williams D. 2004 Development of a novel waterflood conformance control system. In *Proc. 14th SPE/DOE Symp. on Improved Oil Recovery, Tulsa, OK, 17–21 April 2004*. Tulsa, OK: Society of Petroleum Engineers. (doi:10.2118/89391-MS)
111. Ohms D, McLeod J, Graff C, Frampton H, Morgan JC, Cheung S, Chang KT. 2009 Incremental oil success from waterflood sweep improvement in Alaska. *SPE Prod. Oper.* **25**, 247–254. (doi:10.2118/121761-PA)
112. Yañez PAP, Mustoni JL, Relling MF, Chang K-T, Hopkinson P, Frampton H. 2008 New attempt in improving sweep efficiency at the mature Koluel Kaike and Piedra Clavada waterflooding projects of the S. Jorge basin in Argentina. In *Proc. Latin American and Caribbean Petroleum Engineering Conf., Buenos Aires, Argentina, 15–18 April 2008*. Tulsa, OK: Society of Petroleum Engineers. (doi:10.2118/107923-MS)
113. Chang K-T, Cheung S, Frampton H, Neal P, Ng R. 2007 Update on an in-depth conformance control system for improving waterflood efficiency. In *Proc. 6th Int. Conf. on Production Optimization—Reservoir Conformance, Profile Control, and Water and Gas Shutoff, Houston, TX, 6–7 November 2007*. Tulsa, OK: Society of Petroleum Engineers.
114. Frampton H, Denyer P, Ohms DH, Husband M, Mustoni JL. 2009 Sweep improvement from the lab. to the field. In *Proc. 15th EAGE IOR Symp., Paris, France, 27–29 April 2009*. See www.earthdoc.org.
115. Smith JE. 1995 Performance of 18 polymers in aluminium citrate colloidal dispersion gels. In *Proc. SPE Int. Symp. on Oilfield Chemistry, San Antonio, TX, 14–17 February 1995*. Tulsa, OK: Society of Petroleum Engineers.
116. Chang HL, Sui X, Xiao L, Guo Z, Yao Y, Xiao Y, Chen G, Song K, Mack JC. 2006 Successful field pilot of in-depth colloidal dispersion gel (CDG) technology in Daqing oil field. *SPE Reservoir Eval. Eng.* **9**, 664–673. (doi:10.2118/89460-PA)
117. Al-Anazi HA, Sharma MM. 2002 Use of a pH sensitive polymer for conformance control. In *Proc. SPE Int. Symp. and Exhibition on Formation Damage Control held in Lafayette, LA, 20–21 February 2002*. Tulsa, OK: Society of Petroleum Engineers. (doi:10.2118/73782-MS)
118. Bai B, Huang F, Liu Y, Seright RS, Wang Y. 2008 Case study of preformed particle gel for in-depth fluid diversion. In *Proc. SPE Enhanced Oil Recovery Symp, Tulsa, OK, 19–23 April 2008*. Tulsa, OK: Society of Petroleum Engineers.
119. Liu Y, Bai B, Wang Y. 2010 Applied technologies and prospect of conformance control treatments in China. *Oil Gas Sci. Technol.* **65**, 1–20. (doi:10.2516/ogst/2009057)
120. Spildo K, Skauge A, Skauge T. 2010 Propagation of colloidal dispersion gels in laboratory core floods. In *Proc. SPE Improved Oil Recovery Symp., Tulsa, OK, 24–28 April 2010*. Tulsa, OK: Society of Petroleum Engineers. (doi:10.2118/129927-MS)
121. International Energy Agency. 2011 *World energy outlook 2011*. Paris, France: OECD/IEA.
122. Zhang PM, Tweheyo MT, Austad T. 2007 Wettability alteration and improved oil recovery by spontaneous imbibition of seawater into chalk: impact of the potential determining ions Ca^{2+}, Mg^{2+} and SO_4^{2-}. *Colloids Surf. A* **301**, 199–208. (doi:10.1016/j.colsurfa.2006.12.058)
123. Zahid A, Sandersen SB, Stenby EH, von Solms N, Shapiro A. 2011 Advanced waterflooding in chalk reservoirs: understanding of underlying mechanisms. *Colloids Surf. A* **389**, 281–290. (doi:10.1016/j.colsurfa.2011.08.009)
124. Gozalpour F, Ren SR, Tohidi B. 2005 CO_2 EOR and storage in oil reservoirs. *Oil Gas Sci. Technol. Rev. IFP* **60**, 537–546. (doi:10.2516/ogst:2005036)
125. McCoy ST, Pollak M, Jaramillo P. 2011 Geologic sequestration through EOR: policy and regulatory considerations for greenhouse gas accounting. *Energia Procedia* **4**, 5794–5801. (doi:10.1016/j.egypro.2011.02.576)
126. Leach A, Mason CF, van't Veld K. 2011 Co-optimization of enhanced oil recovery and carbon sequestration. *Resour. Energy Econ.* **33**, 893–912. (doi:10.1016/j.reseneeco.2010.11.002)
127. Bryant RS, Burchfield TE. 1989 Review of microbial technology for improving oil recovery. *SPE Reservoir Eng.* **4**, 151–154. (doi:10.2118/16646-PA)
128. Zobell CE. 1947 Bacterial release of oil from sedimentary materials. *Oil Gas J.* **46**, 62–65.
129. Van Hamme JD, Singh A, Ward OP. 2003 Recent advances in petroleum microbiology. *Microbiol. Mol. Biol. Rev.* **67**, 503–549. (doi:10.1128/MMBR.67.4.503–549.2003)
130. Maudgalya S, Knapp RM, McInerney MJ. 2007 Microbial enhanced-oil-recovery technologies: a review of the past present and future. In *Proc. SPE Production and Operations Symp., Oklahoma City, OK, 31 March–3 April 2007*. Tulsa, OK: Society of Petroleum Engineers.